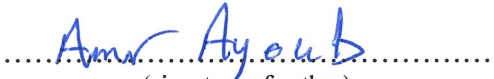# Universitetet
i Stavanger

FACULTY OF SCIENCE AND TECHNOLOGY

MASTER'S THESIS

Study programme / specialization: Petroleum Engineering / Reservoir Engineering	Spring semester, 2017 Open
Author: Amr Ayoub	*Amr Ayoub* (signature of author)

Programme coordinator: Prof. Aly Anis Hamouda
Supervisor: Prof. Aly Anis Hamouda
Co-supervisor: Rockey Abhishek

Title of master's thesis:

Transport Behavior of Nanoparticles (NP) in Stevns Klint Chalk Rock and EOR potential

Credits: 30

Keywords:	
Silica Nanoparticles Zeta potential Ionic strngth Double layer Static adsorption Adsorption / retention Stevns Klint Chalk Scanning Electron Microscope Ion tracking Enhanced Oil Recovery	Number of pages: 85 + supplemental material/other: Stavanger, 15/06/2017 date/year

Title page for Master's Thesis
Faculty of Science and Technology

Acknowledgments

Abstract

This study investigates the adsorption potential of NPs in Chalk cores and the possible EOR mechanisms behind it. The work is divided into two major sets of experiments; static adsorption experiments and core flooding experiments. Static adsorption experiments studies the specific adsorption potential of NPs on the surface of three minerals; Quartz, Kaolinite, and Calcite. Since this work focuses on NPs interactions with Chalk cores, great attention is given to explaining the adsorption that takes place on Calcite mineral and the forces in play as well as comparing the adsorption with the other two minerals. An integral part of studying adsorption of NPs involves performing several measurements on NYACOL DP9711 – source of NPs – to characterize its stability, nominal particle size distribution and its zeta potential at different dilutions in Deionized Water, (DIW) / Synthesized seawater, (SSW) / Low salinity water, (LSW) and at elevated temperatures. The second set of experiments is devoted for core flooding. Core flooding is divided into two main subsets of experiments. The first subset studies the transport and the associated adsorption and desorption that takes place in SK cores. Two cores are flooded with NPs and sample effluents are analyzed intensively. The ion tracking and elemental analysis along with pH allow for underlying the possible major processes that lead to adsorption / desorption and changes introduced to the rock surface. The second subset of experiments, is EOR experiments studying the underlying EOR mechanisms and the potential of Silica Nano Particles as an EOR candidate.

Static adsorption experiments show strong affinity of NPs to adsorb on calcite surface more than quartz and kaolinite. The adsorption is slightly improved in SSW for calcite and this improvement is more pronounced for quartz and kaolinite. From core flooding experiments, adsorption of NPs is proved to take place in chalk cores. The introduction of NP prepared in LSW in chalk cores shows an increment in oil recovery when compared to the primary recovery by LSW and sweep efficiency has improved.

Table of Contents

List of Plots and Figures

List of Tables

List of Abbreviations

[]	activity / effective concentration
abs	UV absorption value
CM	constant mass
conc.	concentration
CSA	constant surface area
DIW	de-ionized water
DLS	dynamic light scattering
DP	nyancol silica nano fluid DP 9711
dp	differential pressure
EDXRF	energy dispersive x-ray fluorescence
EOR	enhanced oil recovery
ESA	electrokinetic sonic amplitude effect
IC	ion chromtograph
ICP-OES	inductive coupled plasma optical emission spectrometry
inj.	injection
K	equilibrium constant
K	kelvin
LDM	laser doppler micro-electrophoresis
LSW	low salinity water
M	molar
mA	milliampere
mD	milli-darcy
mv	milli volt
nm	nano meter
NP	silica nanoparticles
PdI	poly dispersity index
PV	pore volume
PV/D	pore volume per day
Ref.	reference
rpm	rotation per minute
SA	Stearic Acid
sat.	saturation
sat.	saturation
SEM	scannng electron microscope
SK	Stevns Klint
SOR	residual oil saturation

Sp.Ads.	specific adsorption
SSW	synthesized sea water
TDS	total dissolved solids
UV-abs	ultraviolet absorption
Vo	oil volume produced (ml)
Vw	water volume produced (ml)
z-avg	average diameter of silica nano particles

Chapter 1

1. Introduction

Nanotechnology applications have gained a lot of attention over the past few years in the oil industry. Nano-Fluids and Silica Nano Particles (NPs) in particular, have become increasingly more popular as a potential enhanced oil recovery (EOR) candidate for their large surface area compared to their volume, which allows for more interactions with the porous medium. However, the complexity of the processes that encompasses these interactions are not completely understood.

Silica Nano Particles are not expensive to produce, easy to modify their surface, and environmentally friendly, which makes them of great interest for oil field applications [1]. For EOR processes, Silica Nano Particles are becoming increasingly popular in the research area to identify the processes and mechanism involved in an attempt of quantifying and optimizing their potential. Many researches have been made to investigate the adsorption of Silica Nano Particles on Berea but not so many researches are devoted to investigate the adsorption on chalk.

This study investigates the adsorption potential of NPs in Chalk cores and the possible EOR mechanisms behind it. The work is divided into two major sets of experiments; static adsorption experiments and core flooding experiments. Static adsorption experiments studies the specific adsorption potential of NPs on the surface of three minerals; Quartz, Kaolinite, and Calcite. Since this work focuses on NPs interactions with Chalk cores, great attention is given to explaining the adsorption that takes place on Calcite mineral and the forces in play as well as comparing the adsorption with the other two minerals. An integral part of studying adsorption of NPs involves performing several measurements on NYACOL DP9711 – source of NPs – to characterize its stability, nominal particle size distribution and its zeta potential at different dilutions in Deionized Water, (DIW)/Synthesized seawater, SSW/Low salinity water, LSW and at elevated temperatures. The second set of experiments is devoted for core flooding. Core flooding is divided into two main subsets of experiments. The first subset studies the transport

behavior of Silica NPs and the associated adsorption and desorption that takes place in SK cores two cores are flooded) with NPs and sample effluents are analyzed intensively by using ion chromatograph, IC/inductive coupled plasma, ICP/scanning electron microscope with energy dispersive x-ray fluorescence, SEM+EDXRF/ pH/and ultraviolet-visible light spectrophotometry, UV-Vis. The ion tracking and elemental analysis along with pH allow for underlying the possible major processes that lead to adsorption / desorption and changes introduced to the rock surface. The second subset of experiments, is EOR experiments performed on (SK-5 & SK-6) to study the underlying EOR mechanisms and the potential of Silica Nano Particles as an EOR candidate.

This thesis will start with brief theoretical over view in Chapter 2 followed by methodology and procedures of the performed experiments in Chapter 3. After that all the results and findings will be presented and discussed in Chapter 4. Finally, the conclusions and list of findings will be presented in Chapter 5.

Chapter 2

2. Theory

Nanotechnology is becoming increasingly more popular due to their wide range of applications. Silica nano particles have recently attracted a lot of attention due to their high surface area compared to their size range (1-100nm) [2].

NP has many applications in the oil and gas industry including: formation damage mitigation, assisted surfactant / alkaline / low salinity /gas flooding and well treatment after fracturing in unconventional reservoirs. The EOR mechanisms of nanoparticles include wettability alteration, disjoining pressure, interfacial tension reduction, pore channels plugging and improvement in sweep efficiency. Due to their unique properties, Nanoparticles can improve the rock integrity by decreasing the double layer forces between the particles and rock grains by altering zeta potential [3].

2.1. Disjoining pressure

Structural disjoining pressure mechanism occurs due to the establishment of a wedge film in the presence of nanoparticles at three phases contact region. When NPs come between the oil droplet - spread on the substrate - and the rock the IFT will reduce and the oil droplets will be disjoined. When the rock surface becomes covered with hydrophilic NPs, the wettability will be altered and the rock will be less oil wet and more water wet.
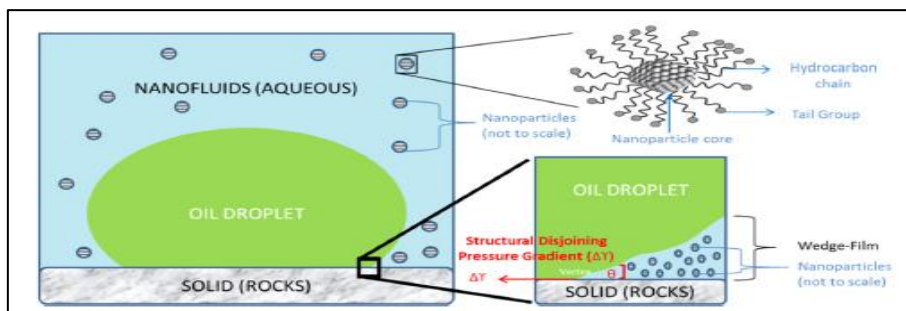
2-1 Disjoining PressureMechanism

2.2. LSW Effect on flooding

LSW improves the oil recovery by changing the rock to more water wet. The main principle is cation exchange with the rock surface. LSW ion concentration is lower than that of the rock, it exchanges cations with the rock surface and, as a result, makes the rock surface more negatively charged [4] . It leads to lowering of electrostatic attractive forces between the rock surface and crude oil, which results in the release of a greater volume of oil. Poor capability of LSW to alter the surface charge of the rock is the main reason for the induced migration of fines during LSW flooding projects [2].

2.3. Derjagin-Landau-Verwey-Overbeek (DLVO) theory.

The study of adsorption, desorption, transportation, blocking, and aggregation of nanoparticles is important to understand the influence of nanoparticles on properties, such as permeability, and porosity. The size of nanoparticles is less than 1 micron (1 micron = 1000 nanometer), thus they are considered Brownian particles. The forces between the nanoparticle and the pore wall are; Van Der Wall attraction potential forces, repulsion forces of electric double layers, Born repulsion (at atomic distances), acid-base interactions, and hydrodynamics. Adsorption of nanoparticles on the substrate of rock surface occurs, when the net of these forces in play is negative, the attraction forces between the pore walls and NPs are greater than the repulsion forces. Desorption occurs if the net forces in play are positive, which is dynamically in balance with adsorption. Blocking of pores occurs only if the nanoparticles aggregates and break up the previous equilibrium of the dispersion system to form clusters greater in diameters than the pore throats [5].

Chapter 3

3. Methodology and Equipment

This chapter is devoted to present an accurate account of the experiments' procedures and the list of materials and equipment being used. There are three main experiments that aim to identify the effect of silica Nano particles on chalk. The first set of experiments start with the characterization of NPs (DP 9711) diluted in DIW and SSW at different temperatures and concentration. Stability of the silica Nano particles against agglomeration is tested at different concentration and under high pressure and temperature. Zeta potential measurements are taken for both NPs and calcite mineral powder at different concentrations. After NPs and mineral characterization and zeta potential measurements are concluded a series of static adsorption experiments are carried out to compare the specific adsorption of silica Nano particles on Calcite, Quartz, and Kaolinite mineral powders at different concentration ratios of minerals to DP diluted in DIW and SSW respectively. The second set of experiments investigate the flow behavior of the NPs in Stevns Klint chalk core to quantify the possible adsorption, desorption and fine migration that takes place in the core through a rigorous analysis of the core effluents. Finally, the last set of experiments are dedicated to investigating silica Nano particles potential as an EOR candidate and the possible recovery mechanisms that are in play.

The first part of this chapter will provide a summary of the materials and equipment being used throughout the experiments along with brief description of the principle of use. The second part will present a detailed description for each of the three main experiments and their procedures.

3.1. List of Laboratory Materials and Equipment

The following tables summarize the list of materials and main equipment used throughout all the experiments.

Table 3.1 List of Powders

Powders (Analysis grade)	Formula	Supplier
Calcite	$CaCO_3$	Honeywell Riedel-de Haën®
Calcium Chloride Dihydrate	$CaCl_2.2H_2O$	Merck KGaA, Germany
Kaolinite	$Al_2Si_2O_5(OH)_4$	Fluka (Part of SAF)
Lithium Chloride	$LiCl$	Merck KGaA, Germany
Magnesium Chloride Hexahydrate	$MgCl_2.6H_2O$	Merck KGaA, Germany
Potassium Chloride	KCl	Merck KGaA, Germany
Quartz	SiO_2	Fluka (Part of SAF)
Sodium Bicarbonate	$NaHCO_3$	Merck KGaA, Germany
Sodium Chloride	$NaCl$	Merck KGaA, Germany
Sodium Sulfate	Na_2SO_4	Merck KGaA, Germany
Stearic Acid	$C_{18}H_{36}O_2$	Merck KGaA, Germany

Table 3.2 Fluids and Chemicals List

Fluids and Chemicals	Formula	Supplier
Acetone	CH_3COCH_3	VWR International AS
Buffer Solutions		VWR Chemicals, USA
DIW/LSW/SSW	H_2O	
Hydrochloric Acid	HCl	Merck KGaA, Germany
Model Oil	N-Decane	Merck KGaA, Germany
Nano Lubricant		ORAPI, Norway
Nitrogen (gas)	N_2	Praxair Norge AS
Silica NPs (DP 9711)	SiO_2	NYACOL® Nano Technologies Inc.
Silicon Grease (SGM-494)		Acc Silicons Europe
Surfactant		OKKjemi, Norway

Table 3.3 List of Equipment

Equipment	Supplier
"AcoustoSizer II-M System"	Colloidal Dynamics LLC, USA
Analytical Balance "MS104-S"	Mettler- Toledo Int. Inc., Switzerland
Centrifuge "5804"	Eppendorf AG, USA
Differential Pressure Deltabar "PMD75"	Endress+Hauser, Germany
GX -271 Liquid Handler	Gilson Inc., USA
"Milli-Q" DIW +Q-Pod and Distilled Water	EMD Millipore
DLS and LDM "Zetasizer Nano ZSP"	Malvern Instruments Ltd, UK
Heat Gun "2000W"	Bosch, Germany
IC "Dionex Ics-5000⁺ DP"	Thermo Fisher Scientific Inc.
Optima 4300 DV ICP-OES	PerkinElmer
Injection Pumps "Gilson 305"	Gilson Inc., USA
Inlet Pressure "Rosemount™ 3051 Coplanar™ Pressure Transmitter"	Emerson, USA
Magnetic Stirrer "VWR VMS-C10"	VWR Int., LLC, USA
Oven "Memmert UM 1000"	Memmert GmbH + Co. KG, Germany
pH "S220 SevenCompact™"	Mettler- Toledo Int. Inc., Switzerland
Precision Balance "Mettler PM 4000"	Mettler- Toledo Int. Inc., Switzerland
Rotator Agitator "Stuart SB-3"	Cole-Palmer, UK
SEM "Supra 35VP FE-SEM"+EDXRF	Carl Zeiss, Germany
Turbiscan	Formulaction, USA
Ultrasonic cleaning baths USC	VWR Int., LLC, USA
UV-Vis "1700 Spectrophotometer"	Shimadzu Corp., Japan
Vacuum pump "Vacuubrand"	GMBH, Germany
Vortex Mixer "Reax Top"	Heidolph Instruments GmbH & Co.KG, Germany

3.1.1. **Nano-Fluid DP9711**

NYACOL DP9711 is a surface modified colloidal silica Nano particles that is stable against agglomeration over wide range of pH and also maintain high stability in brine solutions [6]. The fluid is supplied in 30 wt% concentration of silica which is diluted with DIW, LSW, or SSW to desired concentration. The following table summarizes the typical properties of DP9711.

Table 3.4 Typical Properties of DP9711 [6]

Property	Value
Silica wt%	30
Average Particle Size	20-30 nm
Particle Shape	Spherical
pH @ 250C	3
Viscosity @ 250C	5 cP
Specific Gravity	1.2

3.1.2. **Brines**

Two brines are used throughout the experiments: synthesized sea water and low salinity water SSW and LSW. SSW is prepared by adding reagent grade minerals at certain concentrations to DIW. The salts are dissolved in DIW by stirring them for at least three hours with a magnetic bar and the solution is filtered through 0.22 μm Millipore filter with an aid of vacuum setup to ensure removal of any undissolved impurities. LSW is prepared by diluting SSW 10 times with DIW. The following table summarizes the salts composition for 1 liter of SSW.

Table 3.5 SSW Salt Composition

Mineral	Formula	Amount (g)
Calcium Chloride Dihydrate	$CaCl_2.2H_2O$	1.91
Magnesium Chloride Hexahydrate	$MgCl_2.6H_2O$	9.05
Sodium Bicarbonate	$NaHCO_3$	0.17
Sodium Chloride	$NaCl$	23.38
Sodium Sulfate	Na_2SO_4	3.41
Potassium Chloride	KCl	0.75

The ion composition for SSW and LSW are shown in the table below.

Table 3.6 Ion Composition of Brines [7]

Ion	SSW (mol/l)	LSW (mol/l)
HCO_{3-}	0.002	0.00008
Cl^-	0.525	0.021
SO_4^{2-}	0.0240	0.00096
Mg^{2+}	0.045	0.0018
Ca^{2+}	0.013	0.00052
Na^+	0.450	0.018
K^+	0.010	0.0004
TDS (g/l)	33.39	1.3356
Ion strength (mol/l)	0.657	0.0263

3.1.3. **N-Decane**

N-Decane (N-C_{10}) or normal Decane is supplied in HPLC grade (purity > 99%) [7]. The following table summarizes typical properties of the oil at different temperatures.

Table 3.7 N-Decane Typical Properties [7].

Temperature ^0C	Viscosity (cP)	Density (g/ml)
20	0.92	0.73
50	0.5802	0.7683
70	0.4812	0.7525

For experiments that require core aging Stearic acid at 0.005 (mol/l) concentration is added to the oil before aging the core. Fatty acid alters the wettability of the chalk to more oil wet [8].

3.1.4. **Mineral Powders**

The following table shows the BET surface area measurements for minerals used in static adsorption experiment calculated by water adsorption isotherm [9].

Table 3.8 Surface Area Measurements for Minerals [9].

Powder	Formula	Surface area (m^2/g)
Quartz	SiO_2	0.65
Kaolinite	$Al_2Si_2O_5(OH)_4$	9.95
Calcite	$CaCO_3$	0.23

3.1.5. **AcoustoSizer II-M System**

AcoustoSizer is used to measure the zeta potential and particle size distribution of Calcite mineral at different concentrations. This instrument is designed to take measurements for concentrated colloids without the need of dilution [10]. For that purpose, AcoustoSizer utilizes two principles: ESA or Electro-Kinetic Sonic Amplitude Effect, and Ultrasonic Attenuation. ESA is the ultrasound waves generated by charged particles in the suspension when an external electric field is applied. It permits an oscillation of these charged particles back and forth and phase them, which results in cooperative motion and detectable ultrasound beam [10]. ESA is proportional to the velocity, which is a function in both particle size and charge, hence the determination of both size and zeta potential is made [10]. For weakly charged particles, the size distribution is determined by ultrasonic attenuation. Ultrasonic attenuation utilizes an external ultrasound transducer that generates ultrasound waves in the dispersion and then those waves are received on a second transducer to measure the attenuation caused by the particles in the solvent, which is a function of particle size and concentration [10].

ESA Range [10]:

70 nm < Particle Diameter < 10 µ → size and zeta potential could be measured.

Particle diameter < 70 nm → Only zeta potential could be measured.

3.1.6. **Balances**

- ➤ Precision Balance used to weight cores used in flooding. ***Range:*** (0 - 4100) +/- 0.02 g) [11].
- ➤ Analytical Balance used to weigh minerals and DP 9711. ***Range:*** (0.1 mg – 120 g) [12].

3.1.7. **Centrifuge "5804"**

Centrifuging the samples to remove fines and mineral sediments before taking UV abs measurements. ***Range:*** (200 rpm – 11000 rpm)

3.1.8. **Pressure Gauges**

- ➤ "Rosemount™ 3051 Coplanar™ Pressure Transmitter" used to record the inlet pressure during the core flooding experiments. ***Range:*** (137.89 bar Gauge and 275.79 bar absolute) [13].
- ➤ Differential Pressure Deltabar "PMD75" used to record dp of the system during flooding. ***Range:*** (10 mbar – 40 bar) +/- 0.05 % [14].

3.1.9. **"Milli-Q" DIW +Q-POD and Distilled Water**

The system utilizes a distilled water column connected to Milli-Q DIW system with quality point of delivery system to ensure ultrapure water delivered [15]. DIW is used in dilution and sample preparations as well as core saturation and cleaning procedures.

3.1.10. **DLS and LDM "Zetasizer Nano ZSP"**

Dynamic light scattering technique is utilized to characterize the average size distribution of silica Nano particles in diluted samples at different concentration of DP 9711. Through using a correlation function the diffusion of particles is measured from the intensity of the light scattered by the Brownian motion of NPs. By substituting the diffusion coefficient in Stokes-Einstein equation, the size of NPs is calculated. ***Range:*** (0.3nm – 10 microns) +/- 2 % [16].

Laser Doppler Micro-electrophoresis utilizes an electric field to the NPs dispersion, which causes the particles to move with a velocity relative to their zeta-potential. Electrophoretic mobility is calculated by phase analysis light scattering and hence zeta-potential of NPs is acquired. ***Range:*** (3.8nm – 100 microns) [16].

3.1.11. **IC "Dionex ICS-5000+ DP"**

Ion Chromatography is used to analyze the anions and cations present in the effluents (analyte). The basic principle is that the analyte is injected into the eluent which passes through a column with adsorbent that allows for the dissolved materials to adhere and hence affects their relative speeds in the column, which allows them to separate from one another. Electrical conductivity detector gives a characteristic signal for different species. These signals, which are printed as

peaks on a chromatogram, are calibrated by a reference with known ion content and hence the ion content of the analyte could be calculated based on that reference [17].

Dionex ICS contains eluent generator (EG) where the analyte is injected into and utilizes Palladium Hydrogen reference electrode (PdH), which is pH dependent. Conductivity detector is used to identify different species and aided with suppressor to reduce the noise from the eluent conductance and strengthen the conductance of the analyte. Finally, IC has thermal compartment (TC) with an operating range from $(5 - 85)^0$C and with accuracy of +/-0.1^{0}C, that can be used to heat the column [18].

3.1.12. **Optima 4300 DV ICP-OES**

ICP-OES stands for inductive coupled plasma optical emission spectrometry. ICP is used to detect different elements present in a sample diluted in an aqueous solution both qualitatively and quantitatively. The sample is converted to mist (aerosol) in nebulizer and a few microns of the sample pass through a plasma torch (argon) and become in their excited or ionized state. The atoms emit photons when they returns to their ground state. The emission spectrum contains all peaks for the respective elements present in the sample, which can be identified by using multi-wavelengths to construct the element foot print [19]. Plasma is high energy state of the matter which is considered the fourth state [19]. It is formed by subjecting the gas to temperature range (2000 – 9000) K and the gas atoms become in equilibrium between their neutral and ionized state with their associated electrons [19]. The instrument operates at temperatures $(15 - 35)^0$C, and optimally at 20^{0}C [20].

ICP is utilized to mainly detect silicon in the sample effluents, which indicates the presence of silica nano particles.

3.1.13. **Injection Pumps**

Gilson 305 pumps are used in the core floods experiments. ***Flow Range:*** (10 µl/min – 200 ml/min) [21].

3.1.14. **pH "S220 SevenCompact^{TM}"**

The effluents from the core floods and the fluids injected and prepared pH measurements are taken by "S220 SevenCompact^{TM}"pH meter. Cleaning of the instrument electrode by DIW is followed after each measurement is taken and then the electrode is wiped gently without touching the metal surface on the tip of it. ***Range:*** (-2 – 20) +/- 0.002 [22].

3.1.15. **SEM "Supra 35VP FE-SEM"+EDXRF**

Scanning electron microscope bombard the sample with high energy electrons, which spread on the sample surface. The electrons from the surface are detected and image is rendered [23]. SEM utilizes the principle of x-ray fluorescence, when the sample is bombarded by high energy fast electrons of energy range: (20 – 30) KeV and provide a semi quantitative analysis of the atoms [19]. EDXRF is used to collect the fraction of x-ray fluorescence to construct EDS

histogram, where different elements can be identified quantitatively within a sample volume of $1\mu m^3$ [19]. The following image demonstrates the interaction of the electron beam with the material.
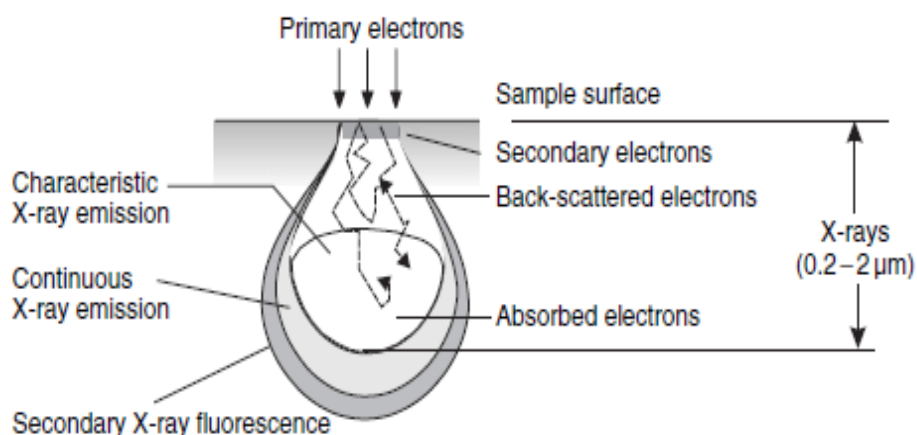
3-1Interaction of Electron Beam with the Material [19]

SEM is used to check Silica Nano particles adsorption on the surface of chalk. SEM is aided with EDAX or energy dispersion x-ray spectroscopy that enables element analysis from the surface and used to check for silicon in the targeted area, where spherical particles in the size range of NPs are spotted. The chalk sample is taken from a cross section of core flooded with 1 (g/l) DP and left to dry in the oven. The sample is retrieved from the oven and coated with palladium inside a glass cylinder - filled with argon to ensure even coating - under 25 mA. The thickness of coating achieved is 20 nm of palladium. SEM was also used to examine some colored sample effluents from pre-flush and post-flush of SK-2. Sample effluents were dried on a carbon film and placed inside SEM sample chamber. EDXRF was performed for a post-flush sample.

3.1.16. **Turbiscan**

Stability of DP is tested at different temperatures using Turbiscan. This instrument is useful to track the size change and flocculation in a sample by using static multiple light scattering technique with an operating **Range** of: 10nm – 1 mm [24].

3.1.17. **UV-Vis "1700 Spectrophotometer"**

When a light is passed through a diluted sample, some of the light will be transmitted and some of it will be absorbed by an amount direct proportion to the concentration of the sample. Beer-Lambert law describes the relationship between absorption and molar concentration of the substance as follows [25].

$$A = \epsilon \times b \times c \qquad\qquad (4.1)$$

Where A is the absorbance, ϵ is the molar absorptivity, b is the path length, and c is the molar concentration.

UV-Vis double beam utilizes a light source that covers the range of both visible and ultraviolet light (190 nm – 1100 nm). To this end it uses two lamps: Tungsten/Halogen lamp for the visible

part, and Deuterium lamp for the UV [26]. As illustrated in the diagram below, the light passes through a diffraction grating slit where it can be adjusted to the desired wavelength intended. After that, the light beam with the desired wave length meets a rotating disc, which allows for three scenarios; transmitting, reflecting, and blocking of the light. If the light is allowed to pass and follow the red line on the diagram through the sample cell and to a mirror which will reflect the light to another rotating disc and eventually to the detector. If the light is reflected from the first disc it will follow the green path and pass through the reference cell and then to the detector. Finally, if the light was blocked by the first disc, no light will pass through any of the cells and it will allow for correction of any current generated in the absence of light. Detector transform the light into current and absorption is related to light intensity as follows [26].

$$A = Log \frac{Io}{I} \qquad (4.2)$$

Where I is the intensity of light measured for the sample cell and Io is for the reference cell.
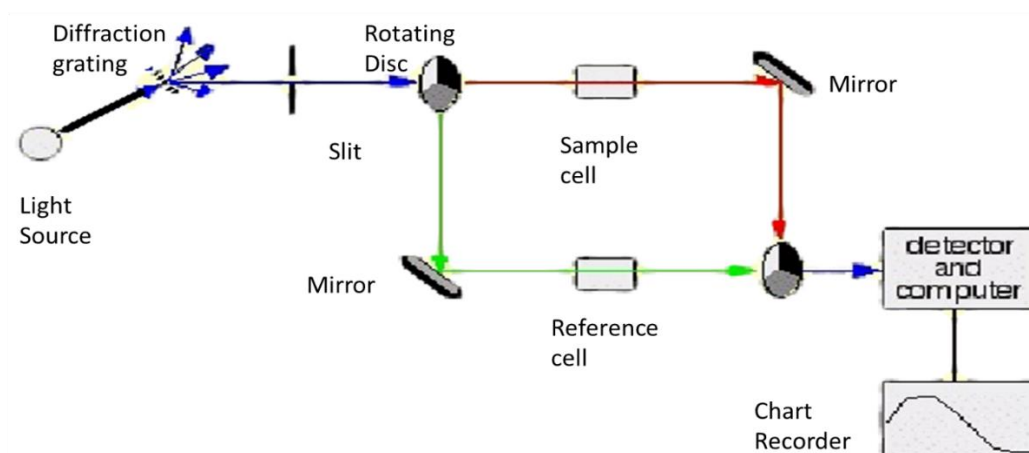
3-2 UV-Vis Double Beam Diagram [26]

UV-Vis is used to analyze samples from static adsorption to measure the concentration change in DP after adding known concentration of DP to known concentration of the mineral and taking the UV abs reading of the sample after centrifuging to remove the mineral and account only for DP concentration change. The glass cuvettes used in the reference and sample cells are made from quartz and specially designed for these types of measurements. **Wavelength Range:** (190 nm − 1100 nm) +/- 0.3 nm. **ABS Accuracy** is +/- 0.002 and +/- 0.004 for ABS $\approx 0.5 \ and \ 1$ respectively [27].

3.2. Characterization of DP 9711 and Calcite Powder

This part will cover a group of tests performed on DP 9711 and Calcite mineral powder. The aim of these tests is to ensure the stability – resistance to agglomeration - of DP at different concentrations and under high pressure as well as measuring its zeta potential by utilizing the use of Turbiscan and Zetasizer Nano ZSP. In addition to DP characterization, zeta potential of concentrated dispersions of Calcite are measured by AcoustoSizer II-M. The Data acquired from these tests are presented in Chapter 5.

3.2.1. DP 9711

➢ Effect of concentration on particle size: DLS measurements are taken for DP prepared in DIW at 1, 2, 4 g/l.
➢ Effect of salinity and temperature on particle size: DLS measurements are taken for DP prepared in DIW, LSW, and SSW at 1 g/l at 25^0C, 50^0C, 80^0C.
➢ Zeta potential measurements – LDM - were taken for 1 g/l DP in DIW, LSW, and SSW.
➢ Stability test at high pressure is carried out for 1 g/l DP in DIW under 80 bars and the sample was tested by using Turbiscan and no flocculation was spotted.

3.2.2. Calcite [$CaCO_3$]

Zeta potential and pH measurements are taken for calcite at 1, 10, 20 g/l in DIW. Samples were stirred for 20 minutes before measurements are taken. The suspension was then placed inside the glass chamber and was continuously circulated in the flow loop through the ESA sensor.

3.3. Static Adsorption Experiments

Static adsorption experiments on Calcite, Quartz, and Kaolinite mineral powders, comprise mainly of four sets of experiments:

1. Constant mass experiments in DIW.
2. Constant mass experiment in SSW.
3. Constant surface area experiments in DIW.
4. Constant surface area experiments in SSW.

The motivation behind these experiments is to study the specific adsorption of silica nano particles on the mineral surfaces as well as comparing the adsorption potential in the three minerals at the equal concentrations of minerals and at equal total average surface area. Measuring the concentration of the silica nano particles in the diluted samples constitutes a major challenge in the experiments. UV-Vis is used to measure the change in concentration of the nano particles after being mixed with mineral powder for 24 hours for quantitative determination of adsorption that takes place on the mineral surface. For consistent and successful quantitative analysis of static adsorption, the following rigorous procedures are followed.

3.3.1. **DP 9711 Preparation**

NYACOL DP9711 is supplied in 30 wt % of silica concentration. All the experiments are done for 1 and 0.5 (g/l) in 30 ml tube. To prepare 1 (g/l) of NP, 3.28 g of DP is weighed on a precision scale and mixed with 1 liter of DIW in 1000 ml volumetric flask. The lower meniscus of water should be parallel to the calibrated line on the flask. The mixture is stirred on a magnetic stirrer for two hours at lower speed of mixing to avoid introducing bubbles in the mixture. To have 0.5 (g/l) DP, in 30 ml tube 15 ml is filled with 1 (g/l) DP and the rest is filled with DIW and then the tube is placed on the vortex mixer for 30 seconds. To prepare 1 (g/l) of DP in SSW or LSW, the same procedures are followed. Procedures for preparing SSW and LSW are mentioned in section (4.1.2).

3.3.2. **Adding Minerals**

Minerals are added to 30 ml tube of liquid to get the required concentration ratio of mineral to DP. Minerals are accurately weighed on precision scale before added to the tube. All tubes are placed on vortex mixer for at least 30 seconds to ensure uniform mixing of the minerals in the fluid. All tubes are labeled properly with their respective mineral powder and concentration of mineral to DP ratio and placed in the rotator agitator at 40 rpm for 24 hours to allow the suspension to reach thermodynamic equilibrium between its different species. The following table summarizes the amounts and concentrations of minerals and DP for all the experiments performed in DIW and SSW.

Table 3.9 Static Adsorption Experiments in DIW and SSW

CM					
Mineral	Weight (g)	Avg surface area (m^2)	Mineral concentration (g/l)	Mineral to NP concentration ratio 1 (g/l) DP	Mineral to NP concentration ratio 0.5 (g/l) DP
Quartz	0.15	0.0975	5	5	10
Kaolinite	0.15	1.4925	5	5	10
Calcite	0.15	0.0345	5	5	10
CSA					
Quartz	0.058	0.0375	1.92	1.92	3.85
Kaolinite	0.0038	0.0375	0.13	0.13	0.25
Calcite	0.164	0.0375	5.46	5.46	10.9
Extra Points for Calcite					
Weight (g)	Avg surface area (m^2)	Mineral concentration (g/l)	Mineral to NP concentration ratio 1 (g/l) DP		
0.03	0.007	1	1		
0.09	0.021	3	3		

Before measurements are made taken by UV-Vis, sample tubes are centrifuged for 10 minutes at 10000 rpm and decanted. 15 ml of the supernatant is centrifuged for another 10 minutes at 10000 rpm to ensure effective separation of the mineral from the sample. Good care should be taken during decanting the samples to avoid disturbing the mineral sediments again into the mixture.

3.3.3. UV-Vis Measurement

Before being able to calculate for the DP concentration present in the sample, it is important to have a reference sample with known concentration of DP where all the later measurements calculation will be based upon. Also. It is important to account for mineral base line correction for the possible residual traces of minerals in the supernatant.

3.3.3.1. Calibration

UV-Vis offer a wide range of wavelength to conduct the measurements. For transparent high diluted samples the visible range of light will not be sensitive to the sample concentration. To determine the correct wavelength where all the subsequent measurements will be taken at, a reference sample of DP at 1 (g/l) is prepared, centrifuged and decanted. 4 ml of the sample is placed in sample cuvette after passing it through 0.2 µm filter by using a syringe. The sample is placed in the sample cell and measured against DIW in the reference cell. Abs values are recorded against different wavelengths range (200 – 300) nm and a new measurement is recorded every 10 nm increment. Values of abs on the ordinate are plotted against λ on the abscissa. The wavelength corresponding to the highest value of λ is chosen for the next measurement. Two other different concentrations of DP are prepared and measured at the designated λ and abs values on the ordinate are plotted against DP concentration on the abscissa. If a straight line is obtained the selected wavelength is approved for all the measurements, otherwise the test is repeated until a straight line is obtained. The wavelength chosen for measurements is 240 nm. The resulting straight line is called the calibration line with a slope used to calculate the unknown concentration of DP present in the sample as will be demonstrated in chapter 5. The same procedures are followed for SSW experiments with DP prepared in SSW and measured against SSW sample in the reference cell instead of DIW.

3.3.3.2. Baseline Correction

Baseline correction for all the minerals is prepared according to each of their respective concentrations as shown in the table below.

Table 3.10 Baseline Correction for Minerals in DIW and SSW

Mineral	Weight (g)	Mineral concentration (g/l)
Quartz	0.15	5
Kaolinite	0.15	5
Calcite	0.15	5
Quartz	0.058	1.92
Kaolinite	0.0038	0.13
Calcite	0.164	5.46
Calcite	0.03	1
Calcite	0.09	3

Baseline correction samples are prepared in similar manner with previous samples but without adding any DP to the mixture. Samples prepared in DIW are measured against DIW reference, while those prepared in SSW are measured against SSW reference after being centrifuged twice and filtered. The abs values of baseline correction are subtracted from abs values of supernatant samples with unknown concentration of DP and mineral samples after receiving the exact same treatment to make sure that the abs measurement corresponds only to DP concentration. The new DP concentration is subtracted from the initial and a mass balance calculation is made to find the amount of NP adsorbed on the mineral surface as shown in chapter 5. The value of adsorption are reported in mg of NPs per unit mass of mineral and mg of NPs per unit avg. surface are of the mineral.

3.3.3.3. Cleaning

It is vitally important to ensure capping of all fluids and minerals when not in use to avoid any possible contamination. An extra care should be given to the glass cuvettes and a rigorous procedure should be followed to avoid any possible effect on the measurements due to uncleanness. Before using the cuvettes they should be placed in plastic containers filled with DIW inside ultrasonic cleaner for 15 minutes and then rinsed thoroughly with DIW. The cuvettes are rinsed with DIW between each measurement and dried with air gun. After concluding the measuring process, the cuvettes are returned again to the plastic containers filled with DIW and placed in the ultrasonic for 15 minutes and then stored in their boxes for the next measurement.

3.4. Stevns Klint Core Flooding

This part consists of six core floods of Stevns-Klint "SK" cores. SK are outcrop chalk cores from Denmark and are 99% pure biogenic with high porosity range 45-50% and relatively low absolute permeability of $\approx$ 1mD [7]. The general outline of experiments is divided into two main sets. The first set of experiments studies the adsorption of silica nano particles and fine migrations in SK cores. The second set of experiments is devoted to examine the silica nano particles potential as an EOR candidate in SK cores. To this end, the first set of experiments utilizes three core floods, and the second set has another three floods summarized in the table below.

Table 3.11 Core Flooding Summary

Core ID.	PV cc	ϕ %	Experiment	Initial Sat. fluid
SK-1	28.9	48.8	Transport behavior of NPs	DIW
SK-2	28.56	47.9	Transport behavior of NPs	DIW
SK-3	33.1	49	Low-pH experiment	DIW
SK-4	32.737	50.6	Drainage	SSW
SK-5	29.7	48.5	Drainage/EOR	SSW
SK-6	33.83	50	Drainage/EOR	SSW

The transport behavior of NP is investigated by analyzing SK-1 and SK-2 effluents and measuring the concentration of NP in them. This was achieved by combining pH, IC, UV, and ICP data to detect the changes before and after injection of Nano-fluid inside the core. SK-3 is used as a control experiment, where low pH slug (DIW + HCl) is injected into the core instead of the Nano-fluid to emphasize the contribution of the NPs in the produced effluents.

The drainage and EOR experiments will be studied for SK-5 and SK-6 due to poor aging of SK-4.

Transport behavior experiments do not require aging of the cores. SK-1 and SK-2 are saturated with DIW and flooded at room temperature with DIW and DP in DIW at 2 and 1 (g/l) respectively. SK-3 is saturated with DIW and flooded with DIW and DIW +90 μl 0.1M HCl. EOR experiments conducted for SK-5 and SK-6 require aging for the cores after drainage. SK-5 and SK-6 were initially saturated with SSW and flooded for drainage - to establish irreducible water saturation – with N-Decane +0.005 M Stearic acid at room temperature. For EOR experiments the cores are aged for two weeks at 50^0C in a cylinder filled with N-Decane+0.005 M Stearic acid. After the cores are retrieved from aging they are flooded with LSW and 1 (g/l) DP in LSW at 70^0C.

3.4.1. **Transport Behavior of NPs**

The experiment consists of two floods as mentioned earlier. Both SK-1 and SK-2 were flooded against 10 bar backpressure and 25 bar confinement pressure at constant flow rate of 10 PV/D. The tables below summarize the flood scheme for SK-1 and SK-2 respectively.

Table 3.12 SK-1 Flood Scheme

Stage	Fluid inj.	pH	No. PV inj.
Pre-Flush	DIW	7	6.75
Slug	2 (g/l) DP + 0.5 M LiCl	5.68	0.5
Post-Flush	DIW	7	8.5

Table 3.13 SK-2 Flood Scheme

Stage	Fluid inj.	pH	No. PV inj.
Pre-Flush	DIW	7	7
Slug	1 (g/l) DP + 0.1 M LiCl	6.01	1.5
Post-Flush	DIW	7	9.75

The aim of this experiment is to detect the change in concentration of the injected Nano-fluid slug by analyzing the flood effluents and to understand the chemistry of ion exchange that takes place inside the core. Ion chromatography (IC) data presented for SK-1 and SK-2 will only include the analysis of: Calcium (Ca^{2+}), Magnesium (Mg^{2+}), Carbonate (CO_3^{2-}) – only available for SK-2 - and Lithium (Li^+) ions, while the rest of the IC data will be given in the appendix. The sample effluents are collected manually each quarter PV in a glass vial. For IC measurements preparation pre-flush bank, colored samples and post-flush bank are prepared and diluted to 1:500 ratio with DIW using GX 271 liquid handler. 1.5 ml of the diluted sample is injected through 0.2 µm filter into a small plastic vial that will be labeled carefully and prepared to be placed for analysis in the IC. As mentioned earlier some of SK-2 samples are analyzed in ICP and SEM+EDXRF. pH are taken for all the samples and UV-Vis Abs are taken for some samples in SK-1 flood. The following schematic illustrates the arrangement of the setup.
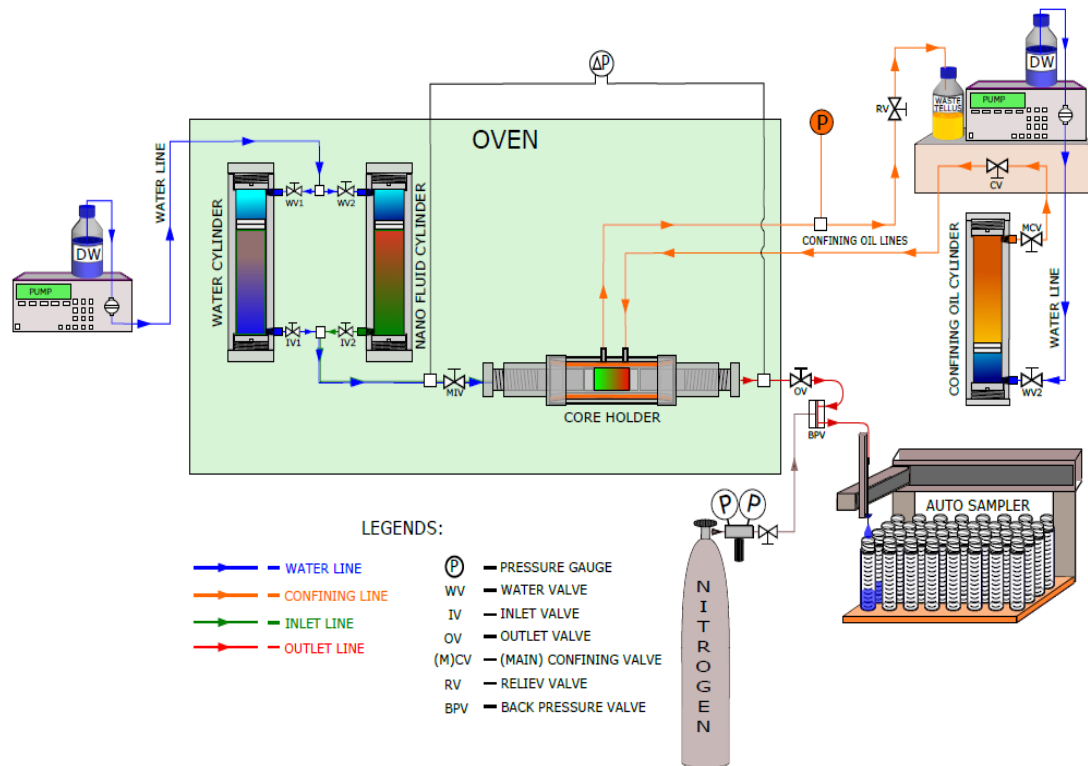
Figure 3-3 Transport Behavior of NP Setup at Room Temperature

3.4.2. Drainage/EOR Experiments/Aging and Flooding Procedures

3.4.2.1. Drainage/EOR

The following table summarizes Drainage/EOR experiments.

Table 3.14 Drainage/EOR Summary

Stage	Core	Initial saturation	Injected fluid	Injection rate (PV/D)	Confinement pressure (bar)	S_{wirr}
Drainage	SK-5	SSW	N-Decane + 0.005 M SA	5	25	0.29
	SK-6	SSW	N-Decane + 0.005 M SA	24	25	0.28

Core	Core	Flood Stages	Injected fluid	Injection rate (PV/D)	Confinement pressure (bar)	Back pressure (bar)	Temp. (C^0)	S_{wi}	S_{orNP}
EOR	SK-5	3	LSW/DP 1(g/l) in LSW	4/16	25	9.8	70	0.29	0.35
	SK-6	4	LSW/DP 1(g/l) in LSW	4/16	25	9.8	70	0.28	0.26

The schematic below shows the main features of the flooding setup for Drainage part.
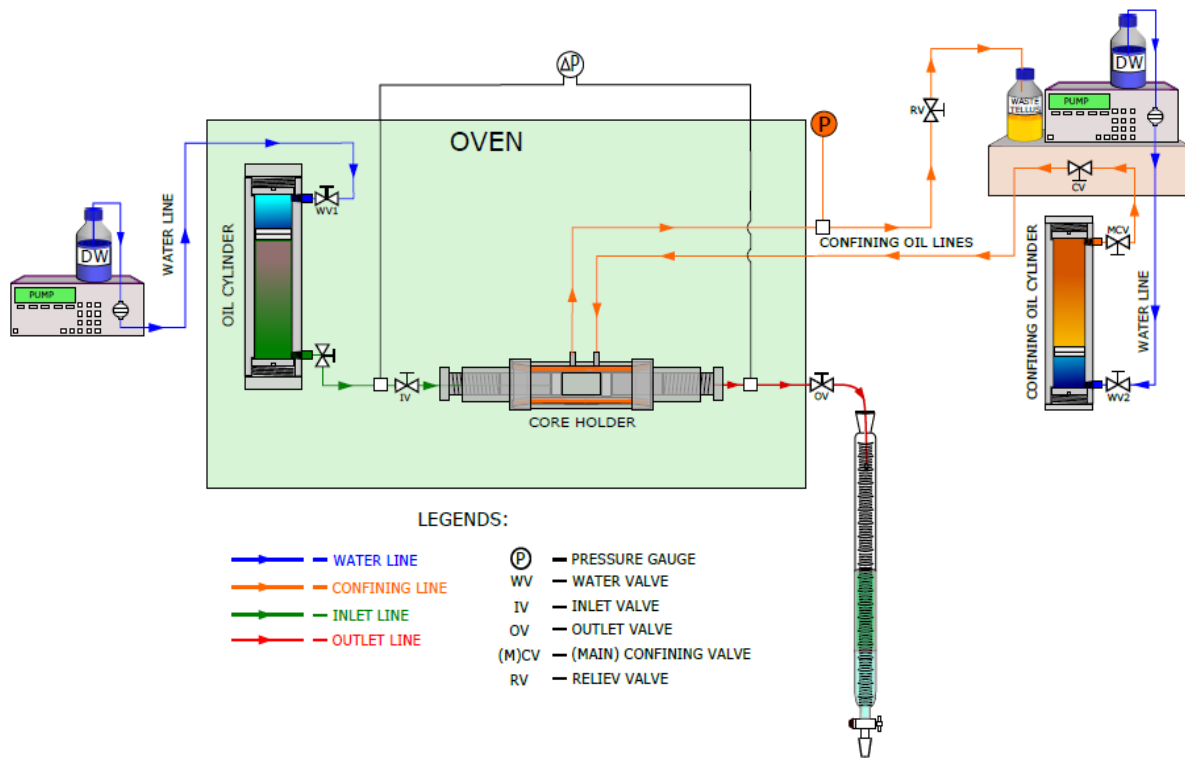
Figure 3-4 Drainage Setup at Room Temperature

The fluid is collected in the graduated burette attached to the system and the total water volume (Vw) and oil volume (Vo) collected is measured. The irreducible water saturation is measured according to the following relation.

$$Swi = \frac{PV - Vw}{PV} \qquad (4.3)$$

The core is weighed after drainage and using the values of core initial dry weight, and the densities for N-Decane and SSW, volumes of each fluid is recalculated and a check is made.

Cores are aged for two weeks at 50^0 C and then retrieved for EOR flood. The setup for EOR experiment at 70^0 C is shown below. The water cylinder contains LSW, while Nano-Fluid cylinder has Nano-Fluid in LSW. Effluent sample is collected each PV, while the fluid is allowed to gather in burette attached to the system. The amount of oil produced is monitored carefully from stage to stage. Residual oil saturation is calculated as follows.

$$Sor = \frac{PV - Vo}{PV} \qquad (4.4)$$

Recovery of Oil % is calculated by the following relation.

$$R\% = \frac{Vo}{PV - Vw} \times 100 \qquad (4.5)$$

The effluents from EOR experiments are collected in similar manner like Transport experiments effluents and prepared for IC by diluting them with DIW with 1:1000 ratio. pH samples are taken for each PV.
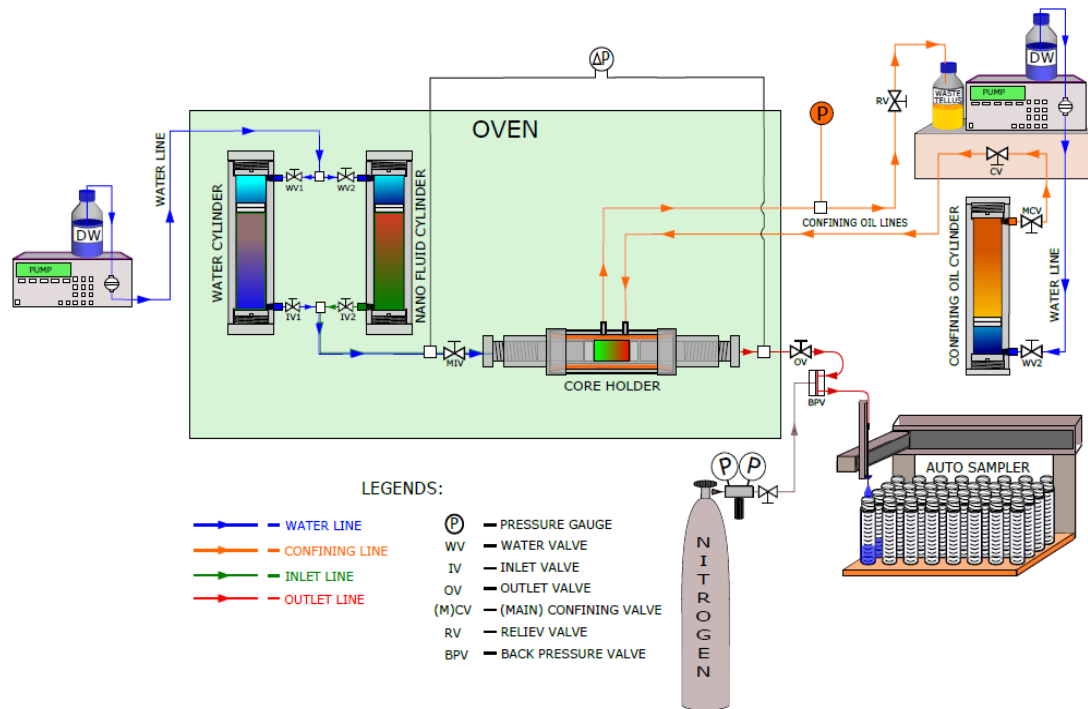
Figure 3-5 EOR Setup at $70^0 C$

3.4.2.2. Aging and Flooding Procedures

All SK cores are cut to the desired length and diameter and stored at 100^0 C in the oven to keep them dry. The saturation of the core takes place under vacuum pressure with DIW/LSW. The dry core weight is measured before saturation. The wet weight of the core is measured after saturation and the PV is calculated by using $\rho DIW = 0.97 \ g/cc$ and $\rho SSW = 1.024 \ g/cc$.

$$PV = \frac{Wet\ Weight - Dry\ Weight}{\rho sat.fluid} \tag{4.6}$$

Porosity (fraction) is PV divided by bulk volume $= \frac{PV}{\frac{\pi}{4} \times D^2 \times L}$, While D and L are the core diameter, and length respectively.

The core is drained using unsteady state (USS) method at constant rate of injection and S_{wi} is established. The core is aged in aging cell filled with N-Decane + 0.005 Stearic Acid and placed in the oven at 50 ^{0}C for at least two weeks. Finally, The core is retrieved gently from the aging cell and weighed.

Chapter 5

4. Results and Discussion

4.1. Characterization of Nanofluid (DP9711) and Calcite Mineral Powder [CaCO₃]

The characterization of Nano fluid is essential to ensure its stability over the range of temperatures and salinity in which the experiments are performed. The following tables summarize zeta potential measurements for both calcite $CaCO_3$ and DP 9711 in addition to average Nano particles diameter distribution "z average" over range of temperatures and concentrations.

Table 4.1 Calcite Zeta Potential and pH

Calcite in DIW Zeta Potential & pH @ 25 °C		
Conc. (g/l)	ZP (mv)	pH
1	54.31	9.11
10	-0.29	10.13
20	-0.8	10.07

Table 4.2 Nano Particles Zeta Potential in Different Mediums

DP 1 (g/l) Zeta Potential @ 25 °C	
ZP (mv)	Medium
-33	DIW
-13	LSW
-6	SSW

Table 4.3 pH for Diluted DP at 1 & 2 (g/l) in DIW and 1 (g/l) in LSW @ 25°C

DP pH @ 25 °C		
Conc. (g/l)	Medium	pH
1	LSW	7.16
1	DIW	6.01
2	DIW	5.68

Table 4.4 Z- average for Nano Particles at different temperatures in DIW, LSW, SSW and at different concentrations in DIW

DP conc. (g/l)	Medium	T°C	Z-Avg (nm)	PdI
	DIW	25	37.52	0.09
		50	38.57	0.078
		79.9	39.40	0.083
1	LSW	25	37.91	0.067
		50	38.18	0.056
		80	38.70	0.045
	SSW	25	56.35	0.105
		50	57.54	0.11
		80	88.11	0.104
2	DIW	25	36.95	0.077
4		25	35.29	0.106

Table (5.1) shows that Calcite has positive zeta potential at 1 (g/l) and it approaches zero with increasing the concentration up to 10 times. The maximum concentration of Calcite used throughout the experiments is around 5.5 (g/l), which is still in the positive region of zeta potential. pH increases with increasing the concentration of Calcite. Table (5.2) describes zeta potential of DP at 1 (g/l), which is negative in DIW, LSW, and SSW. Increasing the ionic strength of the medium, leads to compression of the double layer length (Debye length) and a decrease in the absolute value of zeta potential [28]. Salinity and pH play opposite role on zeta potential in silica systems. Increasing the salinity reduces the zeta potential absolute value, while higher pH is an indication of predominant electrostatic repulsion between silica nano particles and leads to higher zeta potential. From table (5.3) it is obvious that pH decreases with the increase in DP concentration. However, table (5.4) explicitly shows that the average size distribution of the silica Nano particles in DIW is approximately constant at 1, 2, and 4 (g/l) dilutions. The effect of temperature on Z-Avg is negligible in DIW and LSW. However, Z-Avg is sensitive to elevated temperatures in SSW, which is attributed to the increase of the ionic strength of the medium and the increase in TDS. At high temperature the Brownian motion of NPs will increase and in SSW which has higher ionic strength than DIW and LSW and more TDS, the collisions between the particles become more significant and NPs start to become more prone to aggregation.

PdI in table (5.4) refers to the poly dispersity index of the sample, which is a dimensionless variable derived from the cumultant analysis and defines the range where the Z-Avg measurements are representable for the sample. According to ISO standard documents 13321 : 1996 E and ISO 22412 : 2008, DLS measurements are representable in the following range: $0.05 < PdI < 0.7$ [29].

4.2. Static Adsorption Experiments

This section will be devoted for presenting the data obtained from series of experiments investigating the adsorption of silica nanoparticles DP9711, on the surface of quartz, calcite, and kaolinite minerals. These experiments consist of four main sets; two sets conducted in DIW and the other two sets were conducted in SSW. Each set is aimed to investigate the adsorption that takes place on the mineral surface at different concentration ratio between the mineral and the nanoparticles. The first set is a constant mass experiment, where equal amount of each mineral is used in each test tube at 5 g/l concentration and mixed with different concentration of silica nanoparticles; 0.5, and 1 g/l respectively. The second set utilizes a constant surface area for all minerals to be mixed at different concentrations and then added to silica Nano particles at 0.5, and 1 g/l respectively. In all the experiments conducted, the suspension of silica Nano particles can come to thermodynamic equilibrium with the mineral solution by leaving each sample tube on rotation at 40 rpm for 24 hours. The motivation behind this part of experiments is to attempt explaining the behavior of silica nanoparticles with different mineral surfaces and try to understand the forces acting in place as well as comparing the adsorption potential that occurs on minerals' surfaces in DIW and SSW medium respectively.

4.2.1. Constant Mass Adsorption Experiment in DIW

Studying the adsorption of NP (DP) of two concentrations; 0.5 & 1 (g/l) on 5 (g/l) mineral concentration of; Quartz, Kaolinite, & Calcite. An amount of 0.15 (g) of mineral was added to 30 (ml) sample tubes for each mineral in 0.5 & 1 (g/l) concentration of NP (DP) liquid for 10:1 and 5:1 ratio of mineral to NP (DP) respectively. The concentration of NP in (DP) liquid used was calibrated at different concentration in DIW by using the (UV-Abs) at 240 nm wavelength and straight line was achieved of slope equal to 0.1294. Baseline correction for abs readings was taken for all the minerals' traces still present in DIW without DP. After that, those readings were subtracted from the abs readings of each corresponding mineral with DP in DIW and NP concentration corrected for residual minerals was achieved for all the samples. Finally, specific adsorption (mg NP (DP)/m^2 mineral) and (mg NP (DP)/g mineral) were plotted against the concentration of the NP (DP) liquid of 0.5 and 1 (g/l) for each mineral for comparison.

The following table shows the abs values used for calibration at 240 nm wavelength obtained from the UV at two different concentrations of the DP in DIW.

Table 4.5 Calibration Line for Constant Mass Experiment in DIW

DP conc. (g/l)	Abs
0	0
0.1	0.0143
1	0.1293

The calibration line is plotted below; DP concentration values on the abscissa in grams per liter, and abs values on the ordinate. Linear regression best fit is obtained with a slope "S" = 0.1294 and coefficient of determination value "R^2" = 0.9998.
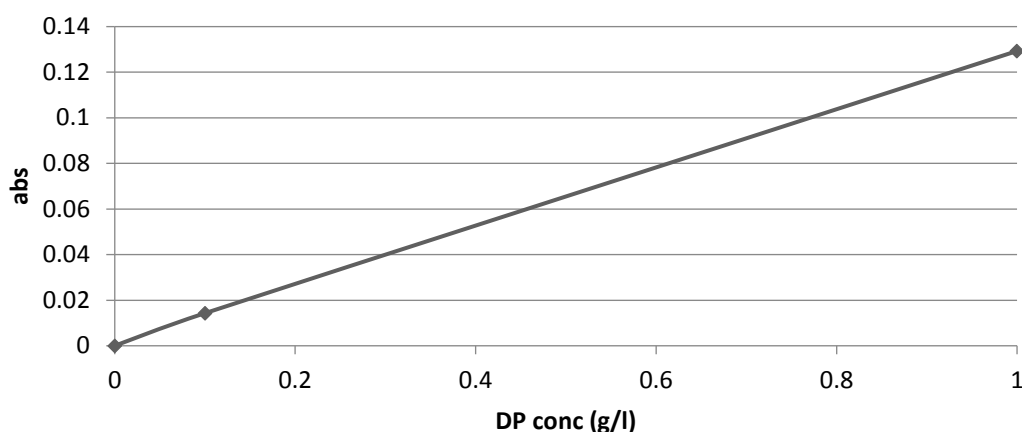
Plot 4.1 Calibration Line for Constant Mass Experiment in DIW

The following tables summarize the abs values and specific adsorption calculated for the three minerals – Quartz, Kaolinite, and calcite - used in the experiment with constant mass in two different concentrations of DP; 0.5 and 1 (g/l).

Table 4.6 UV Abs Readings for Constant Mass Experiment in DIW

Powder	Abs DP (1 g/l)	Abs DP (0.5 g/l)	Abs correction	Surface area (m^2/g)
Quartz	0.1034	0.0626	0.0049	0.65
Kaolinite	0.1155	0.0607	0.0057	9.95
Calcite	0.0895	0.0481	0.0035	0.23

Table 4.7 Specific Adsorption on Quartz

				Quartz		
NP (g/l)	Abs	Abs corr.	NP new (g/l)	NP adsorbed (mg)	Specific adsorption (mg NP/m^2) mineral	Specific adsorption (mg NP/g) mineral
0.5	0.07	0.06	0.47	1.02	10.46	6.80
1	0.1	0.09	0.76	7.16	73.48	47.76

Table 4.8 Specific Adsorption on Kaolinite

				Kaolinite		
NP (g/l)	Abs	Abs corr.	NP new (g/l)	NP adsorbed (mg)	Specific adsorption (mg NP/m^2) mineral	Specific adsorption (mg NP/g) mineral
0.5	0.06	0.06	0.43	2.25	1.51	14.99
1	0.12	0.11	0.85	4.54	3.04	30.29

Table 4.9 Specific Adsorption on Calcite

					Calcite	
NP (g/l)	Abs	Abs corr.	NP new (g/l)	NP adsorbed (mg)	Specific adsorption (mg NP/m^2) mineral	Specific adsorption (mg NP/g) mineral
0.5	0.05	0.04	0.34	4.66	135.07	31.07
1	0.09	0.09	0.66	10.06	291.65	67.08

The slope obtained from the calibration line is used to obtain the concentration values corresponding to each "Abs corr." reading obtained by subtracting the baseline correction values.

$$NP\ new\ conc.(g/l) = \frac{Abs\ corr.}{Slope} \tag{5.1}$$

The amount of NP adsorbed in milligrams on the mineral surface is the difference between the initial concentration and the new concentration calculated.

$$NP\ adsorbed = \frac{NP\left(\frac{g}{l}\right) - NP\ new\ \left(\frac{g}{l}\right)}{1000\ \left(\frac{ml}{l}\right)} \times sample\ volume\ (ml) \times 1000\ \left(\frac{mg}{g}\right) \tag{5.2}$$

Specific adsorption per unit surface area of mineral (m^2) is the amount of NP in milligrams adsorbed divided by the average total surface area of the mineral, while the specific adsorption per unit mass of mineral is calculated by dividing over the mass of mineral.

$$specific\ adsorption(\frac{mg\ NP}{m^2}) = \frac{NP\ adsorped\ (mg)}{mass\ of\ mineral\ (g) \times specific\ surface\ area\ (\frac{m^2}{g})} \tag{5.3}$$

$$specific\ adsorption\ (\frac{mg\ NP}{g}) = \frac{NP\ adsorped\ (mg)}{mass\ of\ mineral\ (g)} \tag{5.4}$$

The following plots compare the specific adsorption values for Quartz, Kaolinite, and Calcite for constant mass experiment in DIW. The first plot is a semi-log plot, where the specific adsorption per unit surface area (m^2) is in logarithmic scale on the ordinate and NP concentration in (g/l) is on the abscissa at 0.5 and 1 (g\l) respectively. The second plot has the specific adsorption per unit mass (g) for each mineral on the ordinate and NP concentration in (g/l) is on the abscissa at 0.5 and 1 (g\l) respectively.

quartz	kaolinite	calcite

NP concentration g/l	0.5	1
quartz	10.46	73.47521103
kaolinite	1.51	3.04
calcite	135.07	291.65

Plot 4.2 Specific adsorption per unit surface area of mineral (m^2) for constant mass in DIW

quartz	kaolinite	calcite

NP concentration g/l	0.5	1
quartz	6.80	47.75888717
kaolinite	14.99	30.29
calcite	31.07	67.08
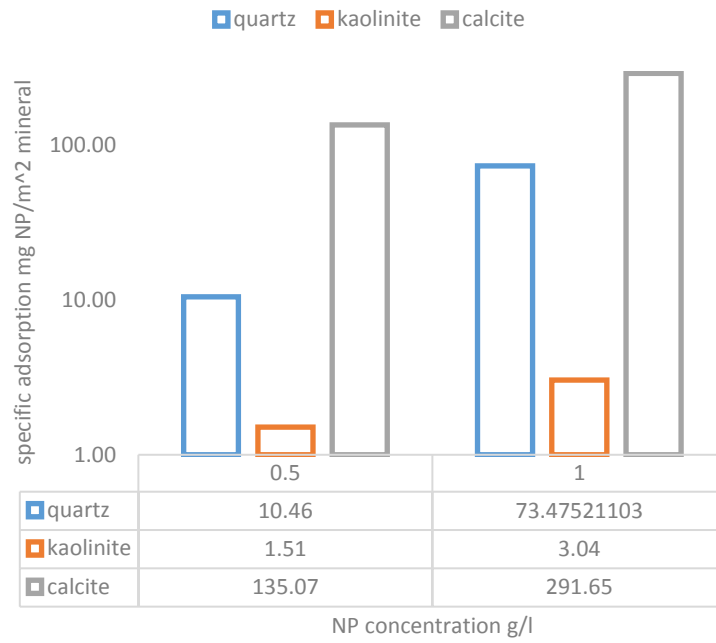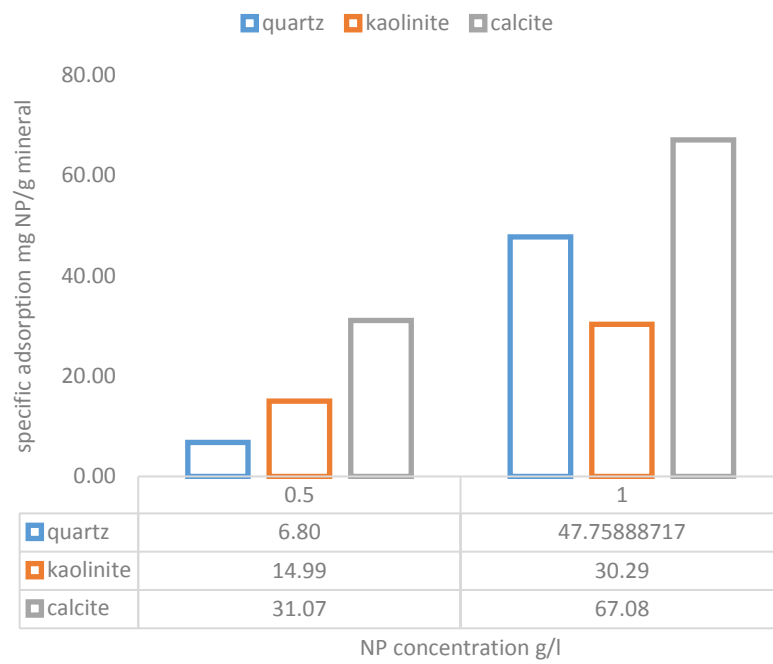
Plot 4.3 Specific adsorption per unit mass of mineral (g) for constant mass in DIW

From the presentation above, specific adsorption in calcite [CaCO$_3$] shows higher values than Quartz [SiO$_2$] and Kaolinite [Al$_2$Si$_2$O$_5$(OH)$_4$] when reported in both two units; milligram of NP per meter square of mineral surface and milligram of NP per gram of mineral, which is also confirmed by scanning electron microscopy "SEM" images taken for a chalk specimen that will be presented later. The reason is mainly attributed to the interaction forces between the negatively charged silica nanoparticles and the positively charged chalk, which is mainly calcium carbonate CaCO$_3$. These forces allow for more NP to deposit on the mineral surface of Calcite and adsorb. Specific adsorption values per unit surface area of calcite are around four times larger than the adsorption values calculated for unit mass. This is due to the small specific area of Calcite (0.23 m^2/g - *approx.*$\frac{1}{4}$). The specific adsorption for Calcite at 1 (g/l) of NP is almost two times the value at 0.5 (g/l) of NP, which indicates a linear relationship for constant mass of the mineral against NP concentration as shown below.
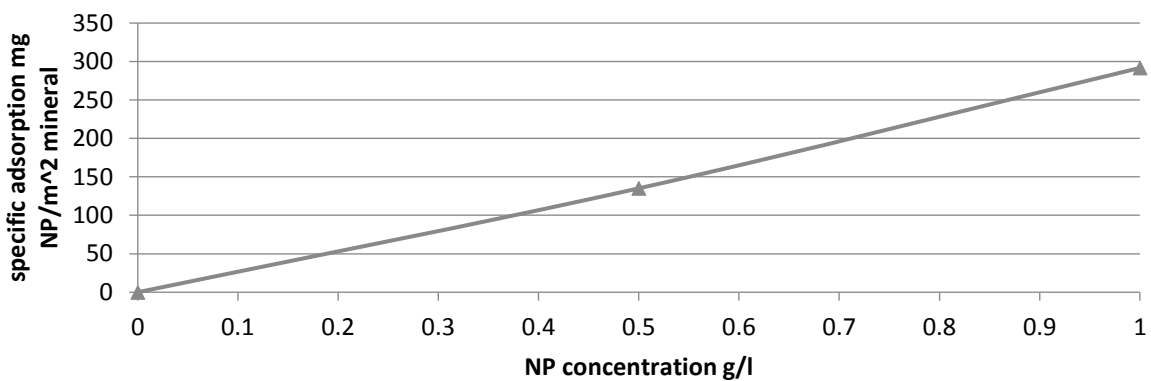
Plot 4.4 Specific adsorption per unit surface area of Calcite in DIW.

$$Specific\ adsorption\ on\ Calcite\ \left(\frac{mg\ NP}{m^2}\right) = 287.35 \times NP\ conc.\left(\frac{g}{l}\right) \quad (5.5)$$
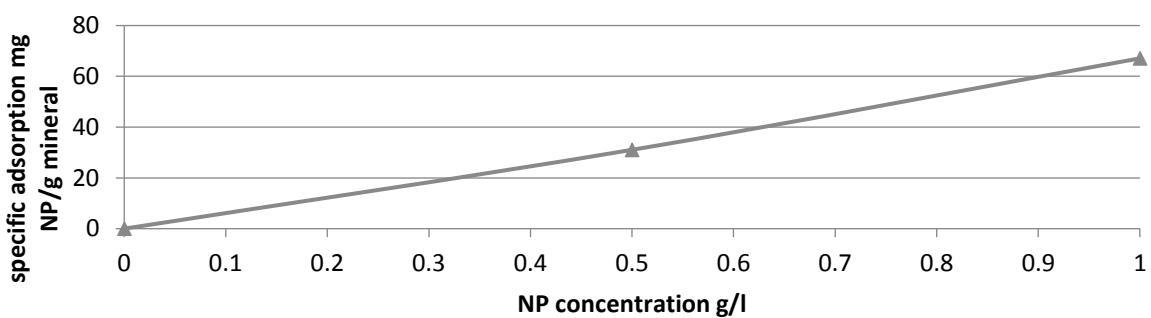
Plot 4.5 Specific adsorption per unit mass of Calcite in DIW.

$$Specific\ adsorption\ on\ Calcite\ \left(\frac{mg\ NP}{g}\right) = 66.09 \times NP\ conc.\left(\frac{g}{l}\right) \quad (5.6)$$

4.2.2. Constant Mass Adsorption Experiment in SSW

Studying the adsorption of NP (DP) of two concentrations; 0.5 & 1 (g/l) on 5 (g/l) mineral concentration of; Quartz, Kaolinite, & Calcite in SSW. This experiment follows the same procedures that have been done in DIW constant mass experiment. The following table shows the abs values used for calibration at 240 nm wavelength obtained from the UV at two different concentrations of the DP in SSW.

Table 4.10 Calibration Line for Constant Mass Experiment in SSW

DP conc. (g/l)	Abs
0	0
0.5	0.0558
1	0.1191

The calibration line is plotted below; DP concentration values on the abscissa in grams per liter, and abs values on the ordinate. Linear regression best fit is obtained with a slope "S" = 0.1176 and coefficient of determination value "R^2" = 0.9984.
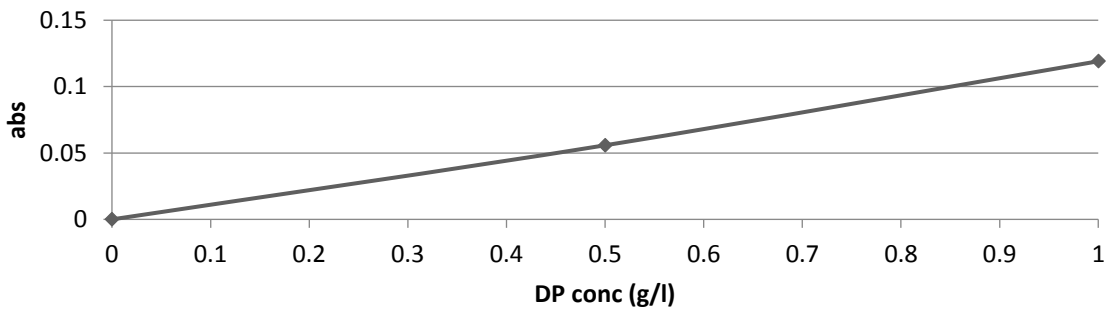
Plot 4.6 Calibration Line for Constant Mass Experiment in SSW

The following tables summarize the abs values and specific adsorption calculated for the three minerals – Quartz, Kaolinite, and calcite - used in the experiment with constant mass in two different concentrations of DP; 0.5 and 1 (g/l).

Table 4.11 UV Abs Readings for Constant Mass Experiment in SSW

Powder	Abs DP (1 g/l)	Abs DP (0.5 g/l)	Abs correction	Surface area (m^2/g)
Quartz	0.0802	0.0433	0.0186	0.65
Kaolinite	0.0784	0.0386	0.0143	9.95
Calcite	0.0867	0.0474	0.0156	0.23

Table 4.12 Specific Adsorption on Quartz

Quartz						
NP (g/l)	Abs	Abs corr.	NP new (g/l)	NP adsorbed (mg)	Specific adsorption (mg NP/m^2) mineral	Specific adsorption (mg NP/g) mineral
0.5	0.04	0.02	0.21	8.70	89.22	57.99
1	0.08	0.06	0.52	14.29	146.52	95.24

Table 4.13 Specific Adsorption on Kaolinite

Kaolinite						
NP (g/l)	Abs	Abs corr.	NP new (g/l)	NP adsorbed (mg)	Specific adsorption (mg NP/m^2) mineral	Specific adsorption (mg NP/g) mineral
0.5	0.04	0.02	0.21	8.80	5.90	58.67
1	0.08	0.06	0.55	13.65	9.14	90.99

Table 4.14 Specific Adsorption on Calcite

Calcite						
NP (g/l)	Abs	Abs corr.	NP new (g/l)	NP adsorbed (mg)	Specific adsorption (mg NP/m^2) mineral	Specific adsorption (mg NP/g) mineral
0.5	0.05	0.03	0.27	6.89	199.65	45.92
1	0.09	0.07	0.60	11.86	343.83	79.08

The following plots compare the specific adsorption values for Quartz, Kaolinite, and Calcite for constant mass experiment in SSW. The first plot is a semi-log plot, where the specific adsorption per unit surface area (m^2) is in logarithmic scale on the ordinate and NP concentration in (g/l) is on the abscissa at 0.5 and 1 (g\l) respectively. The second plot has the specific adsorption per unit mass (g) for each mineral on the ordinate and NP concentration in (g/l) is on the abscissa at 0.5 and 1 (g\l) respectively.

NP concentration (g/l)	0.5	1
quartz	89.22	146.52
kaolinite	5.90	9.14
calcite	0	199.65
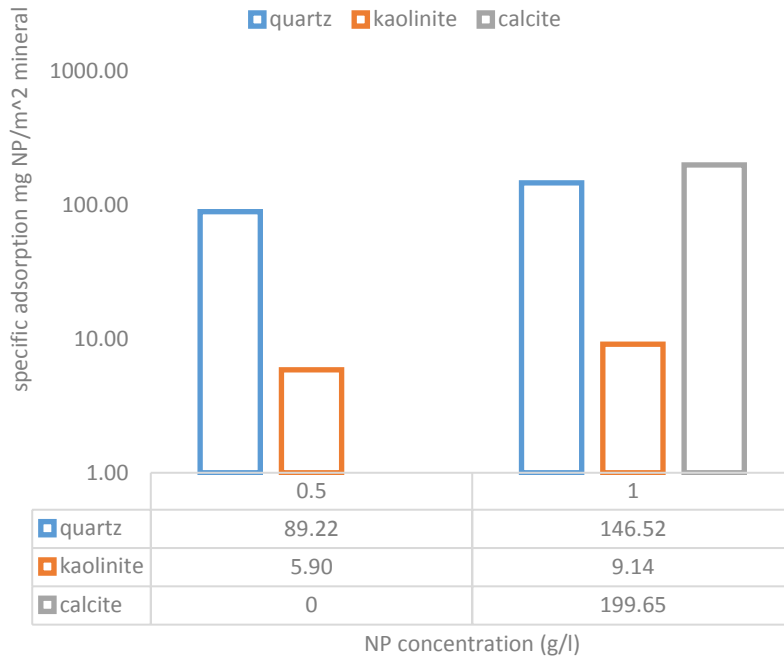
Plot 4.7 Specific adsorption per unit surface area of mineral (m^2) for constant mass in SSW

NP concentration (g/l)	0.5	1
quartz	57.99	95.24
kaolinite	58.67	90.99
calcite	0	45.92
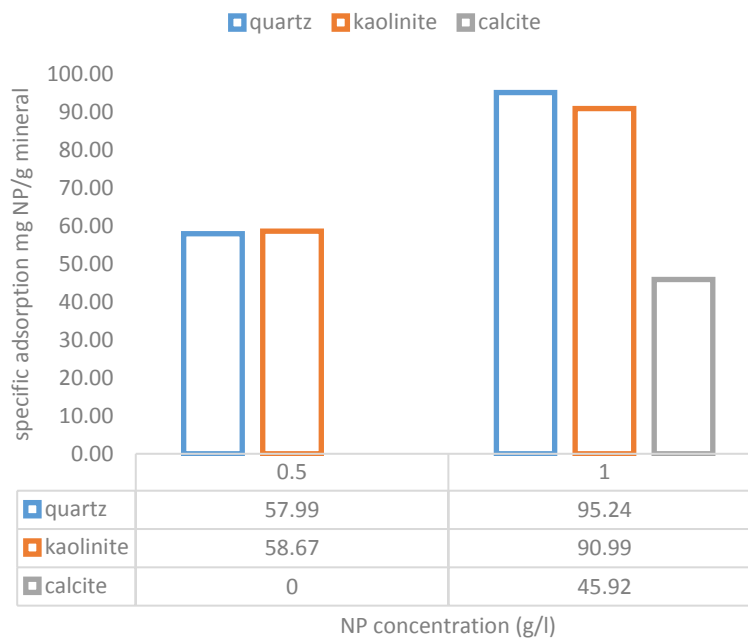
Plot 4.8 Specific adsorption per unit surface area of mineral in SSW

Specific adsorption per unit surface area values are the highest for Calcite in SSW, however for specific adsorption per unit mass of mineral values they are the lowest for Calicte in SSW. Although, the same amount of minerals is used for all three minerals; Quartz, Kaolinite, and Calcite, the average surface area will differ at 0.15 gram for each mineral. Since Calcite has the smallest surface area per unit mass out of the three minerals, the average surface area of 0.15 gram of Calcite will be smaller than the other two minerals. Comparing tables (5.10) and (5.15),

30

shows that specific adsorption of NPs slightly improve in SSW at the same concentration of 5 g/l for the mineral against 0.5 and 1 g/l of DP respectively. The following plots show the linear agreement of specific adsorption on Calcite surface per unit surface area and per unit mass of the mineral respectively versus NP concentration.
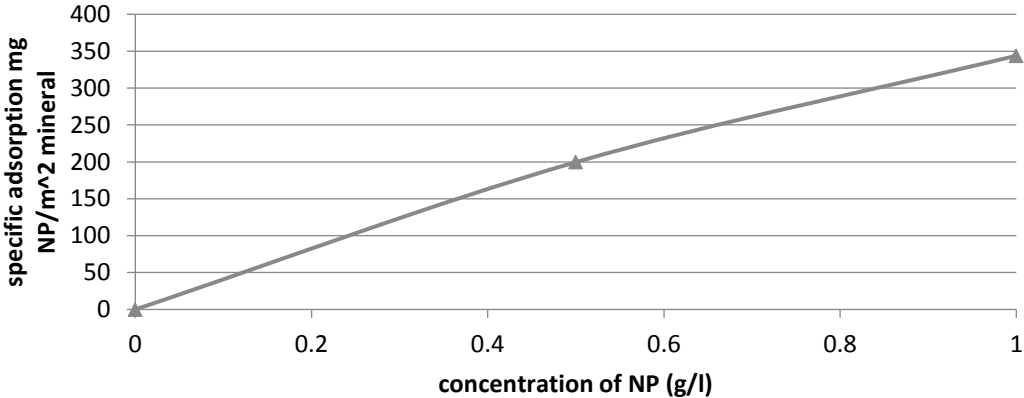
Plot 4.9 Specific adsorption per unit surface area of Calcite in SSW

.

$$Specific\ adsorption\ on\ Calcite\ \left(\frac{mg\ NP}{m^2}\right) = 354.92 \times NP\ conc.\left(\frac{g}{l}\right) \quad (5.7)$$
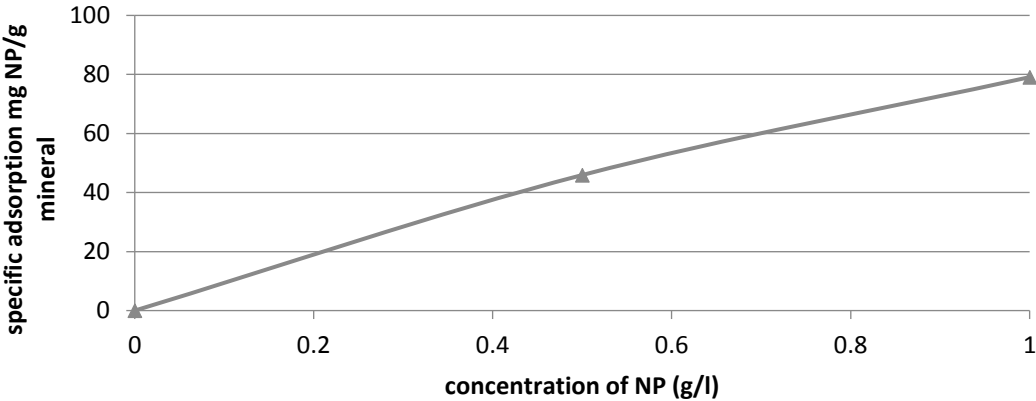
Plot 4.10 Specific adsorption per unit mass of Calcite in SSW.

$$Specific\ adsorption\ on\ Calcite\ \left(\frac{mg\ NP}{g}\right) = 81.633 \times NP\ conc.\left(\frac{g}{l}\right) \quad (5.8)$$

4.2.3. Constant Surface Area Adsorption Experiments in DIW

Specific adsorption per unit surface area of minerals has been tested at constant surface area for, Quartz, Kaolinite, and Calcite in DIW. The motivation behind these experiments were to identify the role of active surface area in static adsorption and to compare the activity of the surface area of the three minerals as well as obtain more points on static adsorption curves for different minerals.

The mineral concentration is varied to reach constant surface area of 0.038 m^2. The weight used of each mineral; 0.058, 0.0038, and 0.164 gram of Quartz, Kaolinite, and Calcite corresponds to 1.9, 0.127, and 5.47 grams per liter respectively. Each mineral is mixed with 1 and 0.5 gram per liter of DP. The following table summarizes the quantity of minerals used and the mineral to NP mass ratio.

Table 4.15 Mineral to NP mass ratio

Mineral	Mass ratio (Mineral to NP)	DP conc. (g/l)
Quartz	3.85: 1	0.5
	1.923: 1	1
Kaolinite	0.251: 1	0.5
	0.127: 1	1
Calcite	10.87: 1	0.5
	5.47: 1	1

The following table shows the abs values used for calibration at 240 nm wavelength obtained from the UV at two different concentrations of the DP in DIW.

Table 4.16 Calibration line of DP liquid for CSA experiments in DIW

DP conc. (g/l)	Abs
0	0
0.5	0.081
1	0.1635

The calibration line is plotted below; DP concentration values on the abscissa in grams per liter, and abs values on the ordinate. Linear regression best fit is obtained with a slope "S" = 0.1632 and coefficient of determination value "R^2" = 1.
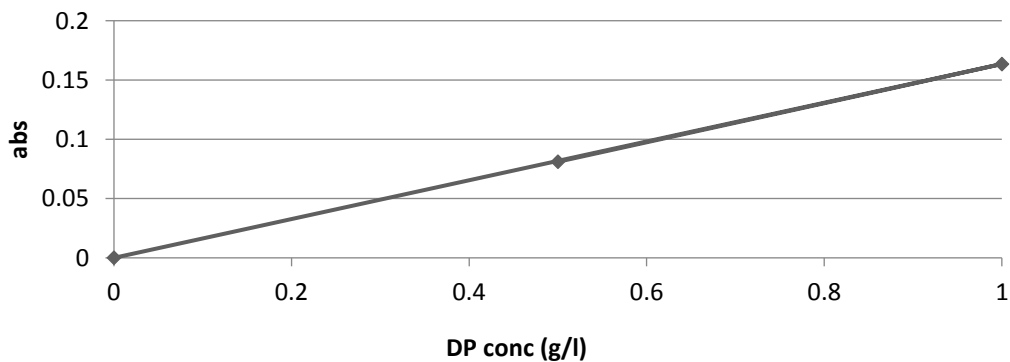
Plot 4.11 Calibration line for CSA in DIW

The following tables summarize the abs values and specific adsorption calculated for the three minerals – Quartz, Kaolinite, and calcite - used in the experiment with constant surface area in two different concentrations of DP; 0.5 and 1 (g/l).

Table 4.17 UV Abs Readings for CSA Experiment in DIW

Powder	Abs DP (1 g/l)	Abs DP (0.5 g/l)	Abs correction	Surface area (m^2/g)	Avg. Surface area (m^2)
Quartz	0.1198	0.0708	0.0067	0.65	0.0377
Kaolinite	0.1317	0.0702	0.0057	9.95	0.03781
Calcite	0.119	0.0593	0.0055	0.23	0.03772

Table 4.18 Specific Adsorption on Quartz

				Quartz		
NP (g/l)	Abs	Abs corr.	NP new (g/l)	NP adsorbed (mg)	Specific adsorption (mg NP/m^2) mineral	Specific adsorption (mg NP/g) mineral
0.5	0.07	0.06	0.39	3.21	85.15	55.35
1	0.12	0.11	0.69	9.21	244.29	158.79

Table 4.19 Specific Adsorption on Kaolinite

				Kaolinite		
NP (g/l)	Abs	Abs corr.	NP new (g/l)	NP adsorbed (mg)	Specific adsorption (mg NP/m^2) mineral	Specific adsorption (mg NP/g) mineral
0.5	0.07	0.06	0.40	3.14	83.14	827.21
1	0.13	0.13	0.77	6.84	180.86	1799.54

Table 4.20 Specific Adsorption on Calcite

				Calcite		
NP (g/l)	Abs	Abs corr.	NP new (g/l)	NP adsorbed (mg)	Specific adsorption (mg NP/m^2) mineral	Specific adsorption (mg NP/g) mineral
0.5	0.06	0.05	0.33	5.11	135.48	31.16
1	0.12	0.11	0.70	9.14	242.21	55.71

The following plots show the specific adsorption per unit surface area and per unit mass of mineral for constant surface area of the three minerals. The first plot reports the specific adsorption in milligrams of NP per meter square of the mineral and the concentration of NP in grams per liter on the abscissa. The second plot is semi-log plot, where the specific adsorption in milligrams of NP per gram of mineral is on the ordinate reported in logarithmic scale.
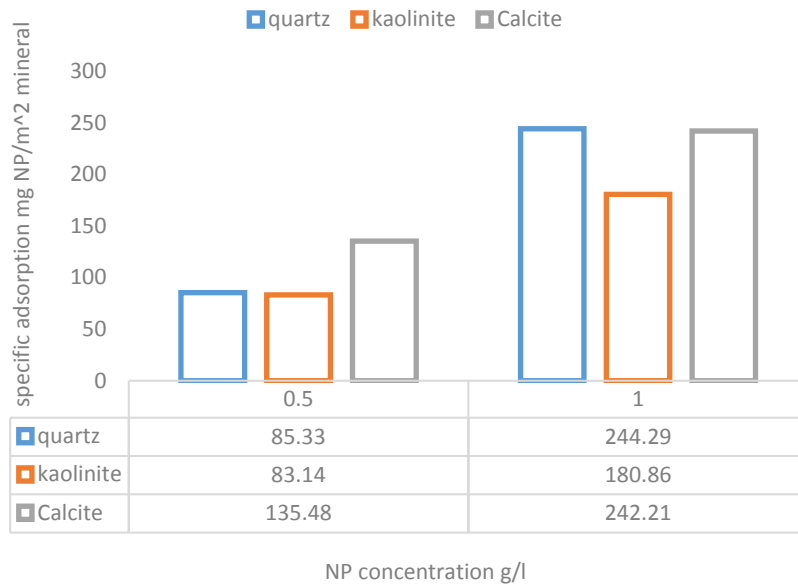
Plot 4.12 Specific adsorption per unit surface area of mineral (m^2) for CSA in DIW

	0.5	1
quartz	85.33	244.29
kaolinite	83.14	180.86
Calcite	135.48	242.21

NP concentration g/l
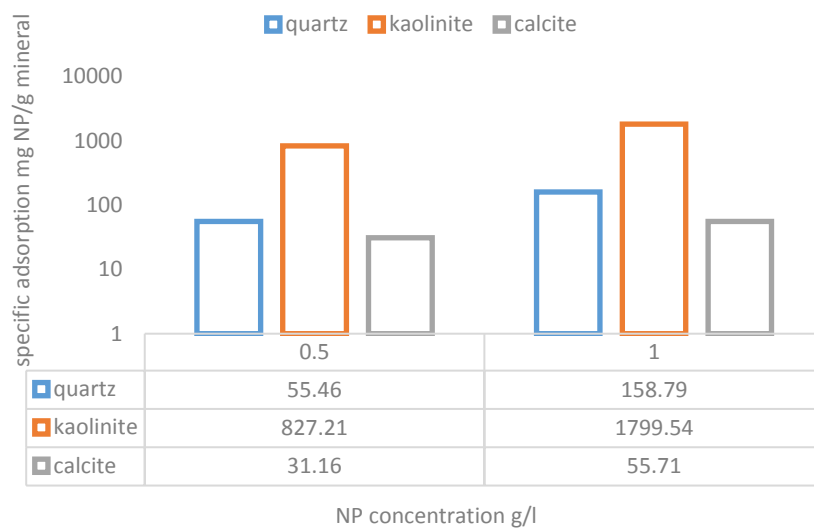
Plot 4.13 Specific adsorption per unit mass of mineral (g) for CSA in DIW

	0.5	1
quartz	55.46	158.79
kaolinite	827.21	1799.54
calcite	31.16	55.71

NP concentration g/l

Calcite shows higher specific adsorption per unit surface area for NPs at 0.5 (g/l) concentration of DP liquid, while it has almost the same value as quartz at 1 (g/l) DP concentration as shown in plot (5.12). Since Calcite has the lowest surface area (m²/g), the amount of mineral weight added to reach an average total surface area of 0.038 m² is the largest among the other two minerals. Hence, Calcite concentration and mineral to NP ratio is greater than Quartz and greater than Kaolinite as shown in table (5-11). The following plots describe the specific adsorption for Calcite in $\frac{mg}{m^2}$ and $\frac{mg}{g}$.

Plot 4.14 Specific adsorption per unit surface area on Calcite for CSA experiment in DIW

$$Specific\ adsorption\ on\ Calcite\ \left(\frac{mg\ NP}{m^2}\right) = 247.96 \times NP\ conc.\left(\frac{g}{l}\right) \quad (5.9)$$
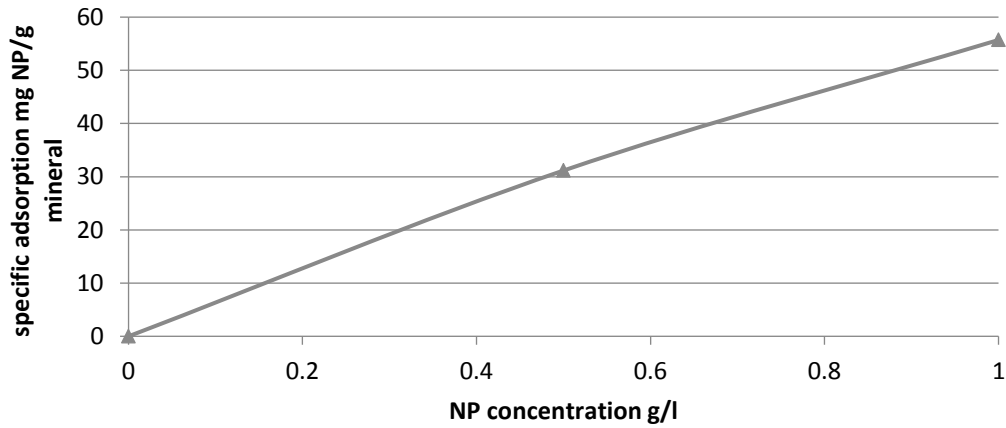
Plot 4.15 Specific adsorption per unit mass on Calcite for CSA experiment in DIW

$$Specific\ adsorption\ on\ Calcite\ \left(\frac{mg\ NP}{g}\right) = 57.03 \times NP\ conc.\left(\frac{g}{l}\right) \quad (5.10)$$

4.2.4. **Constant Surface Area Adsorption Experiment in SSW**

The same adsorption experiment is repeated by mixing the minerals in SSW instead of DIW. The mineral concentration is varied to reach constant surface area of 0.038 m^2. The weight used of each mineral; 0.058, 0.0038, and 0.164 gram of Quartz, Kaolinite, and Calcite corresponds to 1.9, 0.127, and 5.47 grams per liter respectively. Each mineral is mixed with 1 and 0.5 gram per liter of DP. The following table summarizes the quantity of minerals used and the mineral to NP mass ratio.

*Table 4.21 Mineral to NP mass ratio*

Mineral	Mass ratio (Mineral to NP)	DP conc. (g/l)
Quartz	3.85: 1	0.5
	1.923: 1	1
Kaolinite	0.251: 1	0.5
	0.127: 1	1
Calcite	10.87: 1	0.5
	5.47: 1	1

The following table shows the abs values used for calibration at 240 nm wavelength obtained from the UV at two different concentrations of the DP in DIW.

Table 4.22 Calibration line of DP liquid for CSA experiments in SSW

DP conc. (g/l)	Abs
0	0
0.5	0.0558
1	0.1191

The calibration line is plotted below; DP concentration values on the abscissa in grams per liter, and abs values on the ordinate. Linear regression best fit is obtained with a slope "S" = 0.1176 and coefficient of determination value "R^2" = 0.9984.
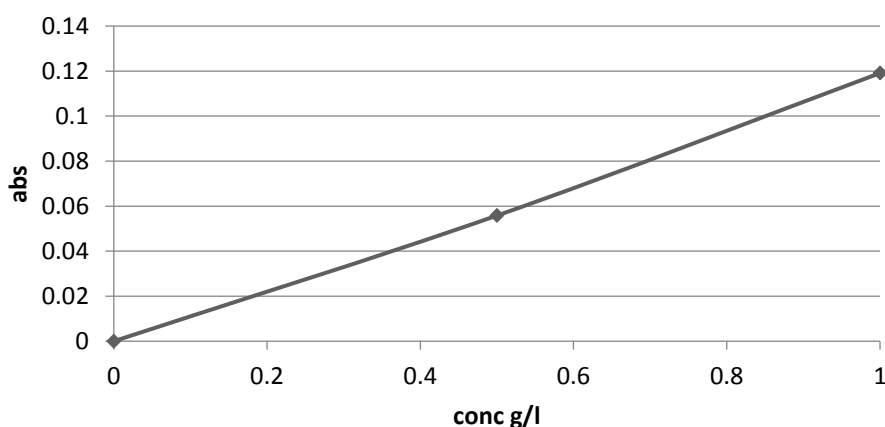
Plot 4.16 Calibration line for CSA in SSW

The following tables summarize the abs values and specific adsorption calculated for the three minerals – Quartz, Kaolinite, and calcite - used in the experiment with constant surface area in two different concentrations of DP; 0.5 and 1 (g/l).

Table 4.23 UV Abs Readings for CSA Experiment in SSW

Powder	Abs DP (1 g/l)	Abs DP (0.5 g/l)	Abs correction	Surface area (m^2/g)	Avg. Surface area (m^2)
Quartz	0.0811	0.0376	0.0077	0.65	0.0377
Kaolinite	0.0669	0.0263	0.0057	9.95	0.03781
Calcite	0.074	0.0328	0.0115	0.23	0.03772

Table 4.24 Specific Adsorption on Quartz

				Quartz		
NP (g/l)	Abs	Abs corr.	NP new (g/l)	NP adsorbed (mg)	Specific adsorption (mg NP/m^2) mineral	Specific adsorption (mg NP/g) mineral
0.5	0.04	0.03	0.25	7.37	195.56	127.11
1	0.08	0.07	0.62	11.28	299.09	194.41

Table 4.25 Specific Adsorption on Kaolinite

				Kaolinite		
NP (g/l)	Abs	Abs corr.	NP new (g/l)	NP adsorbed (mg)	Specific adsorption (mg NP/m^2) mineral	Specific adsorption (mg NP/g) mineral
0.5	0.03	0.02	0.18	9.74	257.73	2564.45
1	0.07	0.06	0.52	14.39	380.53	3786.25

Table 4.26 Specific Adsorption on Calcite

				Calcite		
NP (g/l)	Abs	Abs corr.	NP new (g/l)	NP adsorbed (mg)	Specific adsorption (mg NP/m^2) mineral	Specific adsorption (mg NP/g) mineral
0.5	0.03	0.02	0.18	9.57	253.61	58.33
1	0.07	0.06	0.53	14.06	372.64	85.71

The following plots show the specific adsorption per unit surface area and per unit mass of mineral for constant surface area of the three minerals. The first plot reports the specific adsorption in milligrams of NP per meter square of the mineral and the concentration of NP in grams per liter on the abscissa. The second plot is semi-log plot, where the specific adsorption in milligrams of NP per gram of mineral is on the ordinate reported in logarithmic scale.
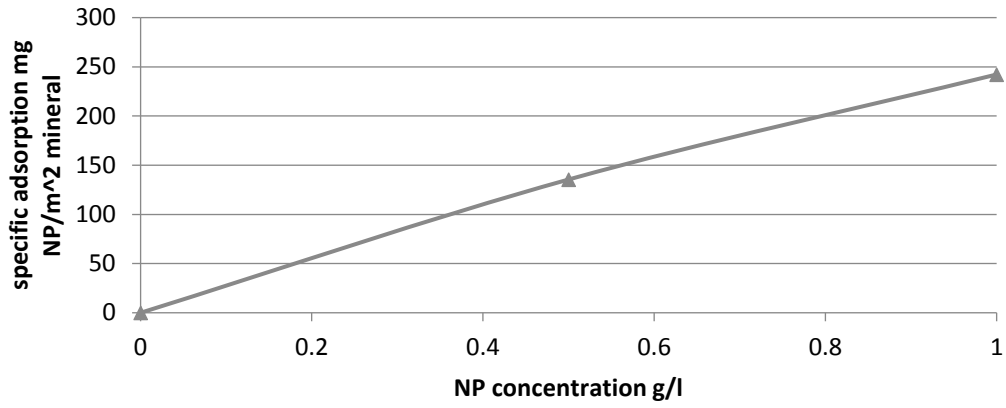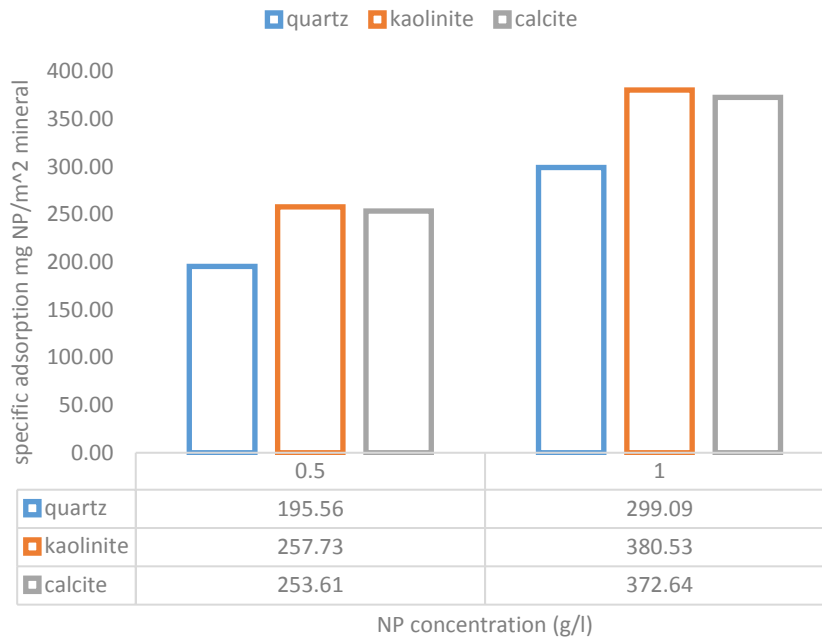
Plot 4.17 Specific adsorption per unit surface area of mineral (m^2) for CSA in SSW

	quartz	kaolinite	calcite
0.5	195.56	257.73	253.61
1	299.09	380.53	372.64
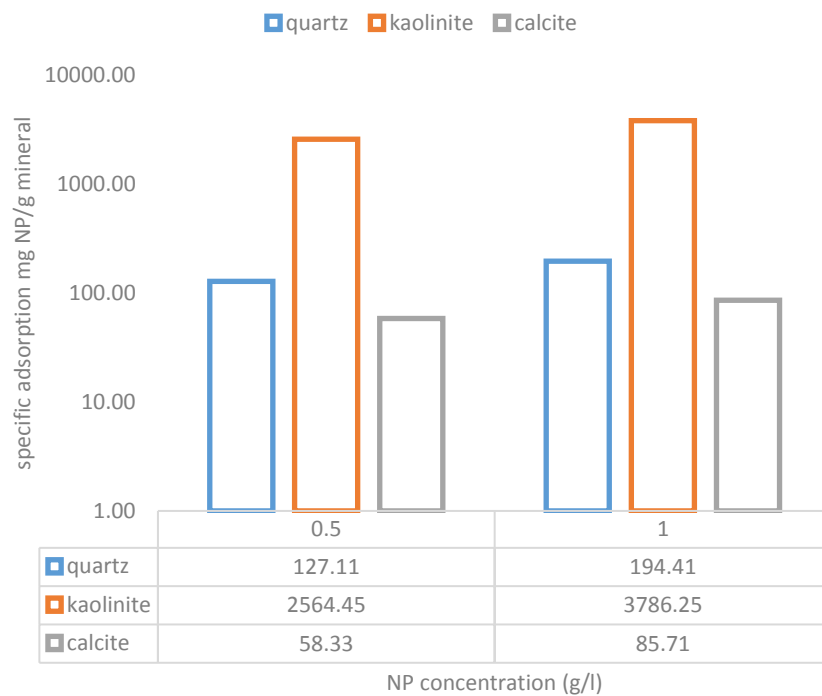
Plot 4.18 Specific adsorption per unit mass of mineral (g) for CSA in SSW

	quartz	kaolinite	calcite
0.5	127.11	2564.45	58.33
1	194.41	3786.25	85.71

From plots (5.17) and (5.18), the specific adsorption values on Kaolinite is the highest. However, specific adsorption values on Calcite per unit surface area are almost the same as Kaolinite. The following plots describe the specific adsorption for Calcite in $\frac{mg}{m^2}$ and $\frac{mg}{g}$.
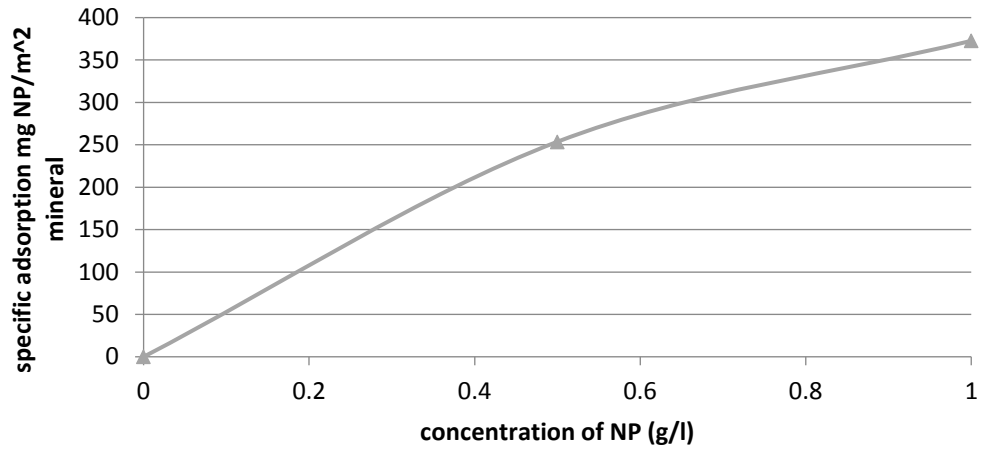
Plot 4.19 Specific adsorption per unit surface area on Calcite for CSA experiment in SSW

$$Specific\ adsorption\ on\ Calcite\ \left(\frac{mg\ NP}{m^2}\right) =$$
$$-110.91 \times NP\ conc.\left(\frac{g}{l}\right)^2 + 454.75 \times NP\ conc.\left(\frac{g}{l}\right) \tag{5.11}$$
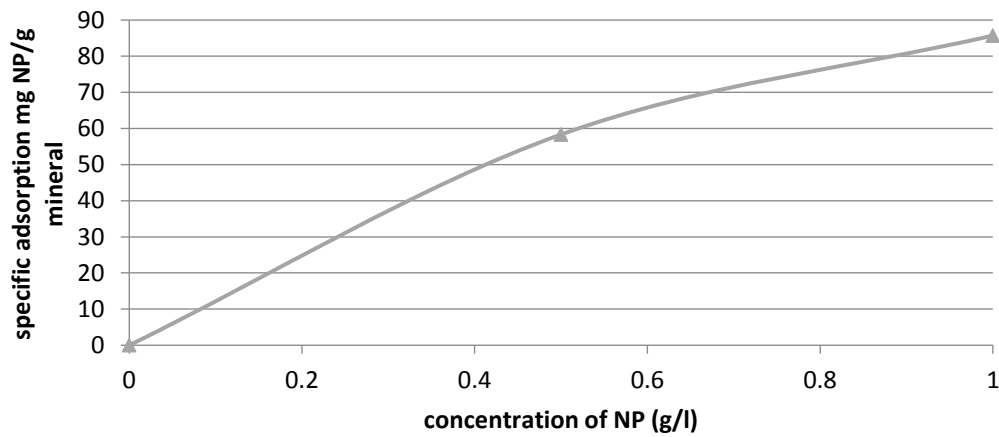
Plot 4.20 Specific adsorption per unit mass on Calcite for CSA experiment in SSW

$$Specific\ adsorption\ on\ Calcite\ \left(\frac{mg\ NP}{m^2}\right) =$$
$$-25.51 \times NP\ conc.\left(\frac{g}{l}\right)^2 + 104.59 \times NP\ conc.\left(\frac{g}{l}\right) \tag{5.12}$$

4.2.5. Specific Adsorption on Calcite Analysis

Specific adsorption, reported in both $\frac{mg\ NP}{m^2\ mineral\ surface}$ and $\frac{mg\ NP}{g\ mineral}$, on Calcite mineral at different concentration ratios of mineral to Nano-fluid is presented on the following plots, which combine the results from CSA and CM experiments in DIW and SSW respectively. More points of mineral concentration at 1 (g/l) and 3 (g/l) against 1 (g/l) of the Nano-fluid are measured and plotted on Calcite specific adsorption curve. The tables below summarize specific adsorption results for Calcite from DIW and SSW experiments.

Table 4.27 Specific Adsorption on Calcite in DIW

Mass ratio (NP to Calcite)	DP conc. (g/l)	Specific Adsorption (mg/m2)	Specific Adsorption (mg/g)
1.00	1	1736.23	399.33
0.33	1	585.51	134.67
0.20	1	291.65	67.08
0.18	1	242.21	55.71
0.10	0.5	135.07	31.07
0.09	0.5	135.48	31.16

Table 4.28 Specific Adsorption on Calcite in SSW

Mass ratio (NP to Calcite)	DP conc. (g/l)	Specific Adsorption (mg/m2)	Specific Adsorption (mg/g)
1.00	1	1778.32	409.01
0.33	1	623.58	143.42
0.20	1	343.83	79.08
0.18	1	372.64	85.71
0.10	0.5	199.65	45.92
0.09	0.5	253.16	58.33

Plots (5.21) and (5.22) show specific adsorption values in both $\frac{mg\ NP}{m^2\ mineral\ surface}$ and $\frac{mg\ NP}{g\ mineral}$ plotted on the ordinate on semi-log plot with the ordinate in logarithmic scale, while silica Nano particles conc. per Calcite conc. is plotted on the abscissa on linear scale.
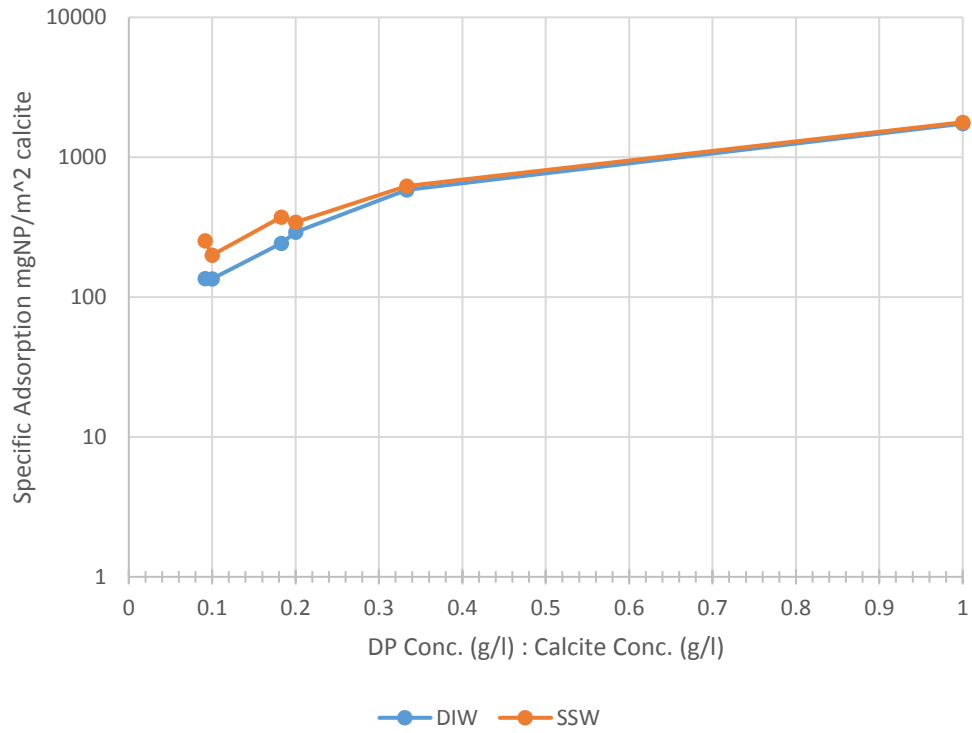
Plot 4.21 Specific Adsorption Curves for Calcite in DIW vs. SSW
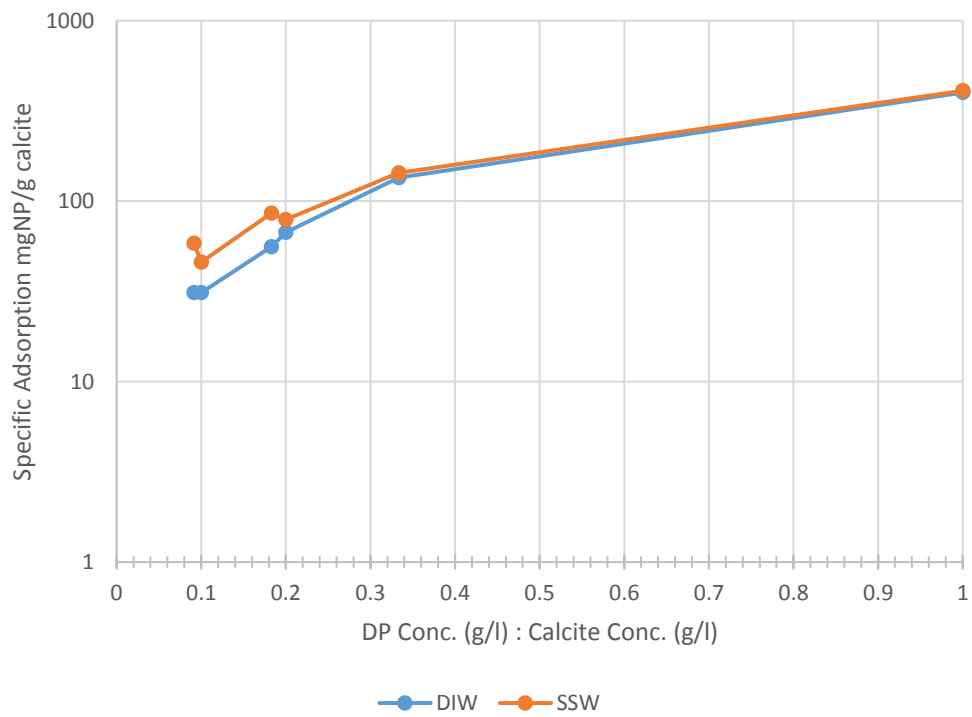
Plot 4.22 Specific Adsorption Curves for Calcite in DIW vs. SSW

Plots (5.21) and (5.22) show that specific adsorption is direct proportion to the silica Nano particles concentration. Specific adsorption increases linearly with the ratio $\frac{\text{NP conc.}}{\text{Calcite conc.}}$. Slight increase in adsorption values is evident in SSW when compared to DIW. This increase becomes more pronounced at $\frac{\text{NP conc.}}{\text{Calcite conc.}} < 0.33$, at higher concentration of mineral (5 g/l and 5.47 g/l) and lower concentration of DP (0.5 g/l). The increase in specific adsorption is inversely proportion to the concentration of Calcite in DIW with exception to single point when Calcite concentration to DP concentration ratio is greater than 10:1, at which specific adsorption of NP is greater at 10.87:1 than at 10:1. However, the increase in specific adsorption with increasing Calcite concentration to DP concentration ratio occurs earlier in SSW at ratios greater than 3:1. Therefore specific adsorption values at 5.46:1 and 10.93:1 is greater than 5:1 and 10:1 of Calcite to DP concentration ratios respectively. It seems that Calcite concentration in SSW has more pronounced effect on specific adsorption of Nano particles values than it has in DIW. This might be attributed to the higher ionic strength of SSW, which amplifies the effect of the increase of Calcite concentration and results in a slight improvement of adsorption on the mineral. Calcite tends to dissolute more in DIW when compared to SSW. Possible increase in active surface area available for adsorption might come from the increase of un-disassociated calcite in SSW compared to DIW. Generally, increasing the ionic strength of the medium will decrease the double layer length and reduces the zeta potential accordingly as aforementioned in section (5.1). Reduction in NPs zeta potential is evident in SSW when compared to DIW. The presence of TDS in SSW also, will play a role in increasing the interactions and collisions among the colloid particles, which is reflected in a slight increase in NPs Z-avg value compared to DIW, and therefore, might cause improvement to adsorption.

To emphasize the effect of SSW on the concentration of Nano particles when compared to DIW, ABS plots for samples at different concentration ratios of DP to calcite and ABS for samples at the same concentrations of Calcite but without DP are presented below for both DIW and SSW. ABS reading is directly proportion to the concentration of the measured sample. Although the ABS values for SSW Calcite baseline correction without DP are always higher than DIW, SSW ABS values for samples with DP 1/0.5 (g/l) are continuously lower than ABS values for DIW. Thus, the lower ABS values of SSW that correspond to DP 1/0.5 (g/l) + Calcite, indicates lower concentration of DP in the measured sample, which is attributed to an improvement in the specific adsorption on calcite in SSW. Running ICP will be recommended to confirm the silicon concentration and correct for the values obtained by using UV spectrophotometry.
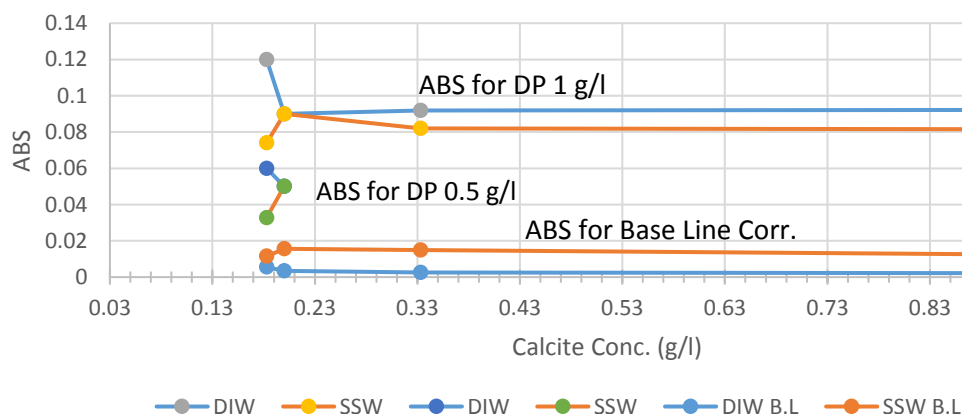
Plot 4.23 ABS Values for Calcite Static Adsorption in DIW and SSW

4.3. Core flooding (SK-Chalk)

4.3.1. Transport Behavior of Nano-Particles

4.3.1.1. SK-1 Flood

The following table lists pH, UV-abs, and IC data for Calcium (Ca^{2+}), Magnesium (Mg^{2+}), and Lithium (Li^+), ions.

Table 4.29 SK-1 pH, IC, UV abs

stage	PV	pH	Li$^+$ (mol/L)	Mg^{2+} (mol/L)	Ca^{2+} (mol/L)	ABS
Pre-Flush	4	7.71	0	0	1.67E-03	0.07
	8	7.54	0	0	1.67E-03	0.11
Post-Flush	8.25	8.08	5.73E-02	4.02E-04	6.66E-03	0.09
	8.5	7.78	4.07E-01	5.24E-04	1.17E-02	0.11
	8.75	8.27	4.77E-01	1.75E-04	5.00E-03	0.15
Colored effluents	9	9.5	1.93E-01	0	1.67E-03	2.03
	9.25	10.69	2.80E-02	0	1.67E-03	2.71
	9.5	10.91	1.04E-02	0	0	0.56
	9.75	10.89	6.14E-03	0	0	0.28
	10	10.88	4.16E-03	0	0	0.19
	10.25	10.71	3.20E-03	0	1.67E-03	0.14
	10.5	10.7	2.94E-03	0	1.67E-03	0.11
	10.75	10.59	1.45E-03	0	1.67E-03	0.09
	11	10.2	4.90E-04	0	1.67E-03	0.09
	11.25	8.04	1.78E-04	0	1.67E-03	0.09
	11.5	8.08	0	0	1.67E-03	0.08
Post-Flush	11.75	8.27	0	0	1.67E-03	0.09
	12	8.5	0	1.57E-04	3.33E-03	0.09
	12.25	8.15	1.34E-04	0	1.67E-03	
	12.5	8.68	0	1.22E-04	1.67E-03	
	12.75	8.21	0	1.05E-04	1.67E-03	
	14	7.6	0	0	1.67E-03	
	14.25	8.65	0	1.40E-04	1.67E-03	
	14.5	8.75	0	1.22E-04	3.33E-03	
	15	8.99	0	1.40E-04	3.33E-03	
	15.25	9	0	1.57E-04	3.33E-03	
	15.5	9.05	0	1.40E-04	3.33E-03	
	16	9.22	0	1.05E-04	1.67E-03	

UV-ABS values are plotted with Li$^+$ concentration, which is from lithium chloride that is used as a tracer. Ca^{2+}, and Mg^{2+} are plotted with pH against PV.
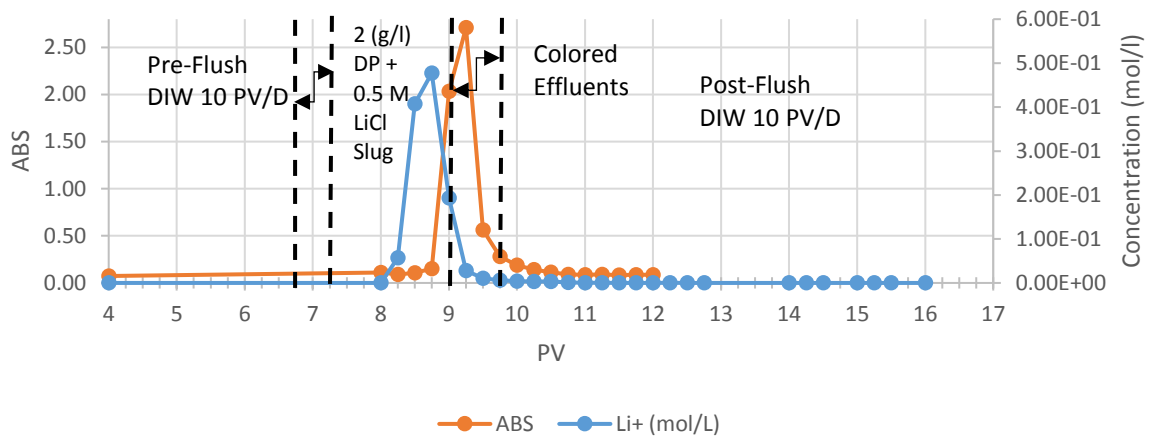
Plot 4.24 SK-1 Tracer vs. ABS
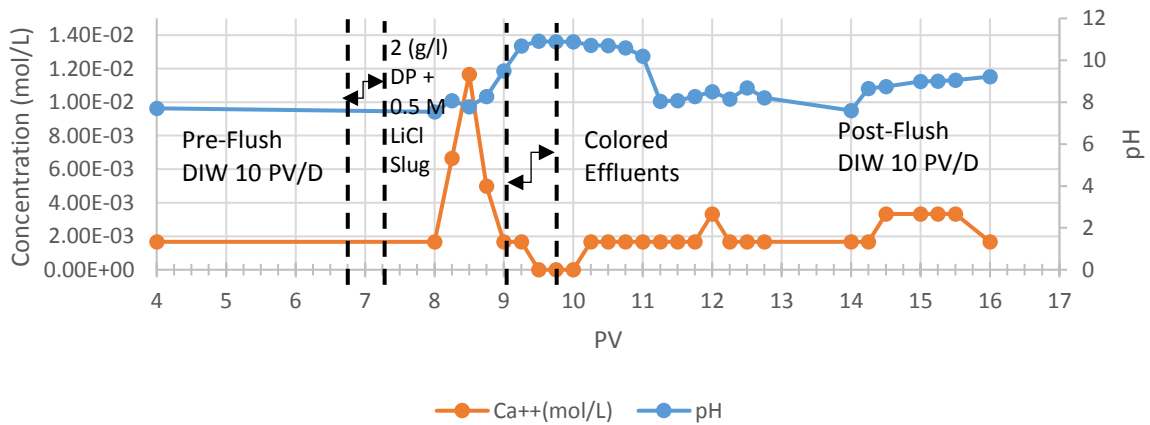
Plot 4.25 SK-1 Ca^{2+}vs. pH
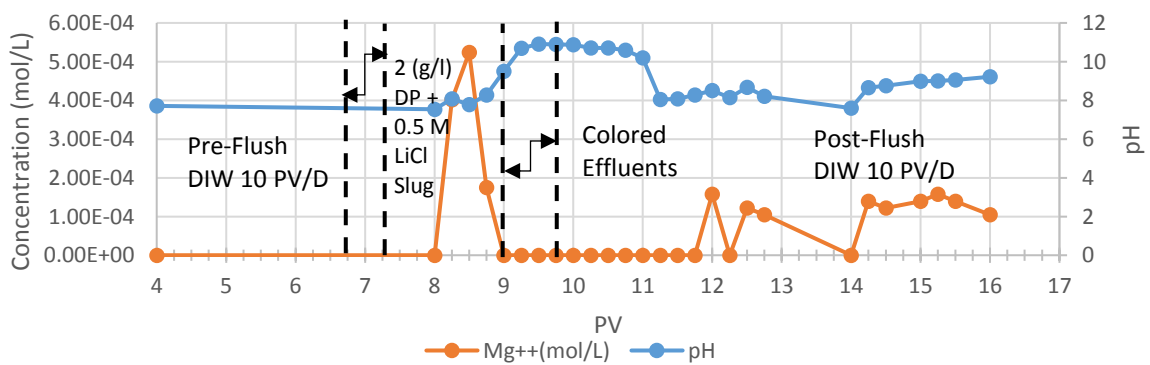
Plot 4.26 SK-1 Mg^{2+} vs. pH

Table 4.30 SK-1 plots Characteristics

Line no.	PV	Stage
1	1-6.75	Pre-Flush
2	6.75-7.25	DP Slug
3	9-9.75	Colored Effluents
4	7.25-16	Post-Flush

44

Li^+ is produced in PV [8.25 – 11.25]. Plot (5.24) shows a spike in Li^+ concentration at point (8.75, 4.77E-01), which is 1.5 PV away from the last PV of DP injected. Another peak is shown on the abs curve at point (9.25, 2.71) 2 PV in the post-flush, which corresponds to a significant increase in pH; (pH > 10), and production of colored effluents. Although, the values of calcium and magnesium ions are low and do not allow for quantitative analysis, however the large increase in pH in this region - after 2 PV of the slug injection ended and during production of colored effluents - might indicate a high production of fines introduced by the injection of DP at 2 (g/l).

4.3.1.2. SK-2 Flood

The following table lists pH, and IC data for Calcium (Ca^{2+}), Magnesium (Mg^{2+}), Carbonate (CO_3^{2-}) and Lithium (Li^+), ions. UV-ABS analysis is not performed for SK-2 effluents due to the colored effluents. It is worth to mention that PV [3.625] and PV [15] are not exact points being measured but rather average mid-points in flush bank intervals; [5 - 24] and [50 – 70] effluent samples which correspond to PVs; [1.25 – 6] and [12.5 – 17.5] respectively. Samples effluent history will be presented in the appendix.

Table 4.31 SK-2 pH, IC Analysis

Stage	PV	pH	Li^+ (mol/L)	Mg^{++}(mol/L)	Ca^{++}(mol/L)	CO_3^{2-}(mol/L)
Pre-Flush	0.25	7.99	0	1.0E-04	1.3E-03	3.2E-01
	0.5	7.92	0	1.6E-04	2.0E-03	3.3E-01
	0.75	7.92	0	1.2E-04	2.0E-03	1.2E-01
	1	7.97	0	0	1.1E-03	1.0E-01
	3.625	8	0	0	5.5E-04	2.7E-01
	6.25	7.63	0	0	6.5E-04	2.9E-01
	6.5	7.68	0	0	0	2.6E-01
	6.75	7.53	0	0	3.7E-04	2.6E-01
	7	7.56	0	0	5.7E-04	2.7E-01
DP Slug	7.25	7.62	0	0	4.3E-04	2.7E-01
	7.5	7.61	0	0	1.1E-03	3.2E-01
	7.75	7.62	0	0	4.7E-04	2.6E-01
	8	7.59	0	0	5.7E-04	2.8E-01
	8.25	7.46	6.7E-03	1.0E-04	2.0E-03	2.4E-01
	8.5	7.09	6.0E-02	2.4E-04	5.3E-03	2.5E-01
Post-Flush	8.75	7.1	8.6E-02	2.2E-04	4.6E-03	3.2E-01
	9	7.25	9.1E-02	1.0E-04	2.0E-03	2.3E-01
	9.25	7.33	9.2E-02	1.2E-04	2.1E-03	2.7E-01
	9.5	7.37	9.3E-02	1.9E-04	3.0E-03	3.4E-01
Colored Effluents	9.75	8.51	8.5E-02	6.2E-04	4.3E-03	1.3E-01
	10	9.23	2.6E-02	3.3E-04	2.9E-03	4.4E-01
	10.25	9.75	1.0E-02	0	6.1E-04	3.7E-01
	10.5	9.98	7.3E-03	0	3.9E-04	3.7E-01
	10.75	10.03	5.0E-03	0	2.0E-04	3.3E-01
	11	9.91	3.8E-03	0	0	3.0E-01

Table 4.32 SK-2 pH, IC Analysis Continue.

Stage	PV	pH	Li⁺ (mol/L)	Mg⁺⁺(mol/L)	Ca⁺⁺(mol/L)	CO₃²⁻(mol/L)
	11.25	9.84	2.6E-03	0	3.1E-04	3.0E-01
	11.5	9.64	1.2E-03	0	0	2.9E-01
	11.75	9.02	2.9E-04	1.6E-04	2.0E-03	4.0E-01
	12	8.06	0	0	1.2E-03	3.1E-01
Post-Flush	12.25	7.96	0	0	4.9E-04	2.6E-01
	15	8.18	0	0	5.5E-04	2.7E-01
	17.75	8.74	0	0	5.9E-04	2.7E-01
	18	9.18	0	0	0	2.5E-01
	18.25	9.01	0	8.6E-05	1.4E-03	3.4E-01
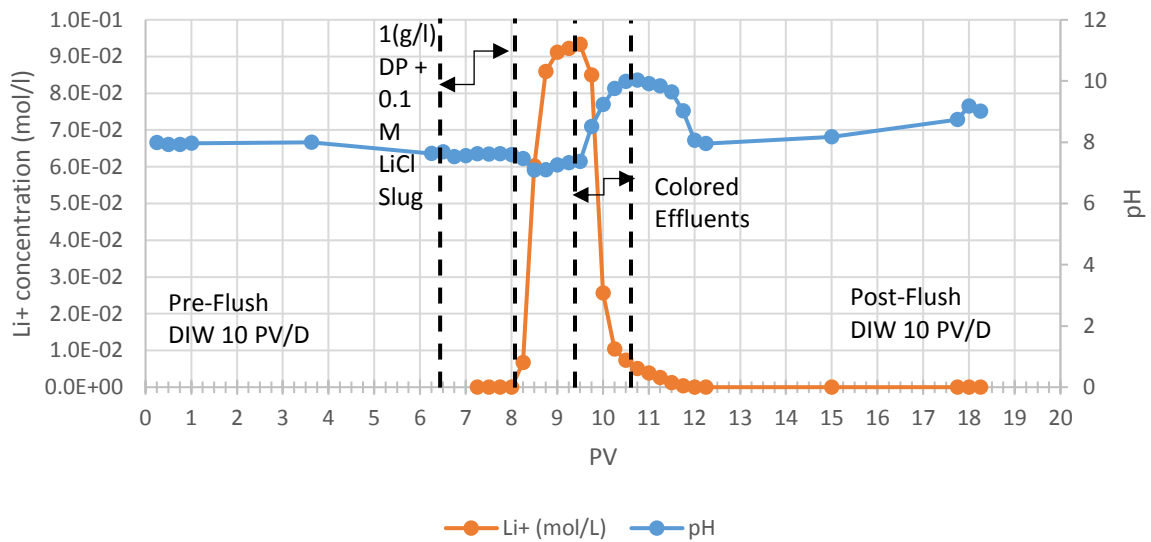
Plot 4.27 SK-2 Tracer vs. pH
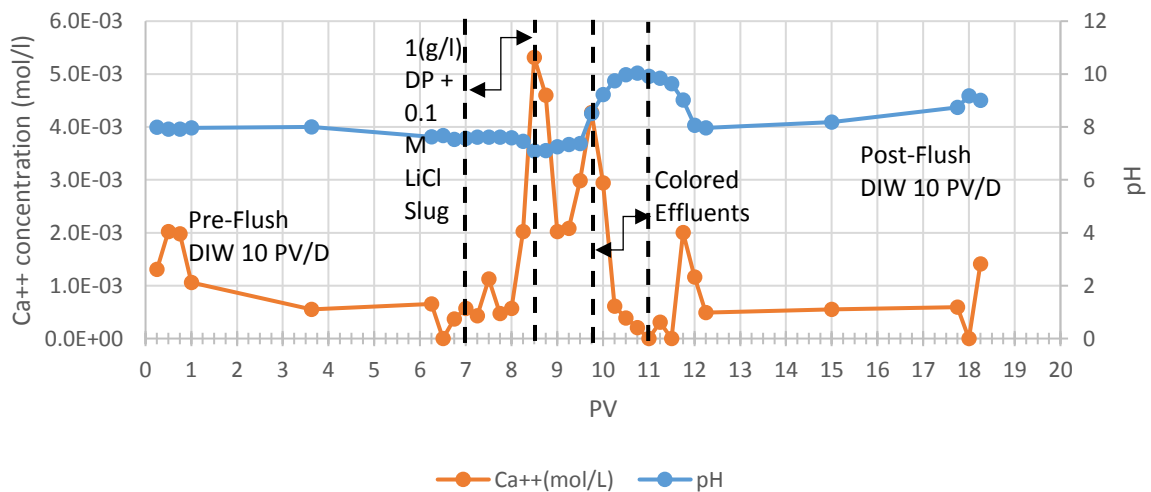
Plot 4.28 SK-2 Ca²⁺vs. pH
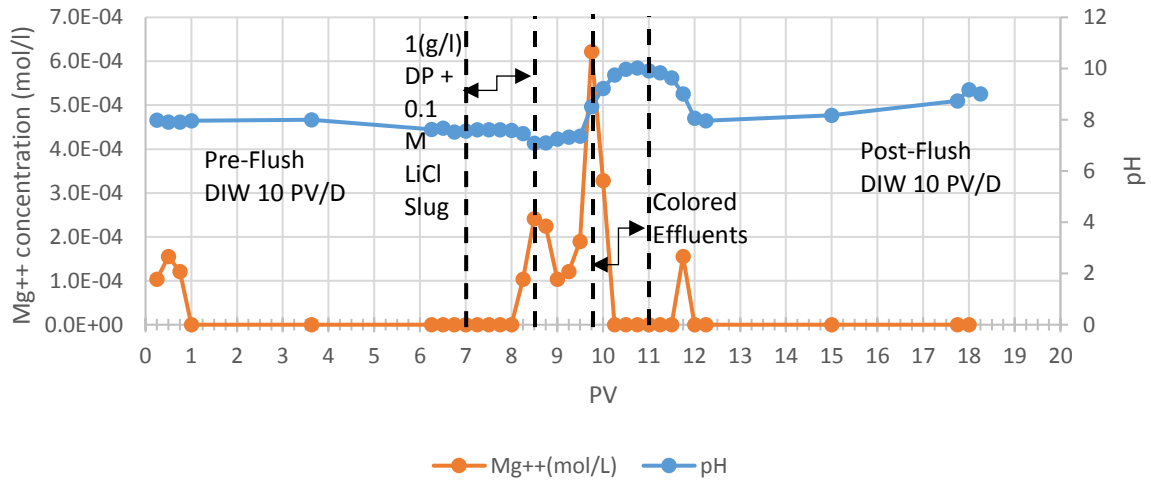
Plot 4.29 SK-2 Mg^{2+} vs. pH
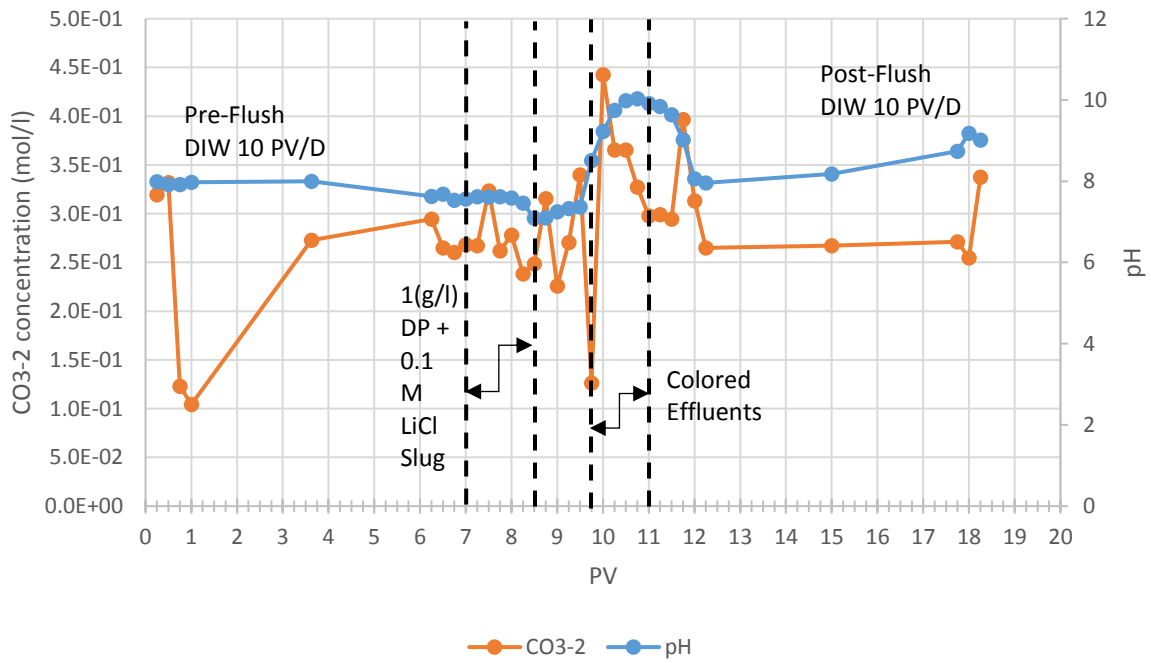
Plot 4.30 SK-2 CO$_3^{2-}$ vs. pH

Table 4.33 SK-2 plots Characteristics

Line no.	PV	Stage
1	1-7	Pre-Flush
2	7-8.5	DP Slug
3	9.75-11	Colored Effluents
4	8.5-18.25	Post-Flush

Li$^+$ is produced in PV [8.25 – 12] approximately 0.75 PVs larger than SK-1 due to larger slug volume of 1.5 PV compared to 0.5 PV from SK-1. With a peak at (9.5, 0.09), (PV, Conc.) respectively, which marks the end of 1 PV of DP injection and only 0.25 PV before the colored effluents which resembles the location of Li$^+$ peak in SK-1. The pH values shown on the plots exhibit an increase - pH > 10 – in the vicinity of the colored effluents region PV [9.75 – 11]. The colored effluents show a corresponding increase in (Ca^{2+}), Magnesium (Mg^{2+}), and Carbonate (CO$_3^{2-}$) concentrations which are still at significantly low values but exhibit a continuous spread and do not form an isolated points on the plots as observed in SK-1. ICP is used to analyze some samples from pre-flush and post-flush with colored effluents for more accurate and better quantitative analysis of the elements present in the effluents. Furthermore, ICP will provide more accurate analysis for the elements present in the effluents, which can be used as a check on IC values obtained earlier. The following plot shows a perfect agreement of calcium and lithium profiles obtained from ICP with calcium and lithium ions obtained from IC. Three points are picked for each series to demonstrate the start and the end point of production and the peak in between against PV.
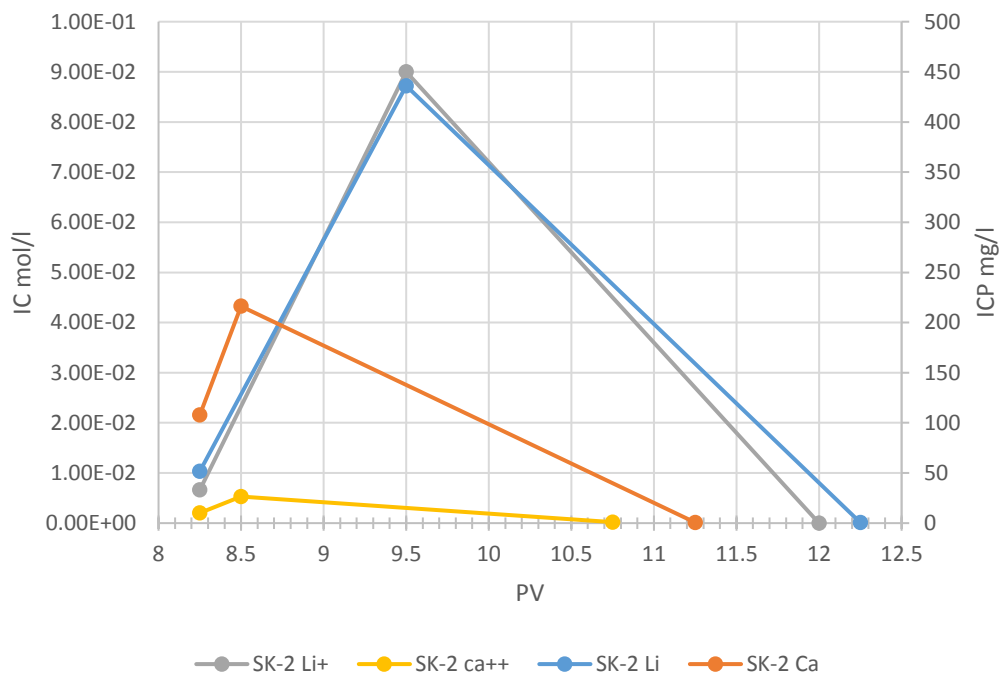
Plot 4.31 Lithium and Calcium Measurements for SK-2

As shown above, IC becomes powerful analytic tool when combined with ICP. Li, Li$^+$ and Ca, Ca$^+$ have the same spread profile against PV with a slightly extended range of detection with ICP (red and blue lines ICP, and IC respectively).

The following table summarizes the data from ICP for SK-2.

Table 4.34 ICP Analysis for SK-2 Effluents

Stage	PV	Ca mg/l	Li mg/l	Si mg/l
Ref 1	Ref. DI water	<0,05	<0,02	<0,1
Pre-Flush	0.25	85.5	<0,02	11.2
	0.5	111	<0,02	13.6
	0.75	112	<0,02	13.4
	1	88.3	0.20	10.5
	3.625	18.6	0.23	1.4
	6.25	9.31	0.04	0.7
	6.5	9.25	0.05	0.8
	6.75	8.99	0.06	0.7
	7	8.93	0.04	0.8
DP Slug	7.25	8.96	0.04	0.9
	7.5	8.51	0.03	0.7
	7.75	8.49	0.03	0.7
	8	9.36	0.06	0.6
	8.25	108	51.5	1.0
	8.5	216	304	1.2
Post-Flush	8.75	117	413	2.1
	9	69.5	429	2.7
	9.25	50.9	435	3.1
	9.5	39.9	436	3.5
Colored Effluents	9.75	24.8	363	3.8
	10	4.54	114	5.4
	10.25	1.57	54.2	6.0
	10.5	0.98	47.8	5.6
	10.75	0.90	40.1	4.5
	11	0.55	33.5	3.7
Post-Flush	11.25	0.64	24.0	3.0
	11.5	0.98	14.0	2.4
	11.75	2.42	4.90	1.9
	12	4.09	1.20	1.7
	12.25	5.02	0.59	1.7
	15	6.10	0.13	5.5
	17.75	7.13	0.04	9.3
	18	7.19	0.05	9.9
	18.25	7.21	0.04	10.2
Ref 2	Ref. DP-LiCl	0.16	461	274

ICP is used for analyzing SK-2 effluents instead of the UV-ABS to investigate the change in NP concentration in the effluents. ICP is mainly used to detect the presence of silicon (Si), which is indicative of the presence of NPs. The concentration of silica NPs is measured in gram per liter by dividing the amount of silicon that ICP measures in the effluents by the amount of silica it registers in a reference sample of 1 (g/l) DP.

Silicon concentration in 1 (g/l) DP fluid sample = 274 (mg/l) → NP concentration (g/l) in the effluent is equivalent to $\dfrac{Si\ concentraion\ (\frac{mg}{l})}{274\ (\frac{mg}{l})}$.

Since the injection of NP slug continued for 1.5 PV, which started at PV [7.25], therefore silica Nano-particles are expected in the effluents corresponding to PV [8.25] to PV [18.25].

However, ICP detects high amount of silicon in the early pre-flush samples, which might be attributed to contamination in the outlet lines from the setup or due to impurities from the core itself, hence those values will be disregarded. The average amount of silicon detected in PVs $[6.25 - 8]$ is taken as a baseline correction. From the concentration of NP in grams per liter, the mass of NP adsorbed is calculated as follows.

$$\text{NP adsorbed \%} = \frac{\left[NP\ inj.conc.\left(\frac{g}{l}\right)*Slug\ volume\ (l)\right] - \sum[NP\ conc.in\ the\ sample\left(\frac{g}{l}\right)*Sample\ volume\ (l)]}{[NP\ inj.conc.\left(\frac{g}{l}\right)*Slug\ volume\ (l)]}\ \%$$

NP concentration (g/l) and mass balance (g), are calculated in the effluents corresponding to $[8.25 - 18.25]$ PVs as shown in the table below.

Table 4.35 NP Concentration (g/l) and Mass Balance in SK-2 effluents

stage	PV	Si	NP Conc. (g/l)	NP Conc. (g/l) corr.	NP mass balance (g)
Base-Line corr.	8	0.7	2.55E-03	0.00E+00	0.00E+00
DP Slug	8.25	1.0	3.81E-03	1.26E-03	8.99E-06
	8.5	1.2	4.40E-03	1.84E-03	1.32E-05
Post-Flush	8.75	2.1	7.68E-03	5.13E-03	3.66E-05
	9	2.7	9.78E-03	7.23E-03	5.16E-05
	9.25	3.1	1.13E-02	8.76E-03	6.25E-05
	9.5	3.5	1.27E-02	1.01E-02	7.24E-05
Colored Effluents	9.75	3.8	1.39E-02	1.13E-02	8.08E-05
	10	5.355	1.95E-02	1.70E-02	1.21E-04
	10.25	6.025	2.20E-02	1.94E-02	1.39E-04
	10.5	5.57	2.03E-02	1.78E-02	1.27E-04
	10.75	4.48	1.64E-02	1.38E-02	9.85E-05
	11	3.72	1.36E-02	1.10E-02	7.87E-05
Post-Flush	11.25	2.99	1.09E-02	8.36E-03	5.97E-05
	11.5	2.395	8.74E-03	6.19E-03	4.42E-05
	11.75	1.885	6.88E-03	4.32E-03	3.09E-05
	12	1.745	6.37E-03	3.81E-03	2.72E-05
	12.25	1.695	6.19E-03	3.63E-03	2.59E-05
	15	5.545	2.02E-02	1.77E-02	1.26E-04
	17.75	9.34	3.41E-02	3.15E-02	2.25E-04
	18	9.875	3.60E-02	3.35E-02	2.39E-04
	18.25	10.24	3.74E-02	3.48E-02	2.49E-04

Total injected mass of NPs in (g) $= 1.5\ PV \times 28.56\ \frac{L}{1000 \times cm^3} \times 1\ \left(\frac{g}{l}\right) = 0.043\ (g)$.

Total NPs' mass produced in the effluents $= \sum NP\ mass\ balance = 1.92 \times 10^{-3}(g)$.

NPs adsorbed $= \frac{0.043 - 1.92 \times 10^{-3}}{0.043}\ \% = 95.52\ \%$.

Concentration of NPs (g/l) is plotted against PV once with tracer Li, and once with Ca as demonstrated in the plots below respectively.
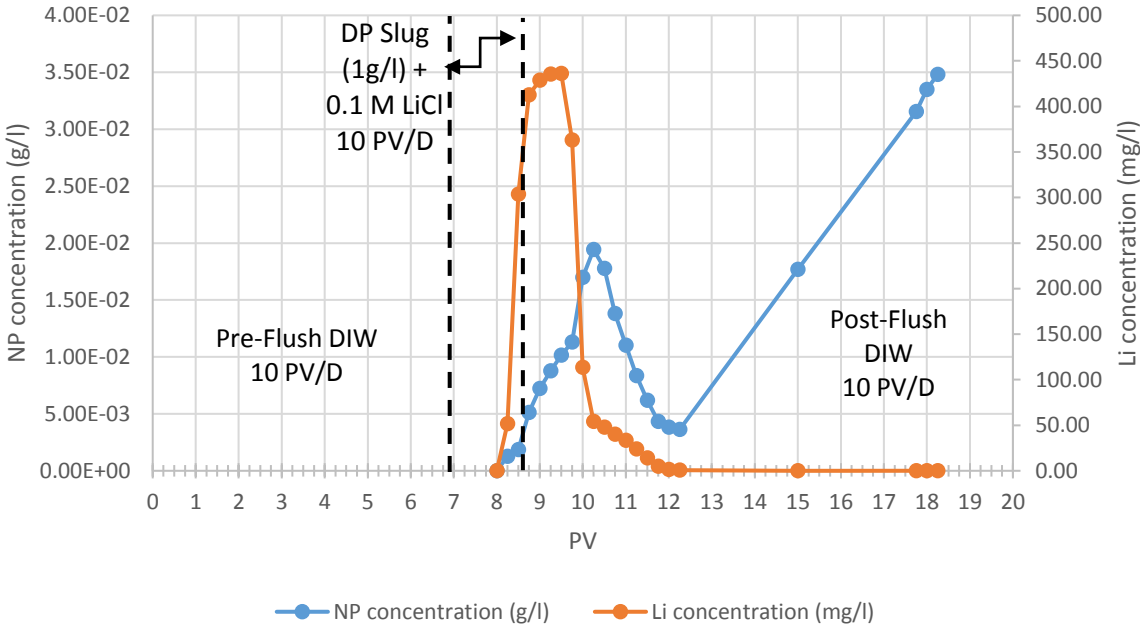
Plot 4.32 NP Concentration (g/l) with Li Concentration (mg/l) SK-2
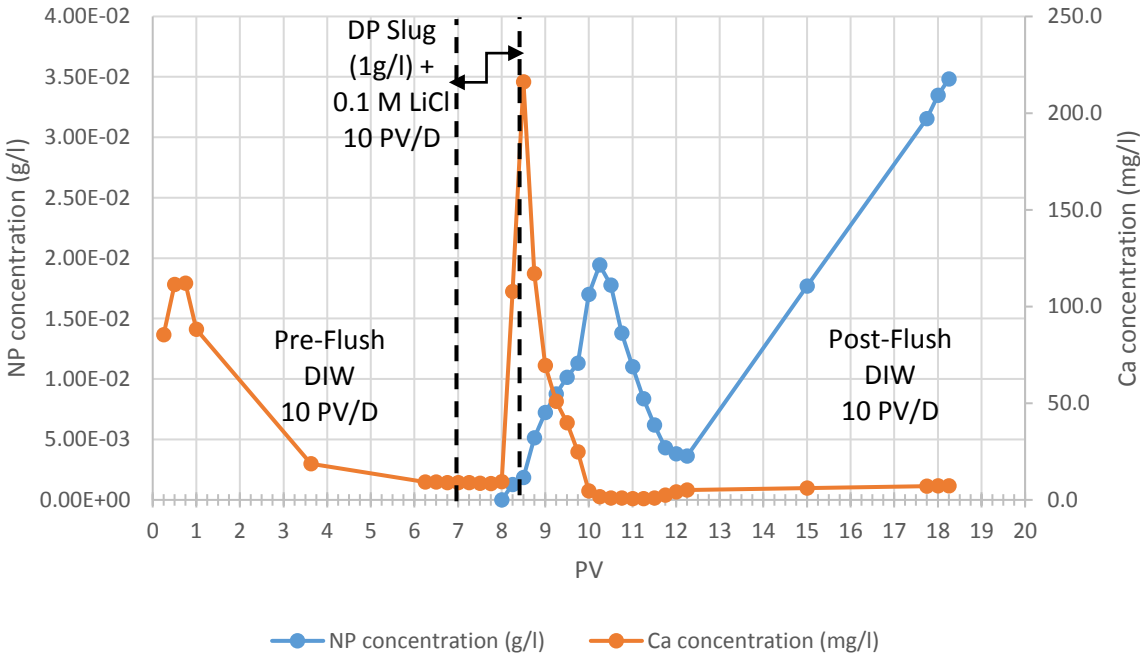
Plot 4.33 NP Concentration (g/l) with Ca Concentration (mg/l) SK-2

Plot (5.32) shows the point at which both NPs and the tracer started to break through the core, which corresponds to PV [8.25] that marks the end of an exact one pore volume of slug injection. The production of the tracer is increasing in the PV interval [8.25 – 9.5], while NPs is increasing in the interval [8.25 – 10.25]. Both the tracer and NPs concentrations are declining

51

until PV [12.25]. NPs concentration starts to pick up and increase until it reaches its highest value that corresponds to the late post-flush at PV [18.25]. The delay in NPs production compared to the tracer production is a clear evident of NPs retention, while the constant increasing rate of NPs concentration in the late post-flush effluents is a sign of NPs desorption.

Plot (5.33) shows a peak of Ca concentration at PV [8.25]. This increase corresponds to the starting point of NPs, and Li production, which might be attributed to some fines released and collected in the effluents. The release of fines is probably triggered by the slightly low-pH of the DP slug and the abrasive nature of NPs. The differential pressure below demonstrates a slight increase in dp after the slug injection, which might be due to fine migration. As shown from the differential pressure profile, no sign of pore blockage is observed and dp stabilizes in the post-flush.
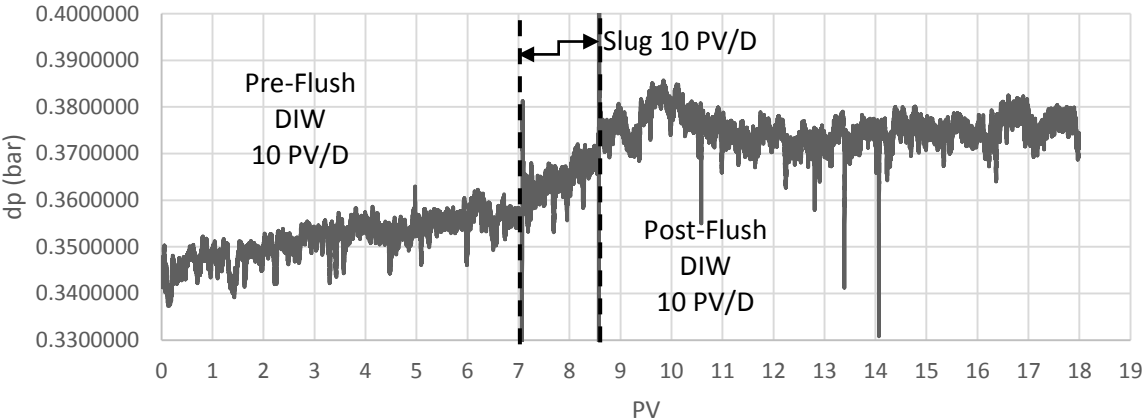
Plot 4.34 dp for SK-2

4.3.1.3. SK-1 and SK-2 IC Data

The following plots show selected points for SK-1 and SK-2 IC and pH data. The points represent Li^+, Ca^{++} Conc. (mol/l) against PV and pH is plotted with Ca^{++}. Three points are taken for each curve, which show the start of increase, peak, and the end of decline.
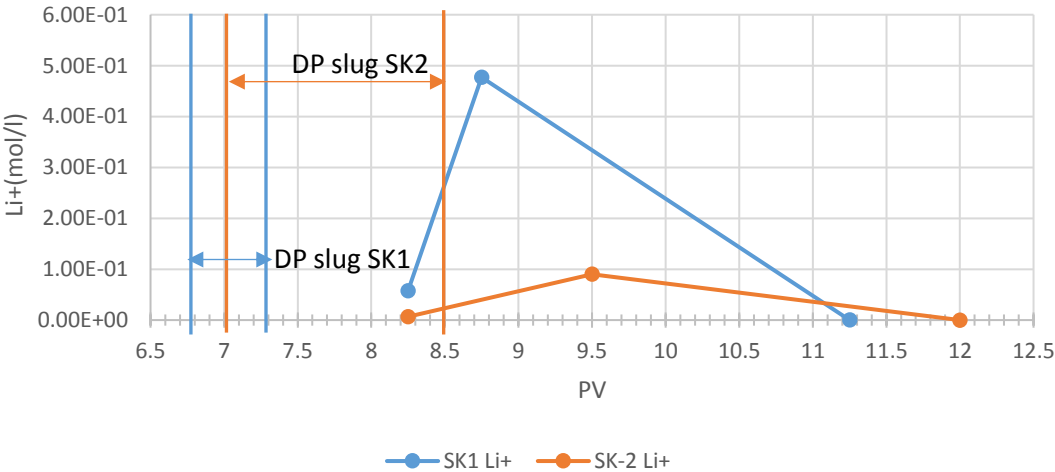
Plot 4.35 Li⁺ Profile (SK-1 vs. SK-2)

52
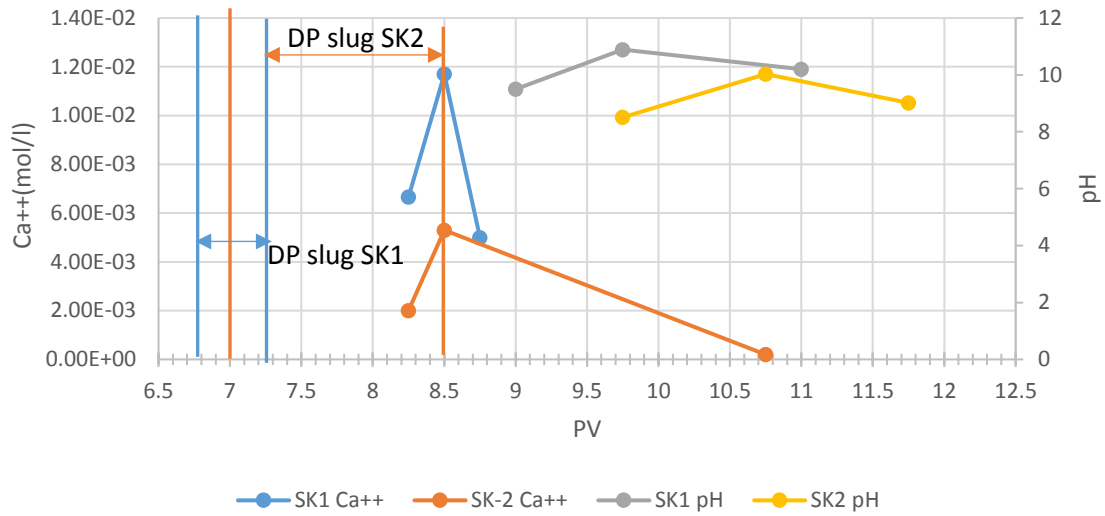
Plot 4.36 Ca⁺⁺Profile (SK-1 vs. SK-2) with pH

The starting point of production of Li^+ and Ca^{++} for SK-1 and SK-2 is at PV [8.25]. SK-1 has a higher concentration slug, (2g/l DP + 0.5 M LiCl), than SK-2, (1g/l DP + 0.1 M LiCl). However, SK-2 has bigger slug volume (1.5 PV) than SK-1 (0.5 PV). Plot (5.35) shows that with injection of only half pore volume of slug (0.5 M LiCl) in SK-1, it took around 4 PVs after the slug injection ended to produce all the amount of tracer (Li^+), while for longer slug injection (1.5 PV) but with lower concentration LiCl (0.1 M) in SK-2, it took around 3.5 PV at the same flow rate of 10 PV/D. Plot (5.36) suggests that the high concentration of DP in SK-1 relative to SK-2 leads to release of more Ca^{++} at PV [8.5]. However, the production of Ca^{++} ended for SK-1 after 1.5 PV in the post-flush away from the end of slug injection, while it took 2.25 PV of post-flush in SK-2 until Ca^{++} stopped. This might suggest that the amount of Ca^{++} released from the core is strongly affected by the injection of NPs and depends on NPs concentration and slug volume. For higher concentration of NPs but smaller slug volumes, Ca^{++} will be released in higher amounts but in relatively shorter period when compared with lower concentration and bigger slug volumes of NPs. This might be reflected in differential pressure (dp) profile, which might stabilize in case of SK-1 faster than SK-2, however this cannot be confirmed due to the absence of dp profile for SK-1. Furthermore, the pH profiles for SK-1 and SK-2 seem to agree with Ca^{++} concentration profiles (SK-1 pH > SK-2 pH). The increase in Ca^{++} production and the corresponding increase of pH due to NPs injection, is due to calcium dissolution which leads to fine migration and increase the dp as shown in dp profile for SK-2 after DP slug is injected. Calcium dissolution and alkalinity are described by the following reactions [30], [31] respectively.

$$CaCO3 + H2O \rightarrow Ca^{+2} + HCO3^- + OH^- \qquad (5.13)$$
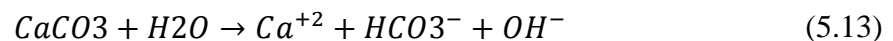
$$Alkalinity = 2[CO3^{-2}] + [HCO3^-] + [OH^-] - [H^+] \qquad (5.14)$$

53

4.3.1.4. SK-3 Flood

In order to test the assumption of NPs desorption and possible fine migration, SK-3 is flooded with low pH slug instead of DP slug. ICP analysis is conducted on SK-3 effluents, and Silicon and Calcium concentration is compared with SK-2. The core was flooded against 10 bar backpressure and 25 bar confinement pressure at flow rate of 10 PV/D. The following table summarizes the flood scheme in SK-3.

Table 4.36 SK-3 Flood Scheme

Stage	Fluid inj.	pH	No. PV inj.
Pre-Flush	DIW	7	7
Slug	DIW + 0.1 M LiCl + 90 μl 0.1M HCl	5.11	1.5
Post-Flush	DIW	7	9

ICP data for SK-3 effluents are shown in the table below.

Table 4.37 ICP Analysis for SK-3 Effluents

Stage	PV	Ca mg/l	Li mg/l	Si mg/l
Pre-Flush	0.25	87.8	0.02	11.7
	3.625	13.5	0.37	1.1
HCl Slug	8	7.28	0.08	1.3
	8.5	267	448	1.7
Post-Flush	10.0	4.10	130	2.1
	15	3.51	0.67	0.3

The silicon concentration is plotted against PV with the tracer Li and with Ca concentration respectively in the following two plots below.
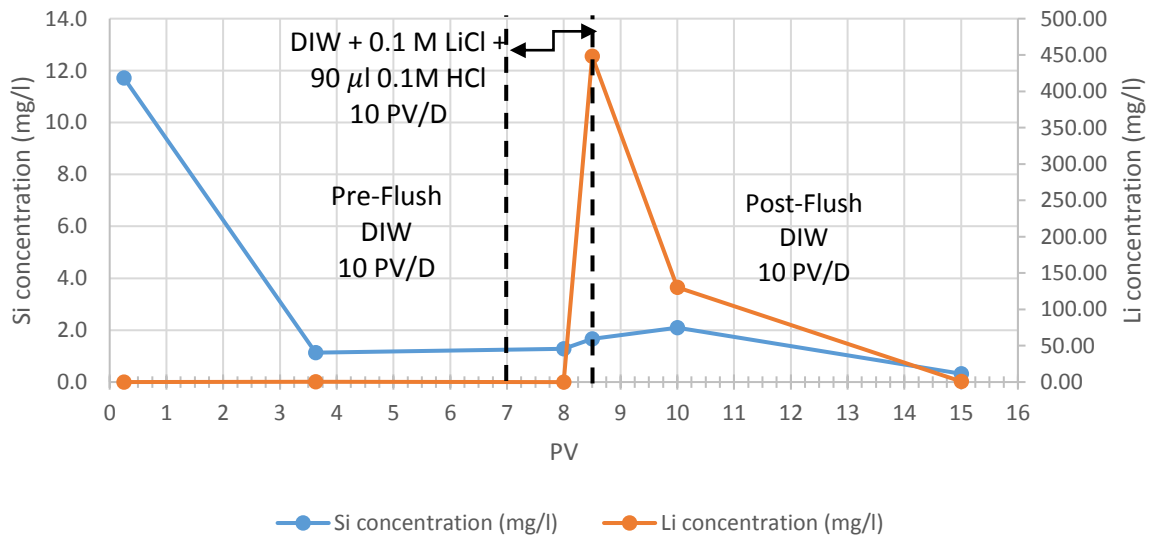
Plot 4.37 Si Concentration (mg/l) with Li Concentration (mg/l) SK-3
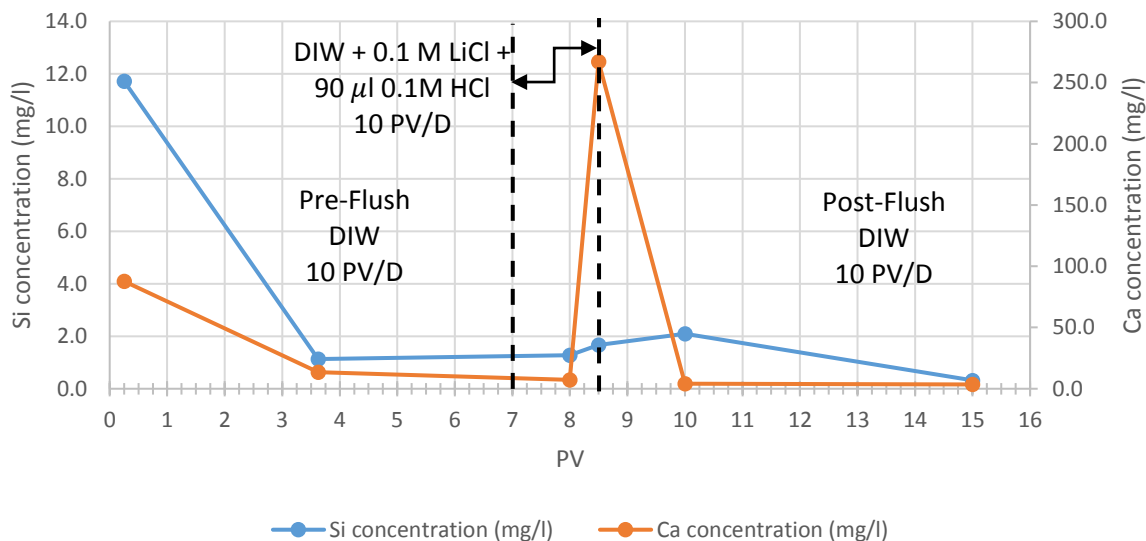
Plot 4.38 Si Concentration (mg/l) with Ca Concentration (mg/l) SK-3

4.3.1.5. SK-2 and SK-3 ICP Data

Silicon concentration from SK-2 and SK-3 is plotted against PV as shown below.
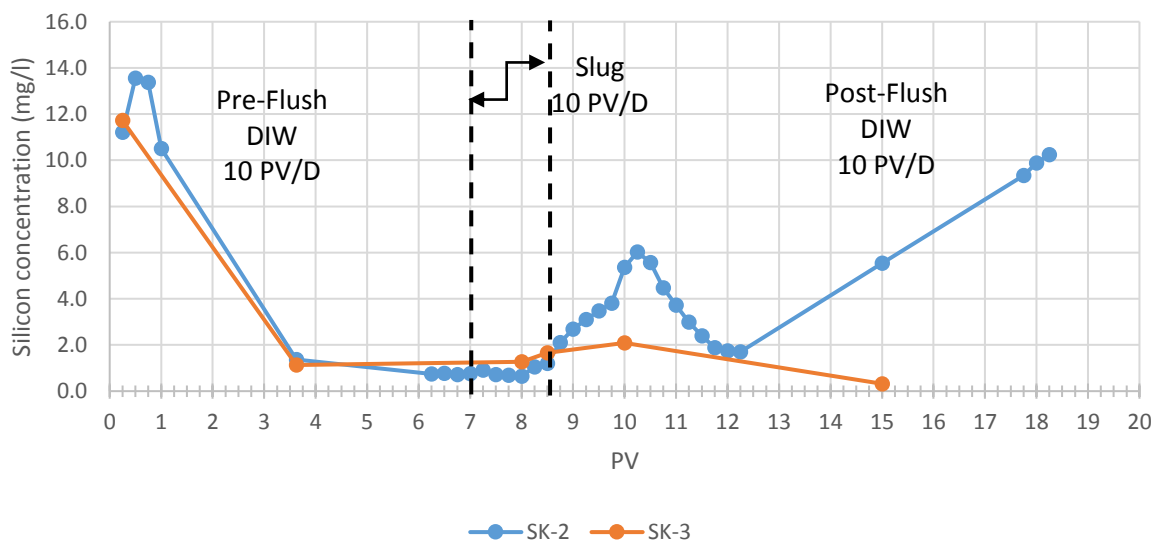
Plot 4.39 Silicon Concentration Comparison, SK-2 vs. SK-3

Low-pH experiment conducted for SK-3 confirms that the Silicon peak in SK-2, in the PV interval [8.25 – 18.25], is a characteristic peak for Silica Nano-particles. In addition, the Silicon concentration peaks in SK-2 and SK-3 from the early pre-flush PVs, are clearly caused by impurities from the core. The increase in Si concentration at the late post-flush in SK-2 is due to increase in production of silica Nano-particles in the effluents, which might be caused by desorption of NPs during the flood.

The following plot compares Ca concentration against PV from SK-2 and SK-3.
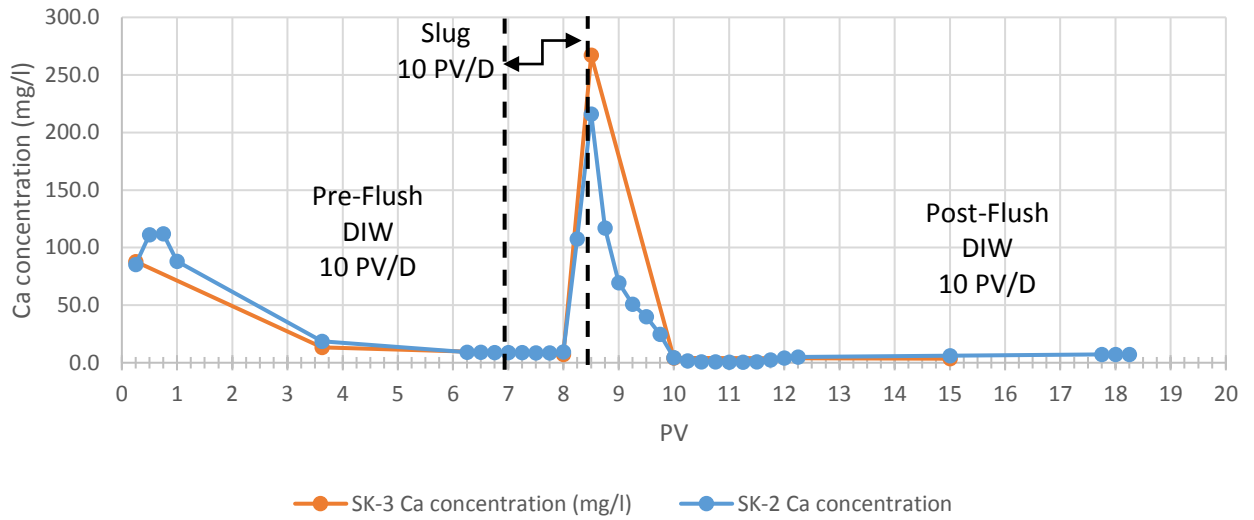
Plot 4.40 Ca Concentration SK-2 vs. SK-3

The increase in Ca concentration in the effluent illustrated by the concentration peak at PV [8.25], is indicative of fine release after the injection of the slug as was seen in SK-1. The relatively lower concentration of Ca produced in SK-2 compared to SK-3, might be attributed to the adsorption of NPs that takes place on calcite which reduces fine migration.

4.3.1.6. SEM+EDXRF

SEM+EDXRF (scanning electron microscopy + energy dispersive x-ray fluorescence) are carried out on DP 1 g/l sample, chalk specimen flooded with 1 g/l DP, and one of the colored sample effluents from SK-2 post flush presented in the figures below. Figure (5-1) shows NPs in DP 1g/l sample. Particles are mostly spherical. The appearance of clusters is due to drying process. The chalk specimen in figure (5-2) shows that it is tighter than Berea sandstone. Also, microfossils are observed. In figure (5-3) NPs can be spotted on the chalk surface. The size range and elemental analysis of these spherical particles confirmed that they are indeed silica particles adhered to the chalk. The post-flush sample analyzed by EDXRF is shown in figure (5-4). Analysis confirms the present of silicon and calcium in the colored effluents, which can be attributed to NPs and fines released from the core. Also, the analysis shows traces of sulfur which might causes the yellowish color of the effluent.
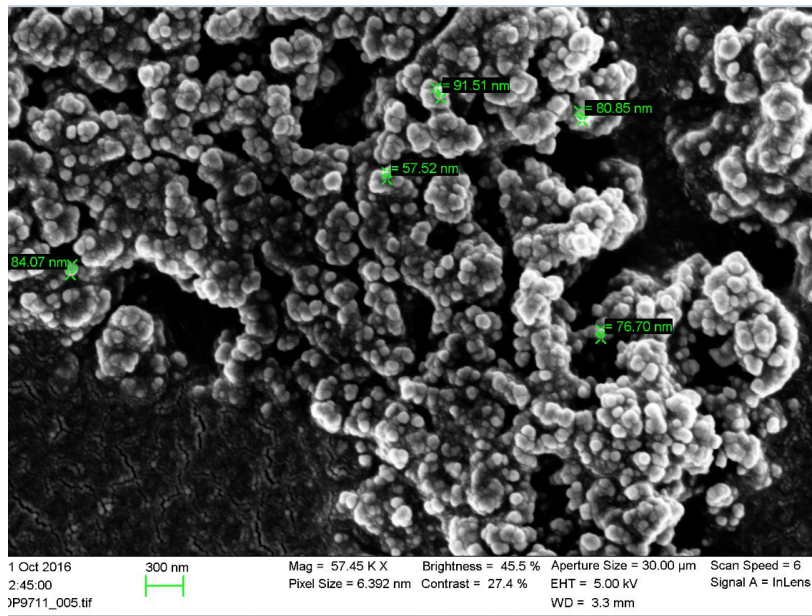
Figure 4-1 DP 1 g/l Sample
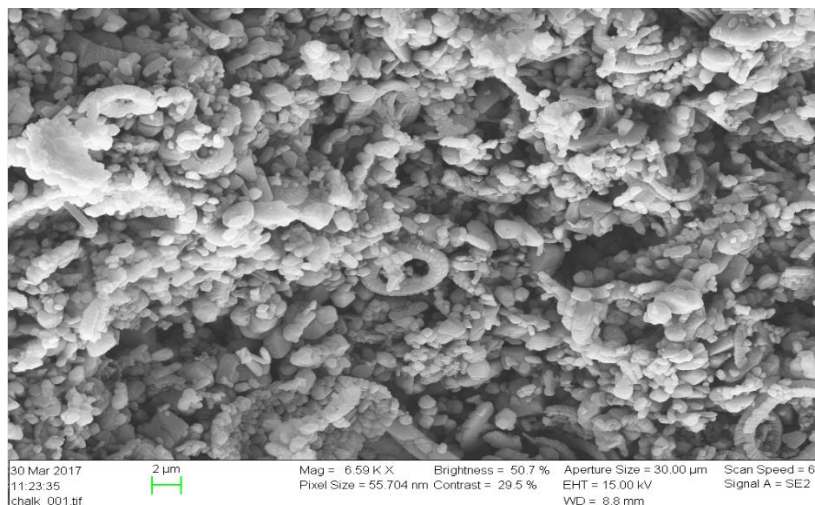
Figure 4-2 Chalk Specimen
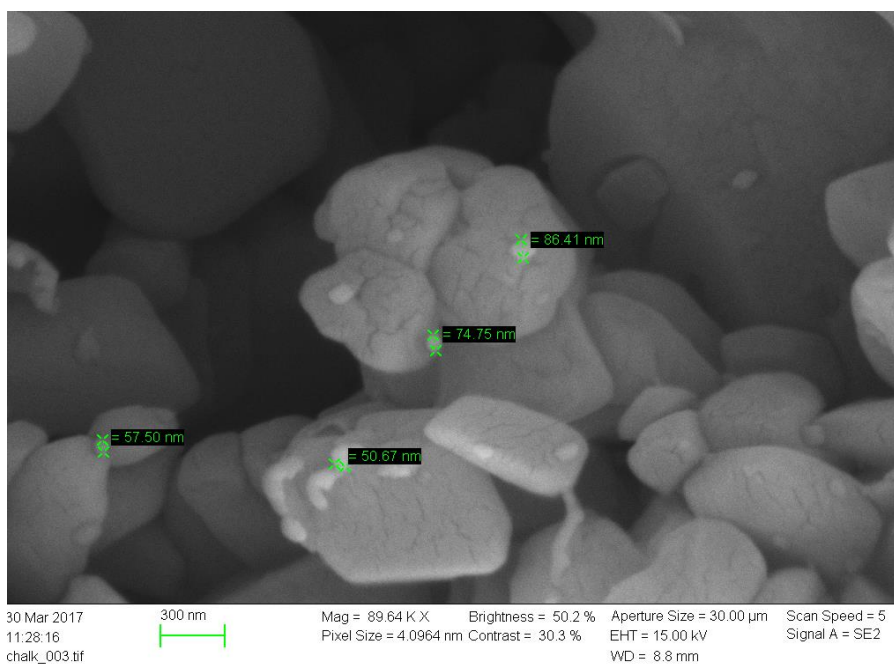
Figure 4-3 Chalk Specimen with NPs Adhered on the Surface
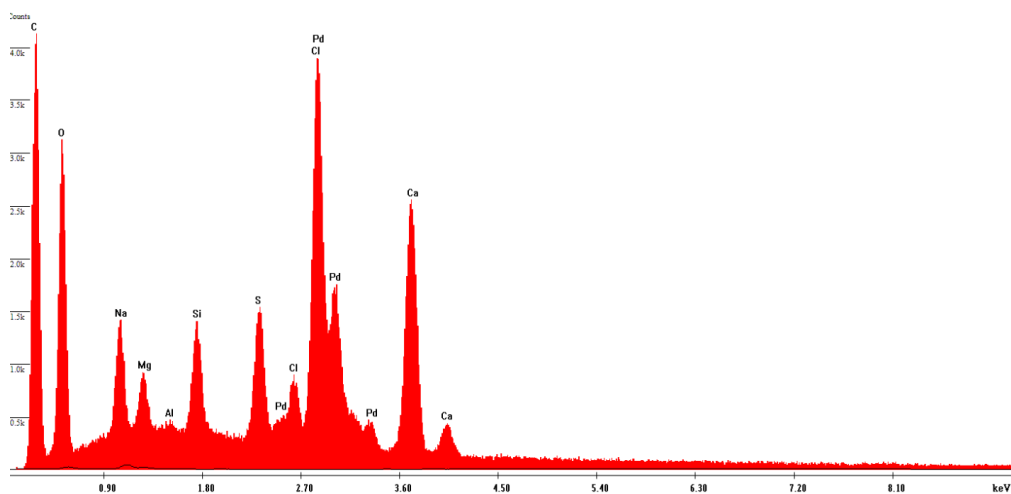
Figure 4-4 EDXRF for SK-2 Colored Effluent

4.3.2. EOR Experiments: SK-5 & SK-6

The aim of this part of experiments is to test silica Nano-particles potential as an enhanced oil recovery candidate. The experiments are divided into two core floods; SK-5 and SK-6. SK-5 is used to investigate the ultimate recovery that could be achieved by injecting silica-Nano particles at early stage of the flood with high flow rate of 16 PV/D after just 3.5 PVs of pre-flush with LSW. SK-6 is utilized to measure the residual oil saturation change introduced by the silica Nano-particles slug after extended LSW flood. Irreducible water saturation is established in the cores after being 100% saturated with SSW, through forced drainage with N-Decane as the displacing phase and SSW as the displaced phase. The following table summarizes the drainage process for SK-5 and SK-6 respectively.

Table 4.38 Summary of Drainage Process

Core	Initial saturation	Injected fluid	Injection rate (PV/D)	Confinement pressure (bar)	S_{wirr}
SK-5	SSW	N-Decane + 0.005 M SA	5	25	0.29
SK-6	SSW	N-Decane + 0.005 M SA	24	25	0.28
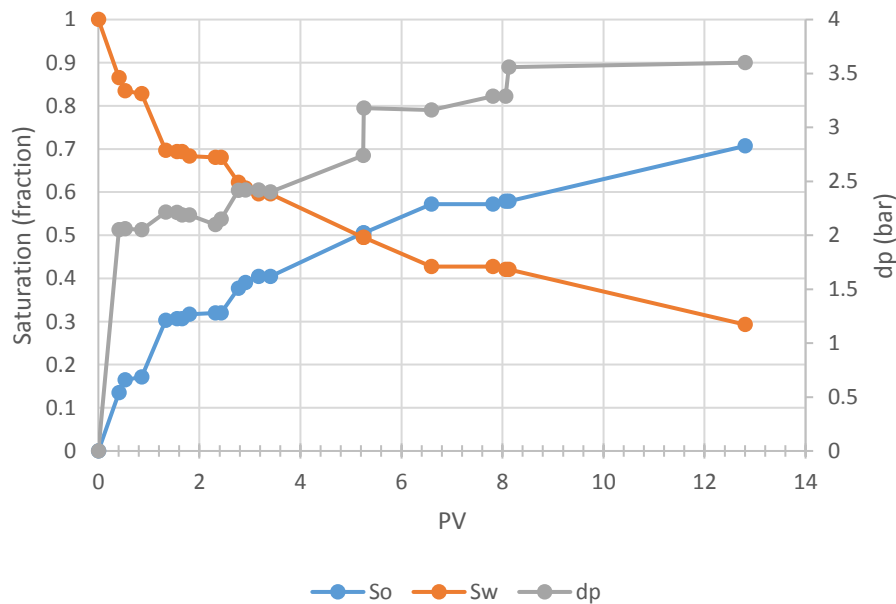
Plot 4.41 SK-5 Saturation Profile with dp
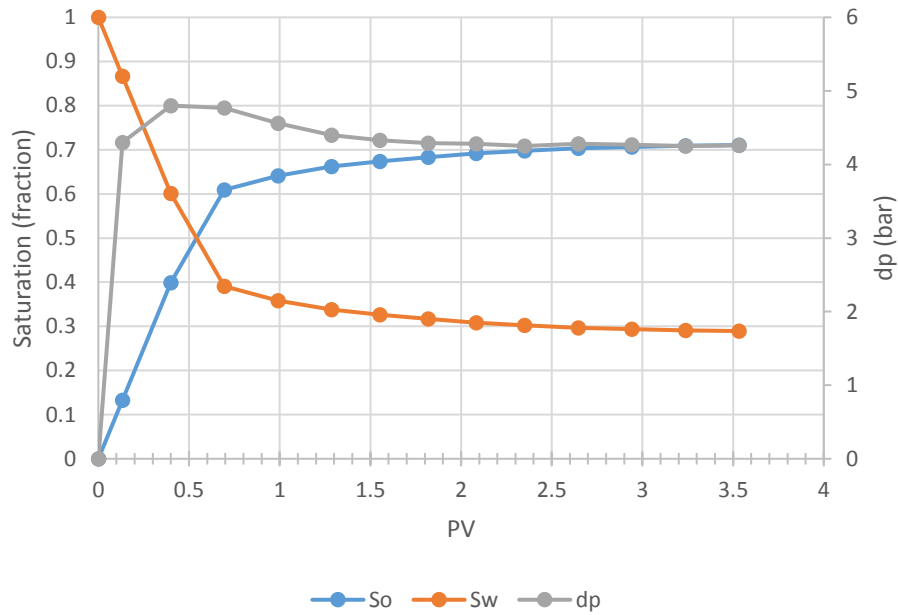
Plot 4.42 SK-6 Saturation Profile with dp

Performing forced drainage by flooding the core at high flow rate facilitates in smoothing the saturation profile curve as shown in plot (5.42) for SK-6. The flood continued until no additional water produced or until dp becomes stable as shown in plot (5.42).

The next table shows EOR flood parameters for the cores after being aged for two weeks at 50^0 C.

Table 4.39 EOR Summary

Core	Flood Stages	Injected fluid	Injection rate (PV/D)	Confinement pressure (bar)	Back pressure (bar)	Temp. (C^0)	S_{wi}	S_{orNP}
SK-5	3	LSW/DP 1(g/l) in LSW	4/16	25	9.8	70	0.29	0.35
SK-6	4	LSW/DP 1(g/l) in LSW	4/16	25	9.8	70	0.28	0.26

4.3.2.1. SK-5 EOR

Forced imbibition of LSW followed by 1(g/l) DP in LSW slug at high flow rate is conducted to examine the ultimate recovery for the core. The flood scheme is illustrated in the following flow chart.

```
┌─────────────────┐      ┌─────────────────┐      ┌─────────────────┐
│  LSW [4.8 PVs]  │      │  DP 1 (g/l) in  │      │  LSW [4 PVs]    │
│                 │ ───▶ │  LSW [4.25 PVs] │ ───▶ │                 │
│     4 PV/D      │      │                 │      │    16 PV/D      │
│                 │      │    16 PV/D      │      │                 │
└─────────────────┘      └─────────────────┘      └─────────────────┘
```
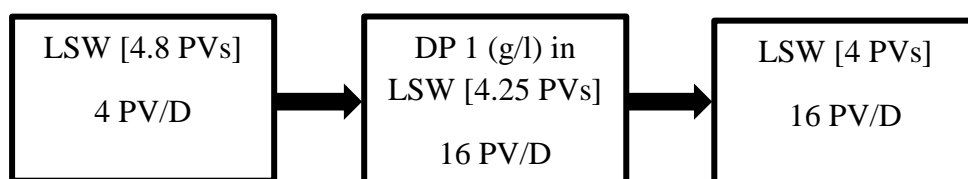
The results from EOR flood are summarized in the following table.

Table 4.40 SK-5 EOR Results

Stage	PV	oil recovered %	dp (bar)
	0.00	0.00	0.338
	0.42	34.76	1.68
	0.47	35.24	1.445
	0.59	37.14	1.46
	0.61	37.14	1.528
	0.62	37.62	1.5
	0.89	39.05	1.28
LSW 4 PV/D	1.16	39.05	1.39
	1.48	40.00	1.28
	1.49	40.48	1.317
	1.75	40.48	1.269
	2.01	40.48	1.327
	2.82	41.90	1.348
	4.67	41.90	0.92
	4.83	41.90	1.5228
	4.91	41.90	2.226
	6.54	46.67	2.43
DP Slug 16 PV/D	6.66	46.67	2.4
	7.66	48.10	2.38
	8.00	49.52	2.6
	8.57	50.00	2.6
	9.03	50.00	2.29
	9.43	50.00	2.214
	10.14	50.00	1.39
LSW 16 PV/D	11.13	50.00	2.429
	12.23	50.00	2.03
	13.22	50.00	2.38

The ultimate recovery of oil achieved for SK-5 is 50 %. SOR from LSW alone is 0.41 and after injecting the slug SOR decreased to 0.35, which represents 5.7% reduction. No incremental oil recovery achieved in the post flush stage with LSW injected at 16 PV/D. Plot (5.44) shows a rise in dp and inlet pressure at the transition from LSW injection to the slug injection. The increase in pressure is a direct response to the increase of the flow rate from 4 PV/D to 16 PV/D, which was carried out to overcome capillary end effect. The fluctuation in dp values might be attributed to the confinement pressure changes that took place during the experiment, which was caused by the elevated temperature of the flood. However, a reduction in dp around 1 bar is observed during the LSW injection in the post flush. A similar behavior of dp with LSW was also reported by A.A.Hamouda and et al [7]. Plot (5.45) demonstrates a corresponding increase in pH at the transition. The pH increase was also reported by A.A.Hamouda and et al [7]. This might be due to the dissolution of Calcium ions [Ca^{2+}] which increase the hydroxylic group [OH^-] concentration in the effluents. The dissolution of Ca^{2+} will introduce some fine migration which might contribute to the dp increase as discussed earlier in section (5.3.1.3).
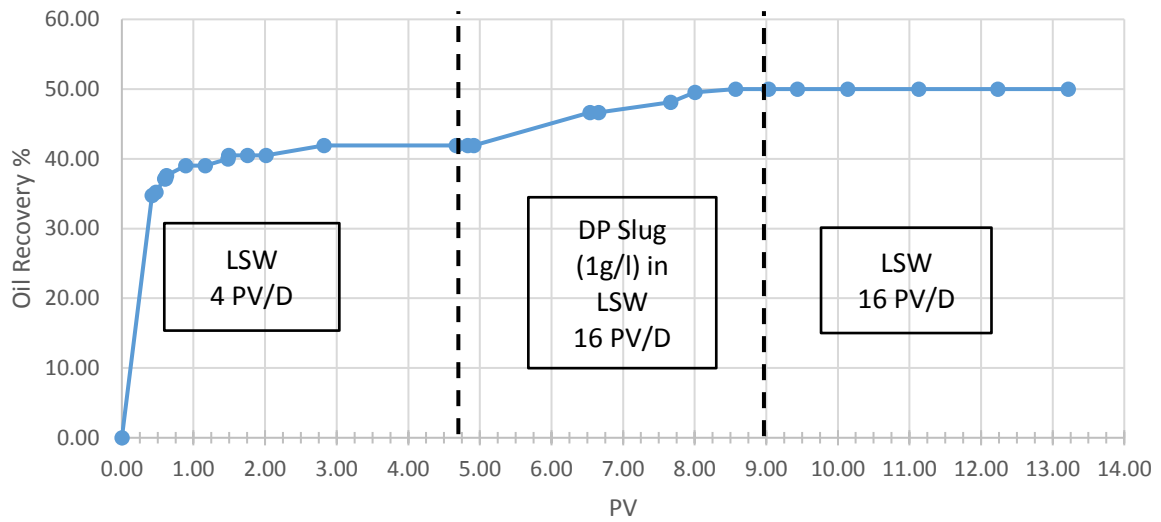
Plot 4.43 SK-5 Oil Recovery %
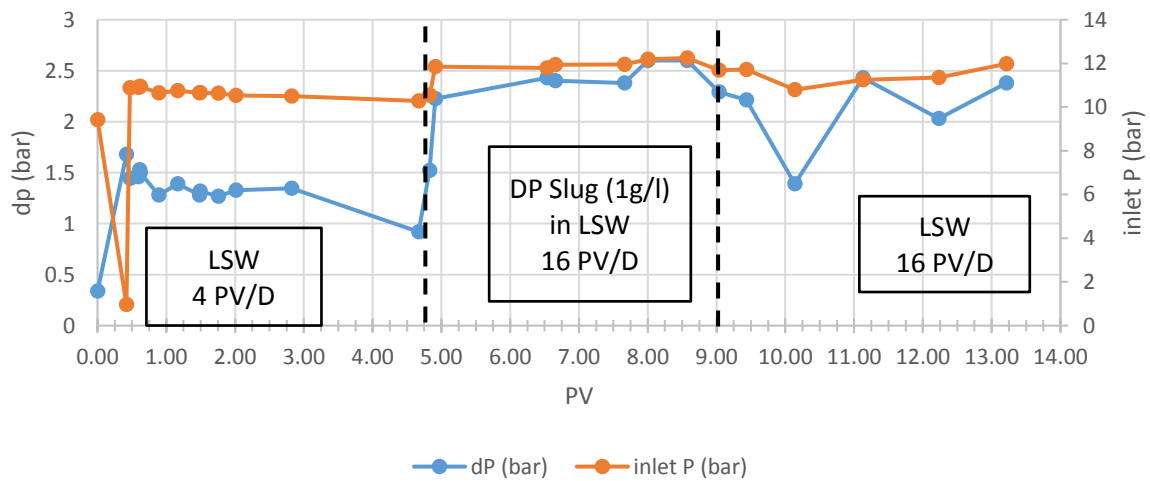
Plot 4.44 SK-5 Pressure Profile
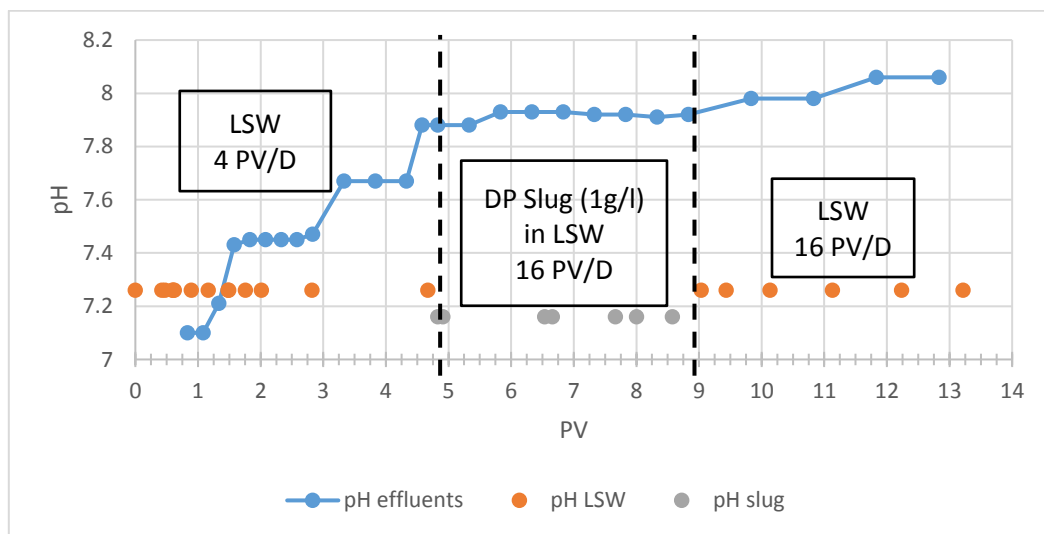
Plot 4.45 SK-5 pH

4.3.2.2. SK-6 EOR

SK-6 was flooded according to the following sequence.

```
┌─────────────────┐   ┌─────────────────┐   ┌─────────────────┐   ┌─────────────────┐
│ LSW [3.5 PVs]   │→  │ LSW [3.5 PVs]   │→  │ DP 1 (g/l) in   │→  │ DP 1 (g/l) in   │
│                 │   │                 │   │ LSW [3.5]       │   │ LSW [3.5]       │
│ 4 PV/D          │   │ 16 PV/D         │   │                 │   │                 │
│                 │   │                 │   │ 4 PV/D          │   │ 16 PV/D         │
└─────────────────┘   └─────────────────┘   └─────────────────┘   └─────────────────┘
                                                                           │
                                                                           ↓
                                                                  ┌─────────────────┐
                                                                  │ LSW [0.75 PVs]  │
                                                                  │                 │
                                                                  │ 4 PV/D          │
                                                                  └─────────────────┘
```
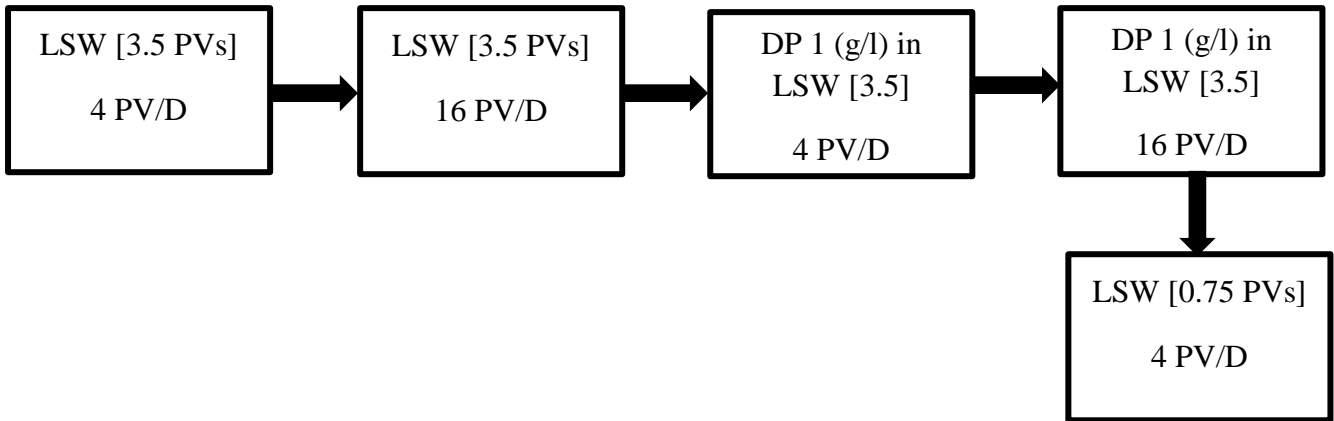
It is worth to mention that PV is calculated according to the injection flow rate, however for pH, IC, and abs measurements, PV is taken according to the volume of effluents produced from the burette.

As shown from the table below, most of the oil is recovered during the first stage of the flood, 3.5 PVs injection of LSW. 60.91 % is the oil recovery from injection of LSW at 4 PV/D, while around 2 % increment of oil recovery achieved after shifting to 16 PV/D of LSW and a total 62.96% of oil is recovered. This is due to overcoming the capillary end effect after increasing the flow rate. 0.41 % increment of recovery was received directly after injecting 0.5 PV of DP slug at 4 PV/D. Another 0.42 % of oil recovery is added after injecting 1 PV of DP slug. SOR from LSW alone is 0.266 and after injecting the slug SOR decreased to 0.260, which represents 0.6% reduction. No additional recovery of oil is received by shifting to 16 PV/D injection of DP slug. An additional 0.75 PV is flooded with LSW as post flush. The ultimate oil recovery from SK-6 is 63.79 %. The plot illustrates the oil recovery for SK-6. The results agree well with previous work with LSW on chalk done by A.A.Hamouda and et-al.,[32].
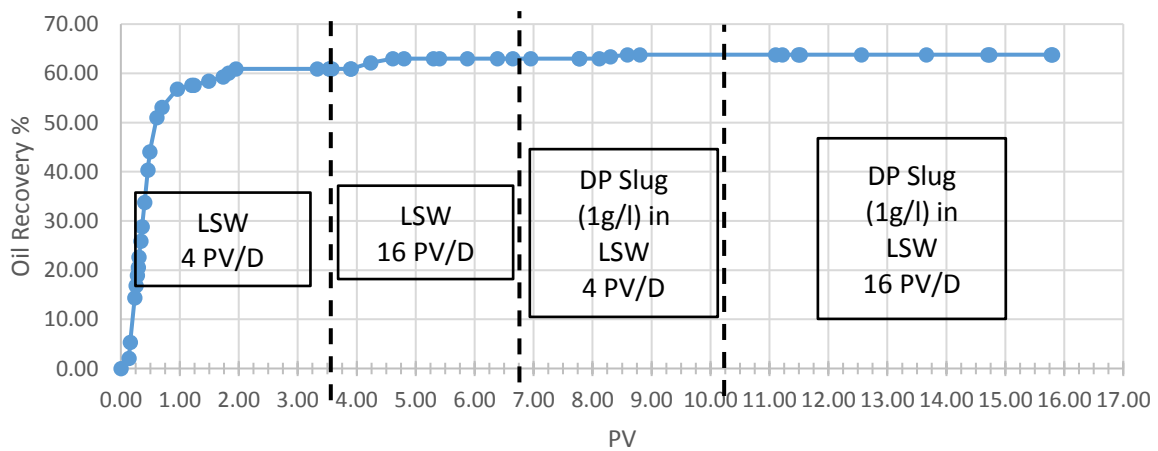
Plot 4.46 Oil Recovery SK-6

EOR data are presented in the table below.

Table 4.41 EOR Data for SK-6

Stage	PV	oil recovered %	dp (bar)
LSW 4 PV/D	0.00	0.00	0.04
	0.14	2.06	0.85
	0.16	5.35	0.81
	0.23	14.40	0.69
	0.26	16.87	0.76
	0.28	18.93	0.85
	0.29	20.58	0.94
	0.30	22.63	1.02
	0.34	25.93	1.21
	0.36	28.81	1.31
	0.40	33.74	1.50
	0.46	40.33	1.63
	0.49	44.03	1.65
	0.61	51.03	1.84
	0.70	53.09	1.20
	0.96	56.79	1.60
	1.20	57.61	1.14
	1.24	57.61	1.55
	1.49	58.44	0.98
	1.74	59.26	1.12
	1.82	60.08	1.27
	1.95	60.91	1.40
	3.33	60.91	1.01
	3.53	60.91	0.86
	3.54	60.91	1.20
	3.58	60.91	1.17
	3.90	60.91	1.30
	3.90	60.91	1.90
LSW16 PV/D	4.23	62.14	2.25
	4.61	62.96	2.20
	4.80	62.96	2.18
	5.30	62.96	2.13
	5.40	62.96	2.17
	5.88	62.96	2.12
	6.38	62.96	2.11
	6.64	62.96	2.13
	6.95	62.96	2.05
	7.77	62.96	2.02
DP 4 PV/D	7.78	62.96	2.34
	8.11	62.96	0.47
	8.30	63.37	0.47
	8.59	63.79	0.45
	8.80	63.79	0.44
	11.10	63.79	0.58
	11.21	63.79	0.36
	11.49	63.79	0.55
	11.52	63.79	0.28
DP 16 PV/D	12.56	63.79	1.88
	13.66	63.79	2.01
	14.70	63.79	2.21
	14.74	63.79	2.21
	15.78	63.79	2.18
	15.80	63.79	2.93

IC, and pH measurements are taken for SK-6 and summarized in table below.

Table 4.42 pH and IC Data for SK-6

stage	PV Produced	Mg++	Ca++	PV	pH
LSW 4 PV/D	1	6.87	1.16	0.25	6.95
	1.25	2.09	1.53	1.25	7.28
	1.5	1.32	0.60	1.5	7.41
	1.75	1.18	0.81	1.75	7.57
	2	1.12	1.62	2	7.54
	2.25	0.86	0.82	2.25	7.6
	2.5	0.92	1.43	2.5	7.57
	2.75	0.72	0.38	2.75	7.64
	3	0.68	0.39	3	7.6
	3.25	0.81	0.73	3.25	7.75
	3.5	0.86	0.65	3.5	7.8
LSW 16 PV/D	3.75	0.77	0.31	3.75	7.76
	4	0.83	0.48	4	7.74
	4.25	4.32	0.90	4.25	7.78
	4.5	1.25	0.35	4.5	7.58
	4.75	1.02	0.85	4.75	7.81
	5	0.92	0.59	5	7.85
	5.25	0.94	1.09	5.25	7.95
	5.5	0.84	0.61	6	7.8
	5.75	0.78	0.28	6.75	7.87
	6	0.89	0.42	7	7.77
	6.75	0.90	0.55	7.25	7.91
DP Slug 4 PV/D	7	1.01	1.10	7.5	7.91
	7.25	0.89	0.58	7.75	8
	7.5	0.82	0.25	8	8
	10	0.99	0.75	8.25	8
	10.25	0.97	0.67	8.5	8
DP Slug 16 PV/D	11.25	1.09	0.77	8.75	8
	12.25	1.03	2.25	9	8
	13.25	0.83	0.61	9.25	8
	14.25	0.98	0.96	9.5	8
LSW 4 PV/D	14.5	0.96	0.81	9.75	8
	14.75	0.88	0.51	10	7.96
	15	0.92	0.37	10.25	8.01
				11.25	7.96
				12.25	8.01
				13.25	8.06
				14.25	8.06
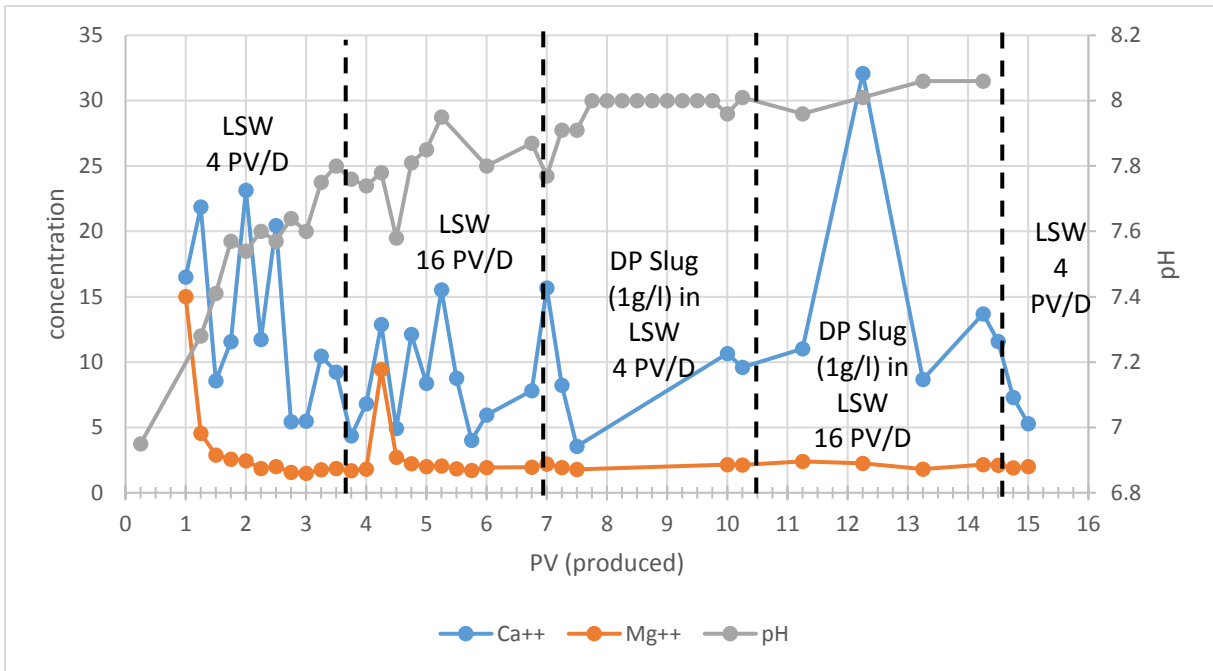
Plot 4.47 IC data with pH SK-6
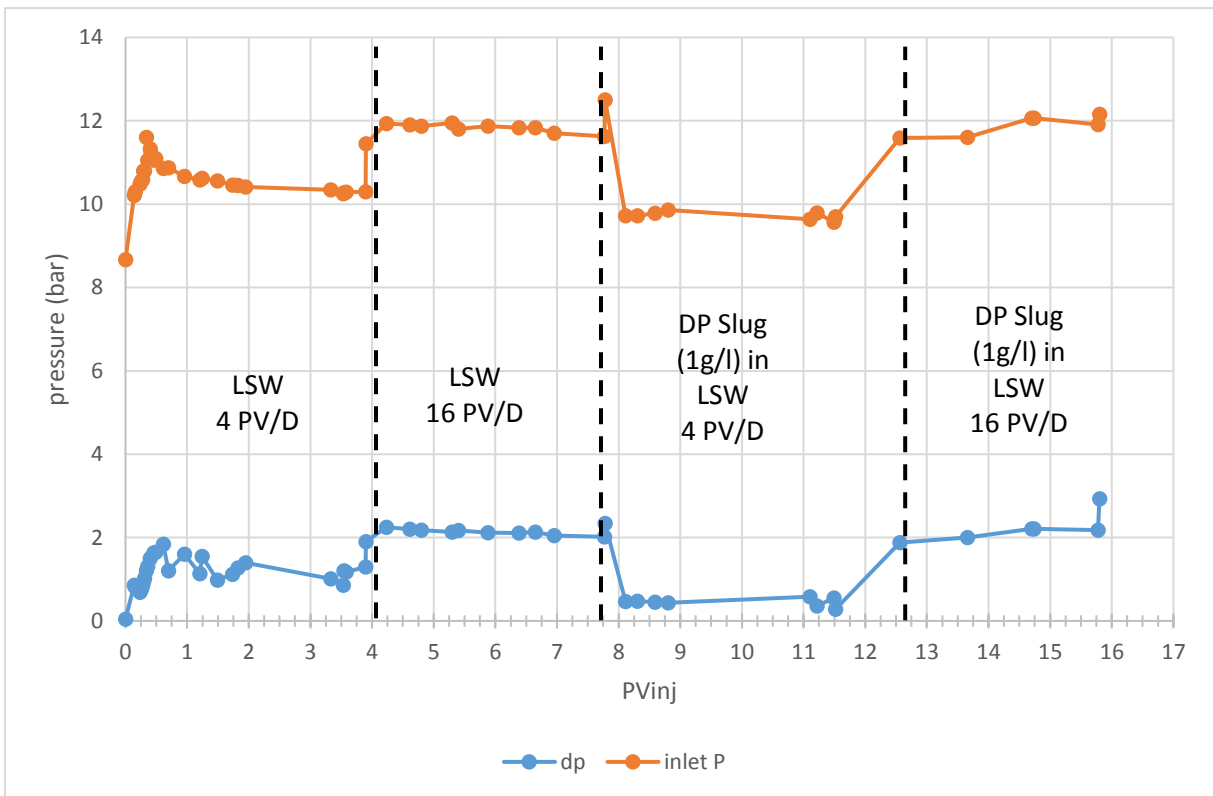
Plot 4.48 Pressure Profile SK-6

Plot (5.47) shows the ions concentration in the effluents relative to the ion concentration of LSW. While Mg^{++} is almost constant, Ca^{++} tends to increase after introducing NPs slug. The increase in Ca^{++} leads to an increase in pH as observed earlier. The production of Ca^{++} reaches its peak around 2 PV after switching to 16 PV/D. This peak corresponds to an increase in dp at the same PV interval. Most likely the dp shown in plot (5.48) will drop and stabilize in response to the decrease of calcium ion production in the effluents. The spike observed in calcium ions production is probably attributed to calcium dissolution and fine migration as explained earlier. However, this increase is followed by a decrease in Ca^{++} production, which is similar to what was observed in SK-1 and SK-2 and might be due to the adsorption of silica NPs on calcite.

The suggested EOR mechanism in place, is the improvement of sweep efficiency that results from calcium dissolution [32]. The wettability of the rock will also change to more water wet because of the suggested adsorption of hydrophilic silica NPs on the chalk surface. Furthermore, the high alkalinity introduced by the dissolution of CaCO3, might react with some of the oil components and enhances oil mobility.

Chapter 6

5. Summary and Conclusion:

The adsorption of surface modified Silica Nano Particles (NPs) adsorption on calcite surface was examined. The potential application of NPs for enhanced oil recovery (EOR) in chalk reservoirs was investigated for Stevns Klint (SK) chalk cores. The main findings from experiments can be summarized in the following points:

1. DP9711 silica Nanofluid (NP) is stable over wide range of salinity and at high temperatures and pressures, which makes it suitable for field application.

2. NPs show negative zeta potential, while calcite mineral has positive zeta potential. Adsorption could occur due to the attractive forces established between the two oppositely charged surfaces.

3. NPs have greater affinity to adsorb on calcite in deionized water (DIW), when compared to quartz and kaolinite.

4. Zeta potential absolute value of NPs decreases in synthetic sea water (SSW) due to reduction in Debye length and double layer shrinkage. This effect slightly improves the adsorption of NPs on calcite mineral in SSW compared to DIW.

5. The Effect of calcite concentration is more pronounced in SSW, when compared to DIW due to higher ionic strength of SSW.

6. The study of NP adsorption in chalk cores SK-1 and SK-2, shows significant adsorption of NPs on chalk - around 95% - followed by constant rate desorption that takes place in the late post-flush.

7. From the observations made in the dynamic adsorption studies in chalk cores, significant reversible adsorption was observed. The desorption appeared to take place at a constant rate. However, even after prolonged post-flush, a significant amount of

NP were retained in the core. The desorption process does not affect the flow behavior in the core as indicated by the flat dp curve.

8. Fine migration due to calcite dissolution is reduced when NPs introduced (SK-2 & SK-3)

9. SEM images confirmed observations made from static adsorption experiments on calcite and EDXRF of SK-2 effluent confirmed production of calcium with some traces of sulfur, and silicon in colored effluents, which are attributed to fines and silica NPs respectively.

10. Ultimate oil recovery reached by using silica NP with LSW is 63.79% and NPs lead to 0.83% increment in oil recovery compared to the primary recovery obtained with only LSW.

11. Ion tracking and pH suggest that the EOR mechanism in place includes the improvement of sweep efficiency due calcite dissolution that leads to fine migration. Furthermore, the hydrophilic silica NPs adsorbed in chalk will probably alter the rock surface to more water wet.

6. References

1.   Metin, C.O., J.R. Baran, and Q.P. Nguyen, *Adsorption of surface functionalized silica nanoparticles onto mineral surfaces and decane/water interface.* Journal of Nanoparticle Research, 2012. **14**(11): p. 1246.

2.   Arab, D. and P. Pourafshary, *Nanoparticles-assisted surface charge modification of the porous medium to treat colloidal particles migration induced by low salinity water flooding.* 2013.

3.   Yuan, B., R.G. Moghanloo, and D. Zheng, Nanoparticles Adsorption, Straining and Detachment Behavior and its Effects on Permeability of Berea Cores: Analytical Model and Lab Experiments, 2016.

4.   Al-adasani, A., B. Bai, and Y.-S. Wu. *Investigating low-salinity waterflooding recovery mechanisms in sandstone reservoirs.* in *SPE Improved Oil Recovery Symposium.* 2012. Society of Petroleum Engineers.

5.   Habibi, A., et al., *Reduction of fines migration by nanofluids injection: an experimental study.* SPE Journal, 2012. **18**(02): p. 309-318.

6.   NYACOL. *NYACOL DP9711 Data Sheet.* [cited 2017 11/6]; Available from: http://www.nyacol.com/app/uploads/2015/04/DP9711-Data-Sheet-20130812.pdf.

7.   Hamouda, A., et al. *Possible Mechanisms for Oil Recovery from Chalk and Sandstone Rocks by Low Salinity Water (LSW).* in *SPE Improved Oil Recovery Symposium.* 2014. Society of Petroleum Engineers.

8.   Hamouda, A.A. and K.A. Rezaei Gomari. *Influence of temperature on wettability alteration of carbonate reservoirs.* in *SPE/DOE Symposium on Improved Oil Recovery.* 2006. Society of Petroleum Engineers.

9.   Tabrizy, V.A., R. Denoyel, and A. Hamouda, *Characterization of wettability alteration of calcite, quartz and kaolinite: Surface energy analysis.* Colloids and Surfaces A: Physicochemical and Engineering Aspects, 2011. **384**(1): p. 98-108.

10.   Dynamics, C. *how do the zetaprobe and acoustosizer II measure zeta potential and particle size.* [cited 2017 10/6]; Available from: www.colloidal-dynamics.com/docs/CD_measurement_techniques.pdf.

11.   toledo, m. *applications technical data accessories.* balances and scales AM/PM/SM 2017 [cited 2017 11/6]; Available from: http://www.mt.com/dam/mt_ext_files/Editorial/Generic/0/AM_PM_SM_TechData_Zubehr_0x00001008400695764001180a_files/am-pm-sm-tdata-e-704701.pdf.

12.   toledo, m. *Analytical Balance MS104TS/00.* 2017 11/06/2017 [cited 2017 11/06]; Available from: http://www.mt.com/ca/en/home/products/Laboratory_Weighing_Solutions/Analytical/MS-TS_Analytical/MS104TS.html.

13.   Emerson. *Rosemount 3051 coplanar pressure transmitter.* [cited 2017 8/6]; Available from: http://www.emerson.com/catalog/en-us/rosemount-3051-coplanar-pressure-transmitter.

14. AG, E.H. *field instruments overview differential pressure Deltabar PMD75*. [cited 2017 8/6]; Available from: https://www.endress.com/en/Field-instruments-overview/pressure/Differential-Pressure-Deltabar-PMD75.

15. Millipore, E. *High Quality Ultrapure Water Purification System* [cited 2017 8/6]; Available from: http://www.azom.com/equipment-details.aspx?EquipID=2470.

16. Malvern. *Zetasizer Nano ZSP Sensitivity, simplicity, versatility*. [cited 2017 8/6]; Available from: https://www.malvern.com/en/products/product-range/zetasizer-range/zetasizer-nano-range/zetasizer-nano-zsp/index.html.

17. Lamont–Doherty Earth Observatory, C.U. *Ion Chromatograph to detect major anions in precipitation (snow), groundwaters and drinking waters from New York*. [cited 2017 13/6]; Available from: http://www.ldeo.columbia.edu/~martins/eda/Ic_lec.html.

18. Scientific, T., *Dionex ICS-5000 Ion Chromatography System Operator's Manual*. 2011, Thermo Fisher Scientific.

19. Rouessac, F. and A. Rouessac, *Chemical analysis: modern instrumentation methods and techniques*. 2013: John Wiley & Sons.

20. evisa, *PerkinElmer Inc. - Optima 4300 DV ICP-OES*.

21. GILSON. *305/306/307 pumps*. [cited 2017 13/6]; Available from: http://www.gilson.com/en/AI/Products/32.35/Default.aspx#.WT-7wVXyhpg.

22. TOLEDO, M. *SevenCompact™ pH/Ion S220 – universal and versatilE*. [cited 2017 13/6]; Available from: http://www.mt.com/no/no/home/products/Laboratory_Analytics_Browse/pH/benchtop_meter/SevenCompact/S220_pH-Ion.html.

23. Argast, A. and C.F. Tennis III, *A web resource for the study of alkali feldspars and perthitic textures using light microscopy, scanning electron microscopy and energy dispersive X-ray spectroscopy*. Journal of Geoscience Education, 2004. **52**(3): p. 213-217.

24. Formulaction. *STATIC MULTIPLE LIGHT SCATTERING*. [cited 2017 13/6]; Available from: http://www.formulaction.com/en/stability-size/static-multiple-light-scattering.

25. Calloway, D., *Beer-lambert law*. J. Chem. Educ, 1997. **74**(7): p. 744.

26. clark, j. *A DOUBLE BEAM UV-VISIBLE ABSORPTION SPECTROMETER*. 2006 2016 [cited 2017 10/5]; Available from: http://www.chemguide.co.uk/analysis/uvvisible/spectrometer.html#top.

27. corporation, S., *UV-Vis Spectrophotometer, UV-1700 series service manual*, S. corporation, Editor.

28. Mondragon, R., et al., *Characterization of silica–water nanofluids dispersed with an ultrasound probe: A study of their physical properties and stability*. Powder Technology, 2012. **224**: p. 138-146.

29. worldwide, m.i. *dynamic light scattering common terms defined*. 2011 [cited 2017 12/6]; Available from: http://www.biophysics.bioc.cam.ac.uk/wp-content/uploads/2011/02/DLS_Terms_defined_Malvern.pdf.

30. Appelo, C.A.J. and D. Postma, *Geochemistry, groundwater and pollution*. 2004: CRC press.

31. Stumm, W. and J.J. Morgan, *Aquatic chemistry: an introduction emphasizing chemical equilibria in natural waters*. 1981: John Wiley.

32. Hamouda, A.A. and E. Maevskiy, *Oil recovery mechanism (s) by low salinity brines and their interaction with chalk*. Energy & Fuels, 2014. **28**(11): p. 6860-6868.

Appendix A:

Effluents History for IC data SK-1,2,&6

Sample No	PV Produced	pH	Li+ (mol/L)	Na (mol/L)	K(mol/L)	Mg++(mol/L)	Ca++(mol/L)	Cl(mol/L)	SO4 (mol/L)	ABS
1	4	7.71	0.00E+00	4.15E-04	2.82E-04	0.00E+00	1.67E-03	5.65E-04	0.00E+00	0.07
2	8	7.54	0.00E+00	5.23E-04	3.05E-04	0.00E+00	1.67E-03	7.45E-04	0.00E+00	0.11
3	8.25	8.08	5.73E-02	5.59E-04	2.82E-04	4.02E-04	6.66E-03	6.29E-02	0.00E+00	0.09
4	8.5	7.78	4.07E-01	8.66E-04	2.82E-04	5.24E-04	1.17E-02	3.50E-01	0.00E+00	0.11
5	8.75	8.27	4.77E-01	7.76E-04	4.46E-04	1.75E-04	5.00E-03	3.92E-01	0.00E+00	0.15
6	9	9.5	1.93E-01	9.92E-04	3.29E-04	0.00E+00	1.67E-03	1.53E-01	0.00E+00	2.03
7	9.25	10.69	2.80E-02	1.52E-03	8.45E-04	0.00E+00	1.67E-03	1.18E-02	0.00E+00	2.71
8	9.5	10.91	1.04E-02	6.13E-04	2.82E-04	0.00E+00	0.00E+00	1.34E-03	0.00E+00	0.56
9	9.75	10.89	6.14E-03	7.94E-04	3.05E-04	0.00E+00	0.00E+00	9.33E-04	0.00E+00	0.28
10	10	10.88	4.16E-03	3.61E-03	2.35E-04	0.00E+00	0.00E+00	4.13E-03	0.00E+00	0.19
11	10.25	10.71	3.20E-03	7.76E-04	2.58E-04	0.00E+00	1.67E-03	1.27E-03	0.00E+00	0.14
12	10.5	10.7	2.94E-03	1.33E-03	3.76E-04	0.00E+00	1.67E-03	2.10E-03	0.00E+00	0.11
13	10.75	10.59	1.45E-03	1.05E-03	2.11E-04	0.00E+00	1.67E-03	1.38E-03	0.00E+00	0.09
14	11	10.2	4.90E-04	5.14E-02	3.76E-04	0.00E+00	1.67E-03	4.85E-02	0.00E+00	0.09
15	11.25	8.04	1.78E-04	7.58E-04	3.52E-04	0.00E+00	1.67E-03	9.84E-04	0.00E+00	0.09
16	11.5	8.08	0.00E+00	6.13E-04	2.58E-04	0.00E+00	1.67E-03	7.53E-04	0.00E+00	0.08
17	11.75	8.27	0.00E+00	5.95E-04	3.76E-04	0.00E+00	1.67E-03	8.47E-04	0.00E+00	0.09
18	12	8.5	0.00E+00	3.74E-02	6.10E-04	1.57E-04	3.33E-03	3.52E-02	0.00E+00	0.09
19	12.25	8.15	1.34E-04	2.04E-03	8.92E-04	0.00E+00	1.67E-03	2.42E-03	0.00E+00	
20	12.5	8.68	0.00E+00	1.59E-03	3.29E-04	1.22E-04	1.67E-03	1.80E-03	0.00E+00	
21	12.75	8.21	0.00E+00	2.20E-03	2.82E-04	1.05E-04	1.67E-03	2.29E-03	0.00E+00	
22	14	7.6	0.00E+00	1.95E-03	3.29E-04	0.00E+00	1.67E-03	1.59E-03	2.71E-05	
23	14.25	8.65	0.00E+00	2.18E-03	4.46E-04	1.40E-04	1.67E-03	2.52E-03	0.00E+00	
24	14.5	8.75	0.00E+00	6.22E-02	2.58E-04	1.22E-04	3.33E-03	5.83E-02	0.00E+00	
25	15	8.99	0.00E+00	2.09E-03	2.82E-04	1.40E-04	3.33E-03	2.38E-03	0.00E+00	
26	15.25	9	0.00E+00	2.40E-03	2.82E-04	1.57E-04	3.33E-03	2.43E-03	0.00E+00	
27	15.5	9.05	0.00E+00	2.78E-03	4.93E-04	1.40E-04	3.33E-03	2.51E-03	0.00E+00	
28	16	9.22	0.00E+00	1.64E-03	2.35E-04	1.05E-04	1.67E-03	1.81E-03	0.00E+00	

Sample No	PV Produced	pH	Li+ (mol/L)	Na (mol/L)	K(mol/L)	Mg++(mol/L)	Ca++(mol/L)	Cl (mol/L)	CO3 (mol/L)	SO4(mol/L)	ICP DP Conc (g/l) corr
1	0.25	7.99		1.1E-03	1.1E-04	1.0E-04	1.3E-03	1.5E-03	3.2E-01	0.0E+00	
2	0.5	7.92		1.2E-03	0.0E+00	1.6E-04	2.0E-03	1.9E-03	3.3E-01	0.0E+00	
3	0.75	7.92		1.8E-03	2.0E-04	1.2E-04	2.0E-03	2.0E-03	1.2E-01	2.4E-05	
4	1	7.97		6.0E-04	0.0E+00	0.0E+00	1.1E-03	9.8E-04	1.0E-01	4.0E-05	
5	3.625	8		6.6E-04	0.0E+00	0.0E+00	5.5E-04	5.6E-04	2.7E-01	0.0E+00	
25	6.25	7.63		1.0E-03	0.0E+00	0.0E+00	6.5E-04	9.5E-04	2.9E-01	0.0E+00	
26	6.5	7.68		7.5E-04	1.1E-04	0.0E+00	0.0E+00	1.0E-03	2.6E-01	0.0E+00	
27	6.75	7.53		6.2E-04	0.0E+00	0.0E+00	3.7E-04	6.1E-04	2.6E-01	0.0E+00	
28	7	7.56		8.1E-04	0.0E+00	0.0E+00	5.7E-04	8.4E-04	2.7E-01	0.0E+00	
29	7.25	7.62	0.0E+00	7.9E-04	0.0E+00	0.0E+00	4.3E-04	8.4E-04	2.7E-01	0.0E+00	
30	7.5	7.61	0.0E+00	2.0E-03	0.0E+00	0.0E+00	1.1E-03	1.9E-03	3.2E-01	0.0E+00	
31	7.75	7.62	0.0E+00	9.2E-04	0.0E+00	0.0E+00	4.7E-04	6.8E-04	2.6E-01	0.0E+00	
32	8	7.59	0.0E+00	1.0E-03	0.0E+00	0.0E+00	5.7E-04	1.0E-03	2.8E-01	0.0E+00	
33	8.25	7.46	6.7E-03	6.4E-04	1.1E-04	1.0E-04	2.0E-03	1.2E-02	2.4E-01	0.0E+00	
34	8.5	7.09	6.0E-02	9.2E-04	0.0E+00	2.4E-04	5.3E-03	5.5E-02	2.5E-01	0.0E+00	0.0E+00
35	8.75	7.1	8.6E-02	2.0E-03	0.0E+00	2.2E-04	4.6E-03	6.8E-02	3.2E-01	0.0E+00	0.0E+00
36	9	7.25	9.1E-02	7.3E-04	0.0E+00	1.0E-04	2.0E-03	6.7E-02	2.3E-01	0.0E+00	0.0E+00
37	9.25	7.33	9.2E-02	1.6E-03	0.0E+00	1.2E-04	2.1E-03	6.8E-02	2.7E-01	0.0E+00	
38	9.5	7.37	9.3E-02	2.8E-03	0.0E+00	1.9E-04	3.0E-03	7.0E-02	3.4E-01	0.0E+00	
39	9.75	8.51	8.5E-02	1.1E-02	2.7E-04	6.2E-04	4.3E-03	7.5E-02	1.3E-01	5.5E-05	1.1E-02
40	10	9.23	2.6E-02	6.0E-03	0.0E+00	3.3E-04	2.9E-03	2.2E-02	4.4E-01	0.0E+00	1.7E-02
41	10.25	9.75	1.0E-02	2.1E-03	0.0E+00	0.0E+00	6.1E-04	4.7E-03	3.7E-01	0.0E+00	1.9E-02
42	10.5	9.98	7.3E-03	1.0E-03	0.0E+00	0.0E+00	3.9E-04	1.5E-03	3.7E-01	0.0E+00	1.8E-02
43	10.75	10.03	5.0E-03	6.6E-04	0.0E+00	0.0E+00	2.0E-04	7.6E-04	3.3E-01	0.0E+00	1.4E-02
44	11	9.91	3.8E-03	4.3E-04	0.0E+00	0.0E+00	0.0E+00	3.0E-04	3.0E-01	0.0E+00	
45	11.25	9.84	2.6E-03	7.0E-04	0.0E+00	0.0E+00	3.1E-04	5.8E-04	3.0E-01	0.0E+00	
46	11.5	9.64	1.2E-03	7.0E-04	0.0E+00	0.0E+00	0.0E+00	5.9E-04	2.9E-01	0.0E+00	
47	11.75	9.02	2.9E-04	4.6E-03	0.0E+00	1.6E-04	2.0E-03	2.8E-03	4.0E-01	0.0E+00	
48	12	8.06	0.0E+00	1.3E-03	0.0E+00	0.0E+00	1.2E-03	1.2E-03	3.1E-01	0.0E+00	
49	12.25	7.96	0.0E+00	8.5E-04	0.0E+00	0.0E+00	4.9E-04	6.8E-04	2.6E-01	0.0E+00	1.3E-03
70	15	8.18	0.0E+00	9.8E-04	0.0E+00	0.0E+00	5.5E-04	7.2E-04	2.7E-01	0.0E+00	0.0E+00
71	17.75	8.74	0.0E+00	6.8E-04	0.0E+00	0.0E+00	5.9E-04	5.6E-04	2.7E-01	0.0E+00	0.0E+00
72	18	9.18	0.0E+00	7.3E-04	0.0E+00	0.0E+00	0.0E+00	5.6E-04	2.5E-01	0.0E+00	0.0E+00
73	18.25	9.01	0.0E+00	2.4E-03	1.6E-04	8.6E-05	1.4E-03	2.0E-03	3.4E-01	0.0E+00	0.0E+00

Sample No	PV Produced	Mg++(mol/L)	Ca++(mol/L)	PV	pH	Ca++	Mg++
1	1	0.027020316	0.008590769	0.25	6.95	16.52071006	15.01129
2	1.25	0.008207675	0.011372308	1.25	7.28	21.86982249	4.559819
3	1.5	0.005200903	0.004455385	1.5	7.41	8.568047337	2.889391
4	1.75	0.004632054	0.006006154	1.75	7.57	11.55029586	2.573363
5	2	0.004388262	0.012036923	2	7.54	23.14792899	2.437923
6	2.25	0.00337246	0.006104615	2.25	7.6	11.73964497	1.873589
7	2.5	0.003616253	0.010633846	2.5	7.57	20.44970414	2.009029
8	2.75	0.002844244	0.002830769	2.75	7.64	5.443786982	1.580135
9	3	0.002681716	0.002855385	3	7.6	5.49112426	1.489842
10	3.25	0.0031693	0.00544	3.25	7.75	10.46153846	1.760722
11	3.5	0.00337246	0.0048	3.5	7.8	9.230769231	1.873589
12	3.75	0.003047404	0.002264615	3.75	7.76	4.355029586	1.693002
13	4	0.003250564	0.003544615	4	7.74	6.816568047	1.805869
14	4.25	0.016984199	0.006695385	4.25	7.78	12.87573964	9.435666
15	4.5	0.004916479	0.00256	4.5	7.58	4.923076923	2.731377
16	4.75	0.004022573	0.006301538	4.75	7.81	12.1183432	2.234763
17	5	0.003616253	0.004356923	5	7.85	8.378698225	2.009029
18	5.25	0.003697517	0.008073846	5.25	7.95	15.52662722	2.054176
19	5.5	0.003291196	0.004553846	6	7.8	8.75739645	1.828442
20	5.75	0.003088036	0.002092308	6.75	7.87	4.023668639	1.715576
21	6	0.003494357	0.003101538	7	7.77	5.964497041	1.941309
22	6.75	0.003534989	0.004061538	7.25	7.91	7.810650888	1.963883
23	7	0.003981941	0.008147692	7.5	7.91	15.66863905	2.21219
24	7.25	0.003494357	0.004283077	7.75	8	8.236686391	1.941309
25	7.5	0.003209932	0.001846154	8	8	3.550295858	1.783296
26	10	0.003900677	0.005538462	8.25	8	10.65088757	2.167043
27	10.25	0.003819413	0.004996923	8.5	8	9.609467456	2.121896
28	11.25	0.004306998	0.005735385	8.75	8	11.0295858	2.392777
29	12.25	0.004063205	0.016689231	9	8	32.09467456	2.257336
30	13.25	0.003250564	0.004504615	9.25	8	8.662721893	1.805869
31	14.25	0.003860045	0.007113846	9.5	8	13.68047337	2.14447
32	14.5	0.003778781	0.006030769	9.75	8	11.59763314	2.099323
33	14.75	0.003453725	0.003790769	10	7.96	7.289940828	1.918736
34	15	0.003616253	0.002756923	10.25	8.01	5.301775148	2.009029